Naval Command,
Control and Ocean
Surveillance Center RDT&E Division San Diego, CA
92152-5001

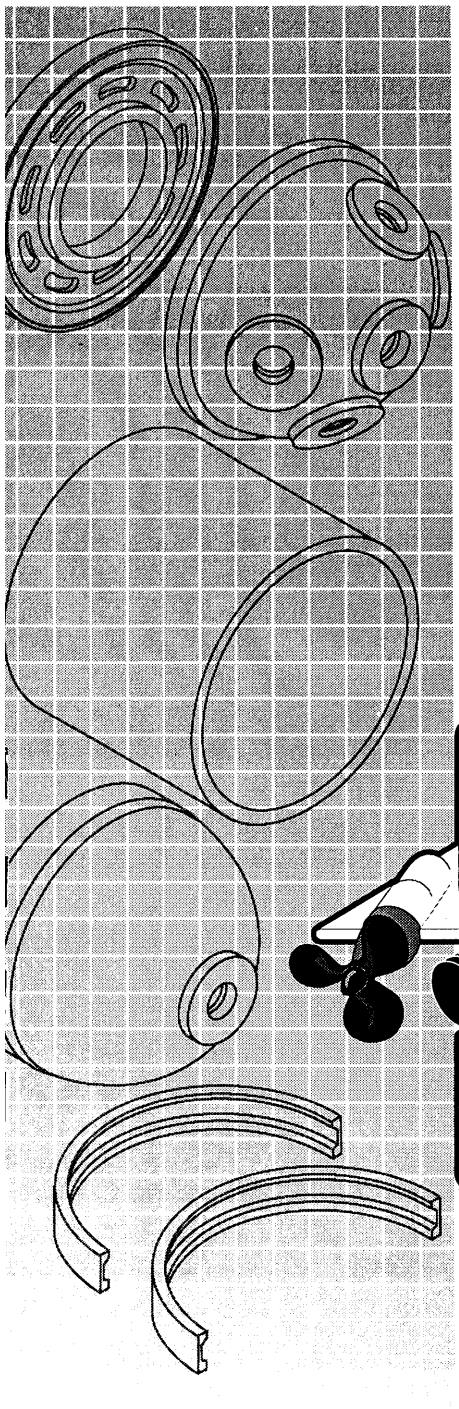

Structural Performance of Cylindrical Pressure Housings of Different Ceramic Compositions Under External Pressure Loading

Part III, Sintered Reaction Bonded Silicon Nitride Ceramic

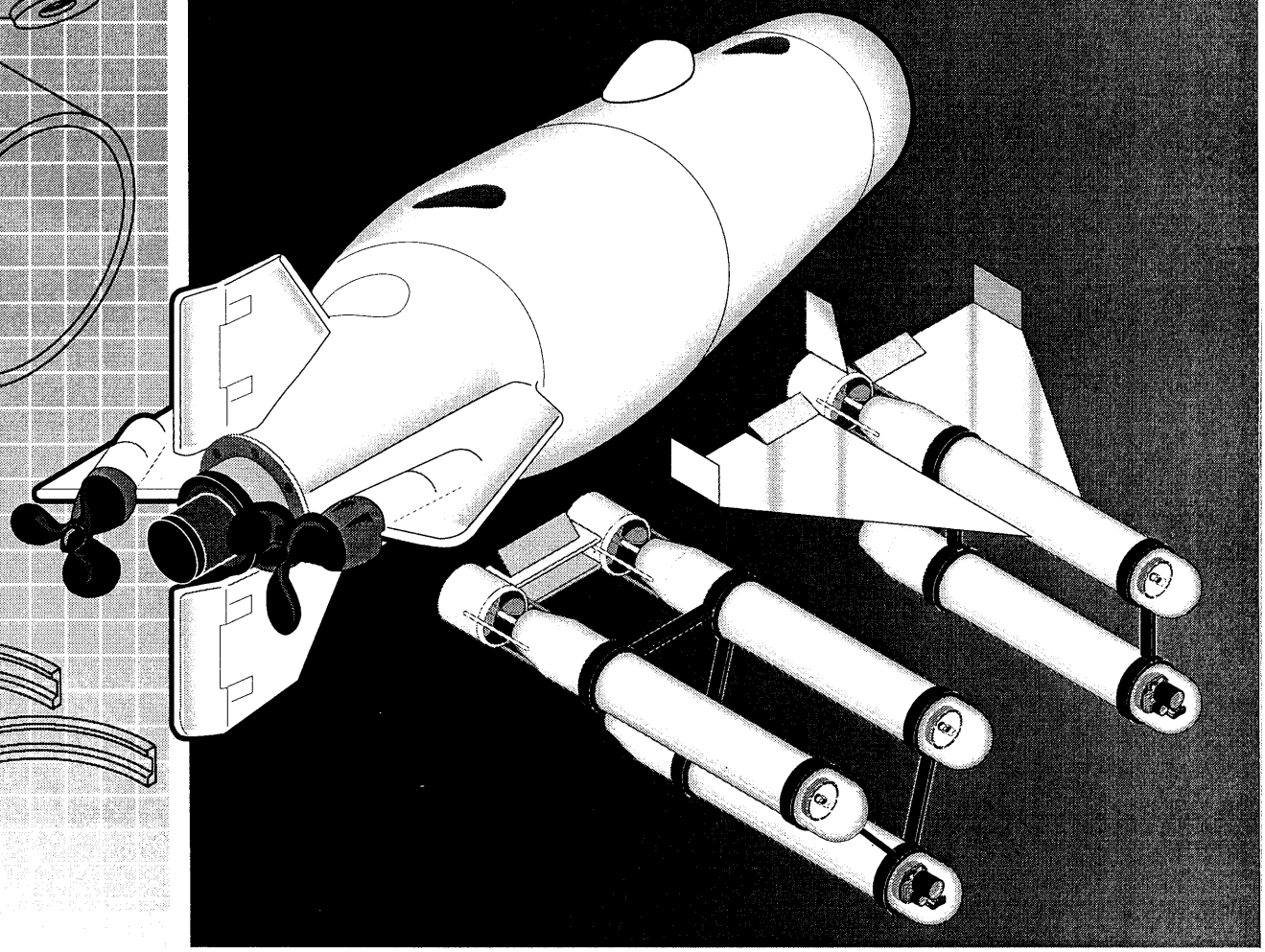

R. R. Kurkchubasche
R. P. Johnson
J. D. Stachiw

Technical Report 1592
June 1994

Approved for public release; distribution is unlimited.

SUMMARY

Ten 12-inch-outside-diameter (OD) by 18-inch-long silicon nitride (Si_3N_4) cylinders were fabricated by CERCOM, Inc., nondestructively inspected, and assembled. They were subsequently instrumented and pressure tested at Southwest Research Institute (SRI) under the supervision of the Naval Command, Control and Ocean Surveillance Center (NCCOSC) RDT&E Division (NRaD) under the Program for the Application of Ceramic to Large Housings for Underwater Vehicles (reference 1). CERCOM's material, designated PSX, was chosen for its high specific compressive strength, high specific elastic modulus, and high fracture toughness. Each cylinder was ultrasonically inspected prior to testing and then fitted with epoxy-bonded titanium end-cap joint rings. After being instrumented with strain gages, the cylinders were pressure tested cyclically and to destruction. CERCOM has demonstrated that it can successfully and repeatably cast 12-inch-OD by 18-inch-long cylinders from PSX. These cylinders are the largest-known monolithic silicon-nitride components ever fabricated. All ten cylinders passed proof testing to at least 10,000 psi. Cylinder failures can be attributed either to cyclic fatigue or to intentional pressurization to critical collapse pressure. Failure of the cylinders by buckling matched closely the predictions made by hand and computer calculations.

CONTENTS

INTRODUCTION 1

BACKGROUND 1

FABRICATION APPROACHES 1

SRBSN PROCESSING 2

OBJECTIVES 3

APPROACH 3

FABRICATION 3

PSX Fabrication Process 3

Powder Processing 3

Cold-Isostatic Pressing (Isopressing) 3

Pre-nitriding Green Cylinder 4

Green Machining 4

Nitriding 4

Sintering 5

QUALITY ASSURANCE 5

Dimensional Inspection 5

Dye Penetrant Inspection 5

Material Characterization 5

Pulse-Echo Ultrasonic Inspection 6

PRESSURE TESTING 6

Test Setup 6

Pressure Testing 7

TEST OBSERVATIONS/DISCUSSION 8

MATERIAL PROPERTIES 8

STRAINS 9

STRUCTURAL PERFORMANCE 9

CYCLIC FATIGUE LIFE **9**

CONCLUSIONS **10**

RECOMMENDATIONS **11**

REFERENCES **12**

GLOSSARY **13**

FIGURES

1. Process flow diagram for SRBSN and SSN fabrication 14
2. Fabrication process for PSX 15
3. Schematic of cold isostatic-pressing tooling set 16
4. Cold-walled, vacuum-nitriding furnace shown with nitrided cylinder 17
5. CERCOM's graphite-based (2200 degrees C) sintering furnace used for densifying Si_3N_4 18
6. Sintered Si_3N_4 cylinder prior to grinding 19
7. Diamond grinding of fully densified Si_3N_4 cylinder 20
8. Typical Vikers indentation for measuring fracture toughness 21
9. Engineering drawing for 12-inch-OD by 18-inch-long Si_3N_4 ceramic cylinder 22
10. Pulse-echo C-scan of Si_3N_4 ceramic calibration standard used for inspection of deliverable components 23
11. 12-inch cylinder test assembly, Type 1 configuration, Sheet 1 24
11. 12-inch cylinder test assembly, Type 1 configuration, Sheet 2 25
11. 12-inch cylinder test assembly, Type 1 configuration, Sheet 3 26
12. 12-inch cylinder Mod 1, Type 2 end-cap joint ring 27
13. 12-inch cylinder spacer 28
14. 12-inch hemisphere 29
15. 12-inch cylinder Mod 1 end-cap joint O-ring 30
16. 12-inch hemisphere clamp end 31
17. 12-inch hemisphere plug 32
18. 12-inch hemisphere washer 33
19. 12-inch hemisphere wooden plug 34

20. 12-inch cyllinder test assembly, Type 2 configuration, Sheet 1 35
20. 12-inch cylinder test assembly, Type 2 configuration, Sheet 2 36
21. 12-inch flat end plate 37
22. 12-inch cylinder test assembly, Type 3 configuration, Sheet 1 38
22. 12-inch cylinder test assembly, Type 3 configuration, Sheet 2 39
23. 12-inch cylinder Mod 1, Type 1 end-cap joint ring 40
24. 12-inch flat end-plate tie rod 41
25. 12-inch flat end-plate feed through 42
26. 12-inch end-plate wooden plug 43
27. Photo of fully machined Si_3N_4 ceramic cylinder prior to bonding of titanium end rings 44
28. Photo of fully machined Si_3N_4 ceramic cylinder with titanium end rings bonded in place 45
29. End-cap joint ring removal fixture 46
30. Pressure vs. strain plot for cylinder 001 47
31. Circumferential cracking on the bearing surface of cylinder 001. The titanium end-cap joint ring was removed after pressure testing to inspect for cracking 48
32. Pulse-echo C-scan of cylinder 001, Sheet 1 49
32. Pulse-echo C-scan of cylinder 001, Sheet 2 50
32. Pulse-echo C-scan of cylinder 001, Sheet 3 51
33. Pulse-echo C-scan of the other end of cylinder 001 52
34. Pressure vs. strain plot for cylinder 002 53
35. Pressure vs. strain plot for cylinder 003 53
36. Pressure vs. strain plot for cylinder 004 54
37. Pressure vs. strain plot for cylinder 005 54
38. Pressure vs. strain plot for cylinder 006 55
39. Pressure vs. strain plot for cylinder 007 55
40. Pressure vs. strain plot for cylinder 008 56
41. Pressure vs. strain plot for cylinder 009, pressurization No. 1 56
42. Pressure vs. strain plot for cylinder 009, pressurization No. 2 57
43. Pressure vs. strain plot for cylinder 010, pressurization No. 1 57
44. Pressure vs. strain plot for cylinder 010, pressurization No. 2 58
45. W/D vs. depth curves for AL-600 96-percent alumina ceramic and PSX ceramic 58

TABLES

1. Typical properties for PSX commercial grade of silicon nitride 59
2. Actual dimensions of deliverable PSX cylinders 59
3. Measured material properties of deliverable PSX cylinders 60
4. Summary of findings made in PSX cylinders using pulse-echo ultrasonic inspection 61
5. Average hoop and axial strains measured on inner mid-bay diameter of PSX cylinders at 10,000-psi external hydrostatic pressure 62
6. Summary of test plans and results for cylinders 001 through 010, Sheet 1 63
6. Summary of test plans and results for cylinders 001 through 010, Sheet 2 64
7. Comparison of cyclic pressure testing performance of PSX Silicon Nitride cylinders and of AL-600 96-percent alumina-ceramic cylinders 65
8. Comparison of the material compositions evaluated for the application of ceramics to large housings for UUVs 66

INTRODUCTION

Unmanned underwater vehicles (UUVs) require pressure-resistant housings for containment of their electronics and power supply. Currently, such housings are fabricated from metals such as aluminum, titanium, or steel. However, these materials result in very heavy housings when vehicles are designed to operate at depths as great as 20,000 feet.

Ceramic materials, because of their high specific compressive strength and high specific elastic modulus, are ideally suited for application to external pressure-resistant housings for underwater applications. A more detailed justification for using ceramic materials in external pressure-resistant housings may be found in the outline for the program under which this work was performed by the Naval Command, Control and Ocean Surveillance Center (NCCOSC), RDT&E Division (NRaD). See reference 1.

One of the objectives of this program was to evaluate various advanced ceramic compositions for use in pressure-resistant housings. Compositions evaluated include zirconia-toughened alumina (ZTA) ceramic (reference)), silicon carbide particulate-reinforced alumina ($SiC/Al_2O_3/Al$) ceramic (reference 3), and silicon-nitride (Si_3N_4) ceramic. The common base of comparison for testing these materials was 96-percent alumina ceramic manufactured by WESGO, Inc. (reference 4). This report summarizes the fabrication, nondestructive inspection, and testing of ten 12-inch-outside-diameter (OD) by 18-inch-long Si_3N_4 ceramic cylinders fabricated by CERCOM, Inc.

BACKGROUND

NRaD has been procuring and testing cylindrical and hemispherical components made from ceramic over the last decade. Most of the work, however, has focused on 94- and 96-percent alumina-ceramic compositions fabricated by Coors Ceramics Company and WESGO. When the program for the application of ceramic to large housings for underwater vehicles began, the most extensive testing had been completed on 94-percent alumina-ceramic housings only. Testing showed limited cyclic fatigue life under repeated pressurixation (references 5 and 6). The eventual failure of components due to repeated pressurization is attributed to radial tensile stress at the ceramic-to-titanium metal-bearing interface (see figure 25 of reference 1). This stress leads to internal circumferential cracks which run through the wall, eventually breaking off in shards, causing leakage or catastrophic failure. It is believed that one way of increasing the cyclic fatigue life of ceramic components is to use compositions having higher fracture toughness than alumina-ceramic composition.

The program for the application of ceramics to large housings for underwater vehicles gave NRaD the opportunity to test some new ceramic compositions exhibiting greater fracture toughness. These include silicon-nitride ceramic, ZTA ceramic, and Lanxide's silicon carbide particulate-reinforced alumina-ceramic composition (90-X-089). Silicon nitride ceramic was chosen for evaluation because of its high fracture toughness, high compressive strength and elastic modulus, and low specific gravity. Sintered reaction-bonded silicon nitride (SRBSN) was chosen because it is the composition CERCOM offered to make for NRaD under competitive contract award. CERCOM was the lowest bidder meeting the physical property requirements chosen by NRaD.

FABRICATION APPROACHES

There are two generic types (based on fabrication route) of silicon nitride that can meet the general material and performance requirements for pressure housings used for deep submergence service: sintered silicon nitride (SSN) produced by Si3N4 powder, and sintered reaction-bonded silicon sitride (SRBSN) produced from Si metal power (figure 1).[1] CERCOM, with extensive expertise producing components using both fabrication approaches, has selected the SRBSN process as the most appropriate for this application.

[1]Figures and tables are placed at the end of the text.

The selection methodology was based not only on the material mechanical property requirements, but also on the manufactured material reliability, fabrication adaptation to the required component size and shape, cost competitiveness, and scale-up ability to larger diameter housings. In short, the SRBSN process offers the flexibility for material and manufacturing design to produce high-quality ceramic pressure housings.

SRBSN PROCESSING

The standard SRBSN process, as shown in figure 1, consists of (1) comminuting and blending silicon metal powder and selected sintering aids, (2) cold forming the powder mixture into a net shape, (3) nitriding the green compact to convert the silicon metal to silicon nitride and concurrently reacting the sintering aids to form second-phase compounds, and (4) thermally consolidating the reaction bonded preform to a fully dense state.

CERCOM presently uses this basic fabrication process to manufacture eight different grades of silicon nitride. Each grade is engineered for a specific application; i.e., properties are developed through grain boundary and microstructural engineering to meet the specific needs of the application. For example, CERCOM manufactures one grade of Si_3N_4 (Cl Si_3N_4) designed specifically for use as an indexable cutting tool for the high-speed machining of cast iron. Another grade, known as NB Si3N4, is manufactured for the use of machining nickel base alloys. In these examples, the chemistry and nature of the grain boundary (crystalline vs. amorphous) for each grade is developed to maximize wear resistance under the conditions found at the interface between the metal work piece and cutting tool.

Another application example relates to the engineering of a suitable silicon nitride used for the balls of ball-valve assemblies in pump mechanisms. These pumps are used in “down-hole” applications for extracting oil where the components are subjected to severe pressure changes and a variety of corrosive environments including salt water/brine. To meet these and other requirements, CERCOM developed a pressureless, sintered grade of Si_3N_4 designated as PSX (see table 1 for typical property data). The intergranular phase (grain boundary) was engineered to be crystalline so that the material would resist corrosion and have good impact resistance (optimal fracture toughness).

As illustrated, silicon nitride can be considered a family of materials in the same manner as stainless steel or brass. In material families certain characteristics are shared, but vary sufficiently to permit the engineering of properties for specific applications. The family concept for silicon nitride originates with the ability to promote sintering with many different densification aids and with the ability to fabricate bodies by a wide variety of available processing routes.

Below its dissociation temperature, the atomic mobility of Si_3N_4 is insufficient to produce the mass transport required for full densification. Additives that promote densification through the formation of a liquid phase are required (alloying). Theoretically, dense silicon nitride can be produced with the addition of one or more oxides, such as MgO, Y_2O_3, Al_2O_3, SiO_2, ZrO_2, and CeO_2. The type and amount of additive used in conjunction with the selected densification process and heat treatment will largely determine the resultant properties of the material. For example, certain additives or additive combinations will produce an amorphous intergranular phase, whereas crystalline phases are produced by other additive selections and/or precise heat treatments. The nature of the intergranular phase will strongly influence the performance characteristics of the material.

As shown, with the many possibilities in additive selection coupled with a wide variety of fabrication routes, the family of silicon nitride is large. From this material family, CERCOM selected the PSX as the most appropriate for submersible applications. PSX is produced using the SRBSN process; where densification is accomplished using a proprietary pressureless sintering (PS) technique. The material is characterized as isotropic with a high fracture toughness—an important requirement for pressure housings. The material also has excellent corrosion resistance because of the crystallized (X) intergranular phase and has excellent strength with good reliability.

OBJECTIVES

The objectives of fabricating and testing CERCOM's PSX ceramic cylinders were:

1. To evaluate CERCOM's ability to fabricate 12-inch-OD by 18-inch-long PSX cylinders. These parts are the largest known monolithic PSX parts ever to be fabricated. Cylinders were to be nondestructively inspected to determine whether this composition could be fabricated relatively free of defects.
2. To determine the structural performance of PSX under external hydrostatic pressure loading. The structured performance parameters investigated included cyclic fatigue life and critical collapse pressure.
3. To compare the performance of the SRBSN Si_3N_4 composition against the performance of the baseline composition, WESGO's AL-600 96-percent alumina ceramic.

APPROACH

The test plan for the ten cylinders included fabrication, quality assurance, and pressure testing.

FABRICATION

PSX Fabrication Process

An overview of the fabrication process for PSX is presented in figure 2. The overall process begins with the selection of raw materials: silicon metal, and Y_2O_3 and Al_2O_3 powders (densification aids). The raw materials require comminution, blending, and homogenization. The processed powders are shaped into cylinders by cold-isostatic pressing. The cylinders are partially nitrided to allow for rapid, conventional green machining. The machined net-shaped parts are nitrided to convert the remaining silicon to silicon nitride and then densified using pressureless sintering technology. Cylinders are finished to final dimensions by diamond grinding, and all components are inspected and characterized to ensure quality. Note that the process flow appears to be "straightforward," and, generally, it is for standard shapes and sizes. However, for the cylinder sizes required for this program, the required logistics for each step became a major technological challenge.

Powder Processing

Powders of silicon metal, Y_2O_3, and Al_2O_3 are sealed into a jar mill with grinding media and a nonaqueous carrier fluid. Comminution and homogenization of the powder blend is achieved by rolling the jar mill for a specified speed and time interval. To maintain process consistency, the slurry viscosity is monitored and adjusted during milling/homogenization, as required, by carrier fluid additions. Silicon nitride grinding media (PSX composition) prevents contamination due to media attrition. All powder handling and processing is performed in a controlled environment to eliminate air-borne contamination which can form inclusions in finished components. After achieving satisfactory homogenization, the powder slurry is dried, screened, and readied for green forming.

Cold-Isostatic Pressing (Isopressing)

A variety of processes have been used for the consolidation of Si metal and Si_3N_4 green parts. The green forming technique of choice for large cylinders is usually isopressing—the technique used here. Isopressing is a well-defined procedure for consolidating silicon-based powders and offers a number of advantages:

1. A uniform, homogenous powder mixture can be handled and pressed without exposure to air and moisture.
2. Isopressed cylinders can be fabricated without binders, eliminating the need for burn-out normally required for injection molded or slip cast processed parts.
3. Isopressed cylinders can be produced with the controlled and uniform porosity required for pre-nitriding and nitriding.
4. Isopressing can be adapted to high-rate, full-scale production.

5. Isopressed cylinders are easily analyzed using standard instrumental techniques and high-resolution computed tomography to assure that critical size inclusions and agglomerates are not present.

6. Isopressing produces green-formed parts with uniform cross sections with relatively high density.

7. Controlled uniform, high-density isopressed parts result in low sintering shrinkage.

The procedure requires a tooling set consisting of a metal mandrel and a rubber bag with end caps (see figure 3 for build-up schematic). The mandrel forms the inside diameter (ID) of the isopressed cylinder, the rubber bag defines the OD, and, together with the end caps, they define the pressing or powder cavity. The rubber bag also transmits the hydrostatic pressure into the pressing (powder) cavity during the pressing cycle.

The metal mandrel is first placed into the rubber sleeve. The blended powders are weighed and charged into the pressing cavity under a controlled environment using vibrational energy. The cavity is capped, sealed, and treated with vacuum to ensure de-airing. The mold then is placed into a hydrostatic chamber, where pressure is isostatically applied to the mold through a fluid. The pressed cylinder is examined visually to ensure the absence of cracks.

Pre-nitriding Green Cylinder

When large silicon metal cylinders are isopressed they have insufficient strength for extensive handling or green machining. There are two techniques that can be used to increase the strength of green-formed silicon metal compacts: (1) argon sintering and (2) pre-nitriding.

Argon sintering involves heating the isopressed form in an argon atmosphere at about 1150 degrees C for several hours, resulting in slight fusion of silicon metal grains at contact points between particles in the compact. The fusion causes some shrinkage which can lead to increased problems during nitriding, particularly for large cross section parts because of diminished gas paths (may lead to incomplete nitriding).

The other technique for achieving acceptable handling strengths for green machining is termed pre-nitriding, which was the process used for this program. Pre-nitriding, simply, uses a shortened nitriding cycle to achieve the partial conversion of silicon metal to silicon nitride, thereby developing sufficient strength for subsequent green machining using conventional cutting tools and techniques. Optimum pre-nitriding conditions are those where about 10 percent of the normal nitrided weight gain is realized. Pre-nitrided cylinders with insufficient weight gains do not have sufficient strength for green machining, whereas cylinders with excessive weight gains become too “hard” and brittle for green machining with conventional tooling.

Green Machining

The OD and the cylinder ends are green machines on a lathe using carbide cutting tools without coolants. The ID of the cylinder is determined by the size of the isopress metal mandrel; therefore, the ID does not require green machining.

Nitriding

Nitriding is carried out in a cold-wall vacuum furnace (figure 4) where all interior construction materials are selected for their overall inertness. Heating elements, hearth, and heat shields are fabricated from molybdenum and high-purity alumina is used as insulation. The green-formed cylinders are placed on Si_3N_4 plates within the furnace hot zone. The furnace vessel is evacuated to outgas the green ware and construction materials. Gas backfill techniques are used to assist this procedure. Once the system integrity is confirmed by a leak check, the temperature is raised to 600 degrees C and held until a vacuum to 10-3 torr or lower is established. This procedure assists the outgassing process and removes all chemically combined water and residual volatiles associated with the system. The furnace then is backfilled to a pressure of 20.0 kPa with a gas containing 3 percent H_2, 25 percent He, and 72 percent N_2 for the remainder of the cycle.

The conversion process takes place in the temperature range of 1100 to 1400 degrees C with two principle nitriding reactions:

$$3\ Si(s) + 2N_2(g) \longrightarrow Si_3N_4(s) \quad (1)$$

$$3\ Si(g) + 2N2(g) \longrightarrow Si3N4(s) \quad (2)$$

Successful nitridation is achieved by precise control over the highly exothermic nature of reactions (1) and (2). The kinetics at a given temperature produce an initial rapid nitriding rate which slows until an essentially complete reaction asymtote is reached (Arrhenius curve). Therefore, the acceptable technique for “exotherm” management is to proceed incrementally, beginning at 1100 degrees C through the nitriding temperature range. At each temperature increment, the nitriding rate is allowed to reach its asumtote level before the temperature is increased again. Continuing this process to the maximum nitriding temperature of 1400 degrees C will result in full conversion of the silicon-to-silicon nitride. The time required at a given temperature for the reaction rate to reach the asymtote level is dependent upon many variables. Some of the most critical variables are Si metal purity, surface area and particle size, compact green density, and cross-sectional thickness. If management of the exotherm is not precise, the kinetics will cascade and the heat generated by the reaction will cause melting of the silicon. Once melted, the silicon coalesces and cannot be nitrided.

Sintering

Sintering is performed in an environmentally controlled graphite vacuum furnace, as shown in figure 5. Thermal consolidation (densification) is accomplished through a liquid-phase sintering technique known as solution-recrystallization. During sintering, the sintering additives form a liquid which promotes the alpha-to-beta phase transformation in Si_3N_4. The sintering temperature is selected to be high enough to form the liquid phase, but low enough not to sublimate Si_3N_4. Special sintering tooling is designed for dimensional control of the component during densification. This technique allows for minimal distortion during sintering. Figure 6 shows the sintered part.

The sintered cylinder is machined with an OD/ID grinding machine (figure 7). Both diameters, as well as length, are diamond ground to print. Test specimens also are machined from the “extra lengths” from all sintered cylinders.

QUALITY ASSURANCE

Quality assurance includes dimensional and dye-penetrant inspection, material characterization, and ultrasonic inspection of each cylinder.

Dimensional Inspection

Dimensional inspection of the ten silicon-nitride cylinders shows that the actual cylinder dimensions do not conform to the drawing dimensions. CERCOM had difficulty pressing parts which had enough stock to grind to the desired drawing dimensions. Dimensions were allowed to be altered slightly, however, the requirement that the wall-thickness-to-diameter ratio remain constant had to be met. Table 2 is a summary of cylinder dimensions. Cylinders 006 and 007 were shortened due to cracks which were found near the ends of the parts.

Dye Penetrant Inspection

Dye penetrant inspection of each cylinder was performed. Only cylinders without cracks were delivered.

Material Characterization

The material characterization consists of elasticity, compression strength, flexural strength, and fracture toughness measurements. All characterization, with the exception of elasticity, is conducted on actual cylinder material. That is, all cylinders were fabricated with excess length. The excess material was removed during diamond grinding of the cylinder and prepared into specimens appropriate for characterization. The elasticity properties were measured from specimens fabricated from “like” processed materials.

Young’s Modulus, shear modulus, and Poisson’s Ratio are measured using the acoustic resonance method, as described in ASTM C848–78. The compression tests follow the procedures outlined in ASTM C773. The flexural strength, or Modulus

of Rupture, is measured using a four-point bending test; performed to MIL–STD–1942 specification using the Type B testing configuration. The Weibull model also is applied for statistical data analysis. That is, both the Weibull Modulus and the characteristic strength are calculated using this model. The Weibull Modulus is a realtive indicator of material reliability. The higher the Weibull Modulus, the more reliable the data for design purposes. The characteristic strenght, always presented in a Weibull analysis, is the stress condition where the probability of failure is 63 percent.

Fracture toughness is measured using the Vickers Indentation Technique. The toughness measurement is based on crack propagation under point loading. After diamond indenting the specimen, four lateral cracks are generated from the corners of the indent (figure 8). The fracture toughness is calculated from the loading and the crack length, using the equation outlines by Hiihara (*J. Mat. Sci. Let.* 1, 1982, pg. 13). Table 3 tabulates the data generated for all fabricated cylinders.

Pulse-Echo Ultrasonic Inspection

Each cylinder was ultrasonically inspected by the pulse-echo ultrasonic inspection technique. The inspection was performed by Sonic Testing and Engineering, Inc. (Southgate, CA). Sonic Testing and Engineering used a 3/8-inch diameter, 3-inch focal length, 10-MHz transducer to perform the inspection. A small tile with flat-bottom drilled holes (see figure 10) was used as a calibration standard. This tile was made from the same composition as the cylinders. Details about the pulse-echo ultrasonic inspection technique and other nondestructive inspection techniques for ceramic components can be found in references 7 and 8. Table 4 lists the results of the ultrasonic inspection. It shows that some of the cylinders had numerous large defects, while others had almost none. The first few delivered cylinders were the “cleanest.” CERCOM attributes the dramatic difference in the number of defects to program changes made between cylinders. Isostatic pressing facilities were changed during the program. Green body quality could have been affected by any number of variables including weather, humidity, facility cleanliness, and processing schedule.

PRESSURE TESTING

Test Setup

Three types of assemblies were tested. They differed in the type of end closure used (hemispherical or flat) and the type of titanium end-cap joint ring used.

Hemispherical end closures were planned for use in cyclic tests, while flat end plates were planned for use in implosion tests (these being more rugged and, therefore, more capable of withstanding the force of the implosion at high pressure, making them reusable). At program initiation, it was not planned to cycle any cylinders above 12,000 psi. The machined hemispherical ends were calculated not to provide enough buckling resistance above 12,000 psi. For this reason, all cyclic tests above 12,000 psi were run using flat-end plates.

The difference in the two titanium end-cap joint ring designs is the external seal. NRaD Mod 1, Type 2 end caps have a lip on the OD. During cylinder assembly, a silicon sealant is applied to this lip. NRaD Mod 1, Type 1 end caps do not have a lip. Type 1 end caps were originally intended for use in proof and implosion tests; Type 2 end caps were originally intended for cyclic tests because they were believed to ensure a better seal under repeated pressurization.

The three types of assemblies can be summarized as follows:

Assembly	End Cap	End Closure
Type I	Type 2	Hemispherical
Type II	Type 2	Flat Plate
Type III	Type 1	Flat Plate

Test assembly Type 1 is shown in figure 11. NRaD Mod 1, Type 2 end caps (figure 12) are epoxy bonded to the ends of the ceramic cylinder using the procedure described in note 4 of figure 11. A 0.010-inch-thick manila paper gasket (figure 13) ensures a minimum 0.010-inch thickness of epoxy on the bearing interface between the ceramic and titanium.

Cylinders 001 through 005 were bonded onto the smoothly machined ceramic surface finish. However, test personnel noticed extrusion of epoxy on the ID of some of the cylindrical test specimens after pressure testing. It was decided that a better bond between the titanium and ceramic could be achieved if the ceramic surface to which the end-cap joint rings would be bonded was grit blasted prior to bonding. The bond surfaces on cylinders 006 through 010 were sandblasted by CERCOM.

In test assemblyType 1, the cylindrical assembly is closed at both ends by titanium hemispheres (figure 14). The assembly is made watertight by a surface seal using a nitrile O-ring (figure 15) for which there is an O-ring gland machined into the titanium end-cap joint ring. The titanium hemisphere is joined to the titanium cylinder via a V-shaped steel clamp band (figure 16).

Each cylinder was instrumented with five CEA-06-250-UT-120 strain gage rosettes. These were located at the center of the cylinder length and spaced 72 degrees apart. Each of the 1/4-inch, 90-degree rosettes had one leg oriented in the hoop direction and the other in the axial direction. Electrical leads for the strain gages were passed through the pole of the upper hemisphere via a plug (figure 17) held in place by a washer (figure 18) and nut on the inside of the hemisphere. The bottom hemisphere had a drain plug which could be opened to determine whether there had been any leakage during testing. A cylindrical wooden plug (figure 19) was placed inside the assembly to mitigate the shock of implosion should failure occur.

Figure 20 shows test assembly Type 2. This test assembly is identical to test assembly Type 1, except that the cylinder ends are closed by flat steel bulkheads (figure 21) instead of titanium hemispheres.

Figure 22 shows test assembly Type 3 which uses NRaD Mod 1, Type 1 titanium end caps (figure 23) instead of the Type 2 end caps used in test assembly Type 2. Test assembly Types 2 and 3 are held together by four 1/2-inch tie rods (figure 24). Strain gage leads are passed through the feed through shown in figure 25. The force of implosion is mitigated by a cylindrical wooden plug (figure 26). Figure 27 shows a fully machined cylinder. Figure 28 is a fully machined cylinder with NRaD Mod 1, Type 2 end caps epoxy-bonded to it.

Pressure Testing

Pressure testing was performed in accordance with the test-plan/result summary shown in table 6. Strains were read at 1,000-psi intervals on the first pressurization for each cylinder. When cylinders were to be purposely taken to failure pressure, strains also were read during the second cycle. In some of the tests where the cylinder withstood all planned pressure testing, at least one end cap was removed using the end-cap removal fixture shown in figure 29.

The method of end-cap removal involves heating the cylinder end to be removed, which breaks down the epoxy, and then pulling the end cap off the cylinder. Adequate force can be applied to remove the end cap by using the mechanical advantage of turning nuts on the four 1/2-inch-diameter tie rods. After the end caps were removed, the cylinder was cleaned and taken to Sonic Testing and Engineering for pulse-echo ultrasonic inspection to determine the presence and extent of internal circumferential cracking.

The following are brief summaries of the pressure testing for each of the cylinders:

Cylinder 001 was proof tested to 16,000 psi and inspected for damage. Strains were read at 1,000-psi intervals and plotted (figure 30). After the proof test, the cylinder was subjected to pressure cycling at 16,000 psi to external pressure (this corresponds to and average maximum membrane stress of 233,010 psi). Testing was terminated after 581 cycles because the cylinder was leaking at one end. The cylinder was shipped back to NRaD, and the end caps were removed. Figure 31 shows the circumferential cracking on the bearing surface of the cylinder. Figure 32 is a full-scale C-scan of this end. Cracking was extensive (up to 5.7 inches in length). The C-scan of the other end (figure 33) shows almost no cracking.

This cylinder demonstrates that extensive internal circumferential cracking can exist in a cylinder without catastrophic failure. It is possible that the

leakage of water into the space between the ceramic and the titanium end-cap joint ring may have accelerated crack growth, a phenomenon known as street-corrosion cracking.

The extrusion of the epoxy on this cylinder convinced NRaD that the smooth ceramic surface was not bonding strongly to the epoxy and the titanium. It was decided that the ends of the remaining deliberable cylinders would be sandblasted to facilitate bonding. The first deliverable sandblasted cylinder was 006.

Cylinder 002 was proof tested to 16,000-psi external pressure. Strains were read and plotted (figure 34). The cylinder was inspected, and no damage was noted. The cylinder was then cycled at 16,000-psi external hydrostatic pressure when it failed on cycle number 337.

Cylinder 003 was proof tested to 13,000-psi external pressure. The strains were read and plotted (figure 35). Subsequently, the cylinder was cycled at 13,000 psi until failure on cycle number 1,379.

Cylinder 004 was proof tested to 9,000-psi external pressure. Strains were read and plotted (figure 36). The test plan called for cycling the cylinder 3,000 times to 9,000 psi. Testing was actually terminated after 3,008 cycles. The cylinder was shipped back to NRaD where one end-cap joint ring was removed and that end of the cylinder was sonically inspected. The pulse-echo ultrasonic inspection revealed no internal circumferential cracking.

Cylinder 005 was proof tested to 12,000-psi external pressure. Strains were read and plotted (figure 37). The cylinder was inspected for damage and then cycled to 12,000 psi until it failed on cycle number 743.

Cylinder 006 was the first cylinder with sandblasted ends to be tested. The cylinder was proof tested to 12,000 psi external pressure. Strains are plotted in figure 38. The cyclinder withstood 2,241 cycles to 12,000 psi without failure or visible damage. Testing was terminated because the test plan only called for 2,000 cycles. This cylinder was not ultrasonically inspected due to budgetary constraints.

Cylinder 007 was proof tested to 11,000-psi external hydrostatic pressure. Strains were plotted in figure 39. This cylinder withstood 3,010 cycles to 11,000 psi without visible damage. Testing was terminated because the test plan called for 3,000 cycles. This cylinder also was not ultrasonically inspected due to budgetary constraints.

Cylinder 008 was proof tested to 11,000 psi. No damage was noted. Strains are plotted in figure 40. The cylinder failed on the 1,665th pressurization to 11,000 psi.

Cylinder 009 was proof tested to 10,000 psi. Strains are plotted in figure 41. The cylinder was inspected for damage and then pressurized to failure which occurred at 22,600 psi. Strains to failure are plotted in figure 42.

Cylinder 010 was proof tested to 10,000 psi. Strains are plotted in figure 43. The cylinder was inspected, and no damage was noted. It then was pressurized to failure which occurred at 21,600 psi external hydrostatic pressure. Strains to failure are plotted in figure 44.

A summary of test plan and test results is shown in table 6.

TEST OBSERVATIONS/DISCUSSION

MATERIAL PROPERTIES

The measured material properties are shown in table 3. All material properties met or exceeded the material property requirements shown on the cylinder drawing (figure 9) with the exception of Weibull Modulus which was measured to be 11.1 with a low of 8.6 in cylinder 006 and a high of 20.4 in cylinder 010.

The average measured specific gravity was 3.27 gm/cc.

The mean Young's Modulus was 43,960,000 psi with a standard deviation of only 340,000 psi. Young's Modulus ranged from 43,500,000 psi to 44,690,000 psi. The average Poisson's Ratio was 0.26.

The mean compressive strength was measured to be 486,600 psi with a standard deviation of

17,900 psi. Flexural strength was measured to be 102,900 psi with a standard deviation of 5,300 psi.

The mean fracture toughness was measured to be 6.1 MPa•m$^{1/2}$ with a standard deviation of 0.2 MPa•m$^{1/2}$, a minimum value of 5.8 MPa•m$^{1/2}$, and a maximum measured value of 6.2 MPa•m$^{1/2}$.

STRAINS

Axial and hoop strains were measured and plotted for the proof cycle and in cylinders 009 and 010 for the pressurization to failure. Strain plots show that both the axial and the hoop strains remain within close range of each other circumferentially (standard deviation does not exceed 10 percent on axial strains and 7 percent on hoop strains) and remain linear up to within about 1,500 psi of failure, at which point the hoop strains diverge rapidly due to the buckling deformation of the cylinder (see figures 42 and 43). Table 5 summarizes strain readings at 10,000-psi external pressure. Strain measurements taken on the second pressurization to 10,000 psi in cylinders 009 and 010 show no significant difference in strain readings between the first and second cycle as was found in the silicon-carbide particulate-reinforced alumina ceramic (Lanxide composition 90-X-089). Therefore, silicon nitride does not appear to exhibit a compaction effect.

Young's Modulus and Poisson's Ratio were calculated for each cylinder using the simultaneous solution of the following equations:

A thick-wall stress equation from reference 9 was used to compute the expected stress at 10,000-psi external psi on the ID of the cylinder:

$$\sigma_{\text{axial}} = \frac{-qa^2}{a^2 - b^2}$$

$$\sigma_{\text{hoop}} = \frac{-q2a^2}{a^2 - b^2}$$

where q = external pressure
a = outer radius
b = inner radius

Then, the following two equations were solved simultaneously for compressive modulus and Poisson's Ratio:

$$\epsilon_{\text{axial}} = \frac{1}{E}(\sigma_{\text{axial}} - \gamma\sigma_{\text{hoop}})$$

$$\epsilon_{\text{hoop}} = \frac{1}{E}(\sigma_{\text{hoop}} - \gamma\sigma_{\text{axial}})$$

where E = compressive (Young's) modulus
γ = Poisson's Ratio

The average calculated Poisson's Ratio was found to be 0.275. This value, with its standard deviation of 0.006, is not within range of the measured value of 0.262 with standard deviation of 0.006. The mean calculated Young's Modulus was 45.25 Msi with a standard deviation of 1.11 Msi; this exceeded the measured Young's Modulus of 43.96 Msi.

STRUCTURAL PERFORMANCE

The structural performance of the ten silicon nitride cylinders tested was very good. None of the cylinders failed on the first (proof) cycle. Proof pressures ranged from 10,000 psi to 16,000 psi. Critical collapse pressure exceeded 21,600 psi. The good structural performance is more impressive when one considers the number of defects detected in the cylinders during pre-service ultrasonic inspection.

CYCLIC FATIGUE LIFE

Cyclic fatigue life data shows that the silicon-nitride cylinders had poor (low) fatigue life at a high stress level (190,000 psi membrane stress). Testing showed that fatigue life improved significantly when membrane stress levels were below 175,000 psi. This is demonstrated by cylinders 004, 006, 007, and 008.

The sandblasting of the cylinder ends seemed to have a dramatic effect on the cyclic performance of the cylinders. It can be stated that cylinders 006 through 008 performed significantly better than cylinders 001 through 005. The difference is especially noteworthy between cylinders 005 and 006. Cylinder 006 had sand-blasted ends, while cylinder 005 did not. When cycled at the same level of stress (approximately 175,000 psi), cylinder 005 failed after 743 cycles while cylinder 005 exceeded 2,241 cycles. These two cylinders did not differ significantly in the number of internal defects, size,

or in material properties (cylinder 006 had lower flexural strength but higher fracture toughness).

The very poor performance at a high stress level (233,000 psi) of cylinders 001 and 002 show that cyclic fatigue life degrades quickly with increased levels of stress. However, the excellent performance of cylinders such as cylinder 004, which withstood 3,008 cycles to 9,000 psi (131,000 psi) and showed no signs of internal circumferential cracking during pulse-echo ultrasonic inspection, shows that the material performs extremely well at the intended design stress level of 131,000 psi at an ocean depth of 20,000 feet.

Silicon nitride still presents some level of unpredictability in cyclic fatigue life as evidenced by cylinders 007 and 008. These cylinders both had sandblasted ends and were tested to the same level of stress (160,000 psi), yet their performances differed dramatically, with cylinder 007 withstanding 3,010 cycles and cylinder 008 failing on cycle number 1,665.

CONCLUSIONS

The objectives of this study were met:

1. Evaluate CERCOM's ability to fabricate 12-inch-OD by 18-inch-long Si_3N_4 cylinders. Nondestructively inspect the cylinders to determine whether this ceramic composition can be fabricated relatively free of defects.

   CERCOM was able to fabricate the cylinders, but not without difficulty. The difficulties appeared to be related to logistics, rather than technical feasibility problems. CERCOM had numerous problems pressing quality parts, leading to a high reject rate and eventually forcing CERCOM to make parts with modified dimensions to meet NRaD's delivery requirements. The fact that the first five cylinders delivered met dimensional requirements and appeared to have the highest quality (in terms of number and size of defects detected) demonstrated that the difficulties were not of a technical nature.

2. Determine the structural performance of $S_{i3}N_4$ under external hydrostatic pressure loading.

   The structural performance parameters investigated include critical collapse pressure and cyclic fatigue life.

   The structural performance of the silicon nitride cylinders was excellent. None of the cylinders failed on proof test, even with the numerous defects found in some of the cylinders. The critical collapse pressure exceeded the design pressure (9,000 psi) by more than a factor of two. The structural performance of silicon nitride can be considered predictable.

   The cyclic performance of the silicon nitride cylinders is not as predictable as would be desired. However, the conclusion can be drawn that the cyclic life can exceed 1,000 cycles at stress levels below 175,000 psi. Cyclic performance degrades significantly at stress levels above 175,000 psi. Evidence indicates that cylinders with ends sandblasted before end-cap joint rings are epoxy-bonded to them perform better cyclically than those without sandblasted ends. The data generated by cyclic pressurization of the cylinders was not sufficient to draw any conclusions about the relationship between any one material property and cyclic performance.

3. Compare the performance of the SRBSN silicon nitride composition against the performance of the baseline composition, WESGO's AL-600 96-percent alumina ceramic (reference 4).

   Table 7 compares the cyclic fatigue performance of PSX silicon nitride cylinders and AL-600 cylinders subjected to external pressure cycles. This table indicates that the structural performance of PSX silicon nitride is comparable to AL-600. AL-600 cylinders showed a clear trend of decreased fatigue life as the peak external pressure of each cycle was increased. The relationship between cyclic life and peak external pressure for each cycle was not as defined for the PSX silicon nitride cylinders tested for this report. The more predictable behavior of the AL-600 cylinders can be attributed to the WESGO's substantial prior experience in fabricating large hull shapes from their alumina-ceramic com-

positions. On the other hand, the silicon nitride cylinders that were evaluated represented the largest parts fabricated by CERCOM using their PSX composition, and, consequently, some manufacturing difficulties were encountered.

Table 8 contains the material properties of CERCOM's PSX silicon nitride and WESGO's AL-600 96-percent alumina ceramic. The properties of WESGO's ZTA ceramic (reference 2) and Lanxide's 90-X-089 $SiC/Al_2O_3/Al$ composition (reference 3) are included for comparison. As the table shows, Si_3N_4 has better properties than AL-600 96-percent alumina ceramic with the exception of compressive modulus and Weibull Modulus. Ninety-six percent alumina ceramic's higher elastic modulus turns out to be important as designs are often driven by buckling requirements. The difference in Weibull Modulus could account for the difference in the predictability of the material during cyclic testing.

It should be noted that Si_3N_4 has the highest compressive strength, the highest flexural strength, and the lowest specific gravity of the four compositions evaluated as part of the program for the application of ceramic to underwater pressure housings. Figure 45 shows W/D vs. depth curves for Si_3N_4 and 96-percent Al_2O_3. The example is for a housing having a length-to-diameter ratio of 1.5. The maximum design stress level for both materials is chosen for a cyclic fatigue life of 1,000 cycles to design depth. Although the curves change for different length-to-diameter ratios, the general trend remains the same.

RECOMMENDATIONS

The following recommendations are made based on the testing of the ten CERCOM PSX Si_3N_4 12-inch-OD by 18-inch-long by 0.412-inch-thick cylinders.

1. CERCOM composition PSX silicon nitride is recommended for use in the construction of external pressure housings of up to 12-inch-OD by 18-inch-long measurements. Use of the composition for cylinders with dimensions greater than this is recommended only after a thorough test-and-evaluation program.

2. If CERCOM's PSX silicon nitride composition is to be used in an underwater external pressure application and 1,000 cycles to design depth are expected, then the design should be such that maximum nominal membrane stress does not exceed 160,000 psi. The engineering properties to be used for engineering calculations and to be called out on the engineering drawing should be:

Compressive strength:	460,000 psi
Compressive Modulus:	43.9 Msi
Flexural Strength:	100,000 psi
Fracture Toughness:	6.0 ksi ($in^{1/2}$)
Specific Gravity:	3.275 g/cc
Poisson's Ratio:	0.26

   Standard finite-element analysis and buckling analysis can be used to analyze pressure-housing designs using CERCOM's PSX silicon nitride.

   Furthermore, the cylinder assembly design should incorporate Mod 1, Type 2 end-cap joint rings bonded in accordance with note 4 of figure 9 to a ceramic surface which has been roughened by sandblasting on the OD and ID circumferential surfaces of the part.

3. Prior to putting the cylindrical assembly together, the ceramic cylinder should be inspected ultrasonically. A pulse-echo ultrasonic inspection using a 3/8-inch diameter, 3-inch focal length, 10-MHz transducer is recommended. The circumferential scanning interval should be 0.010 inch.

4. Cylinders should be inspected by an ultrasonic method for internal circumferential cracks every 100 dives to 75 percent or more of design depth. A handheld thickness-detector unit may be sufficient to perform this inspection. Detection of internal cracks extending beyond the titanium end-cap joint rings should signal the removal of that ceramic cylinder from service.

5. Because silicon nitride shows promise for future application to housings for underwater service, it is recommended that the fabrication process be scaled up to 20-inch-OD by 30-inch-long cylinder sizes.

REFERENCES

1. Kurkchubasche, R. R., R. P. Johnson, J. D. Stachiw. 1993. “Application of Ceramics to Large Housings for Underwater Vehicles: Program Outline,” NRaD TD 2585 (Oct) NCCOSC RDT&E Division, San Diego, CA.
2. Johnson, R. P., R. R. Kurkchubasche, J. D. Stachiw. 1993. “Structural Performance of Cylindrical Pressure Housings of Different Ceramic Compositions Under External Pressure Loading: Part II—Zirconia Toughened Alumina Ceramic,” NRaD TR 1593 (Dec) NCCOSC RDT&E Division, San Diego, CA.
3. Kurkchubasche, R. R., R. P. Johnson, J. D. Stachiw. 1993. “Structural Performance of Cylindrical Pressure Housings of Different Ceramic Compositions Under External Pressure Loading: Part IV—Silicon Carbide Particulate Reinforced Alumina Ceramic,” NRaD TR 1594 (Dec) NCCOSC RDT&E Division, San Diego, CA.
4. Johnson, R. P., R. R. Kurkchubasche, J. D. Stachiw. 1993. “Structural Performance of Cylindrical Pressure Housings of Different Ceramic Compositions Under External Pressure Loading: Part I—Isostatically Pressed Alumina Ceramic,” NRaD TR 1590 (Aug) NCCOSC RDT&E Division, San Diego, CA.
5. Stachiw, J. D. 1993. “Exploratory Evaluation of Alumina Ceramic Housings for Deep Submergence Service—Third Generation Housings,” NRaD TR 1314 (Jun) NCCOSC RDT&E Division, San Diego, CA.
6. Stachiw, J. D. 1990. “Exploratory Evaluation of Alumina Ceramic Cylindrical Housings for Deep Submergence Service—Fourth Generation Housings,” NOSC TR 1355 (Jun) Naval Ocean Systems Center, San Diego, CA.
7. Kurkchubasche, R. R., R. P. Johnson, J. D. Stachiw. 1993. “Evaluation of ND Testing Techniques for Quality Control of Alumina Ceramic Housing Components,” NRaD TR 1588 (Sep) NCCOSC RDT&E Division, San Diego, CA.
8. Kurkchubasche, R. R. 1993. “Non-destructive Evaluation Techniques for Deep Submergence Housing Components Fabricated from Alumina Ceramic,” Marine Technology Society Conference Proceedings, 1993.
9. Young, Warren C. 1989. “Roark’s Formulas for Stress and Strains, Sixth Edition,” McGraw-Hill Company.

GLOSSARY

alumina	aluminum oxide
ASTM	American Society for Testing of Materials
FEA	finite element analysis
FEM	finite element models
Modulus of Rupture	flexural strength
ID	inside diameter
L	Length
L/OD	length-to-outer-diameter ratio
MOR	modulus of rupture
NDE	nondestructive evaluation
OD	outside diameter
PS	pressureless sintering
PSX	CERCOM's pressureless, sintered grade of Si_3N_4
SF	safety factor (factor of safety)
SSN	sintered silicon nitride
specific strength	strength-to-density ratio
SRBSN	sintered reaction-bonded silicon nitride
t	thickness
t/OD	thickness-to-outer-diameter ratio
UUV	unmanned underwater vehicle
W/D	weight to displacement
ZTA	zirconia-toughened alumina

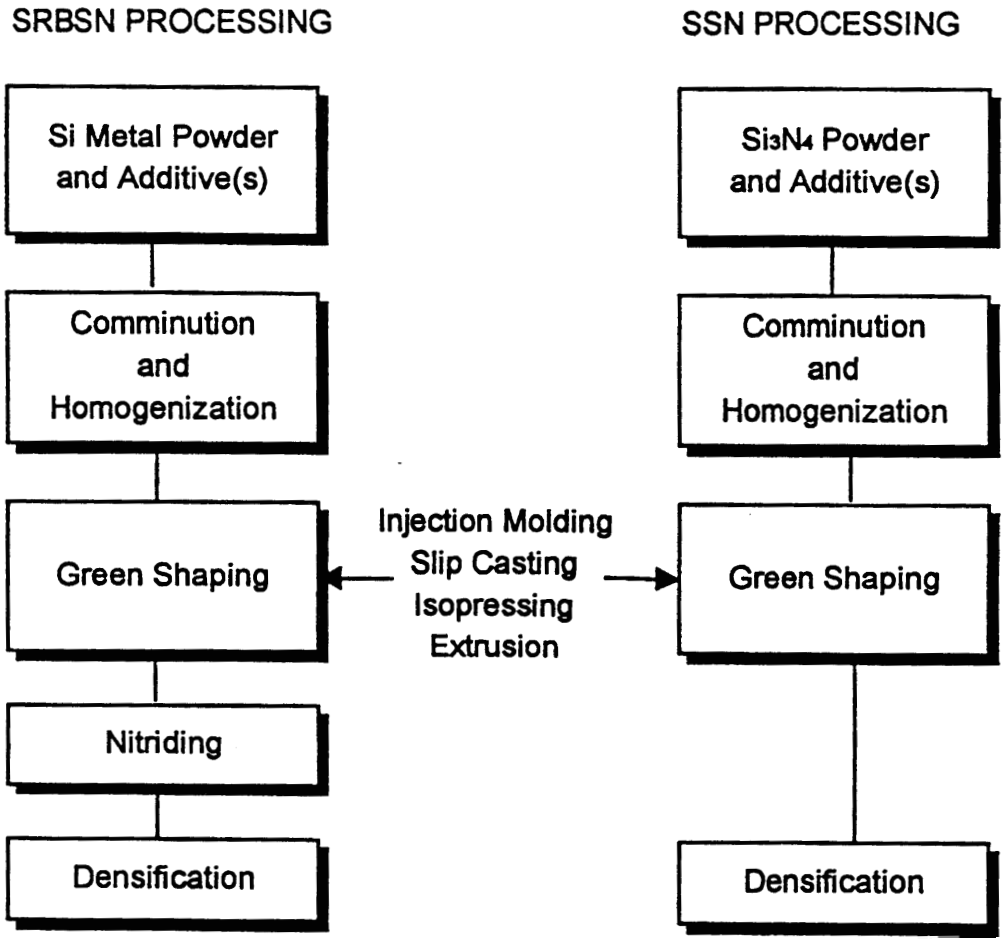

Figure 1. Process flow diagram for SRBSN and SSN fabrication.

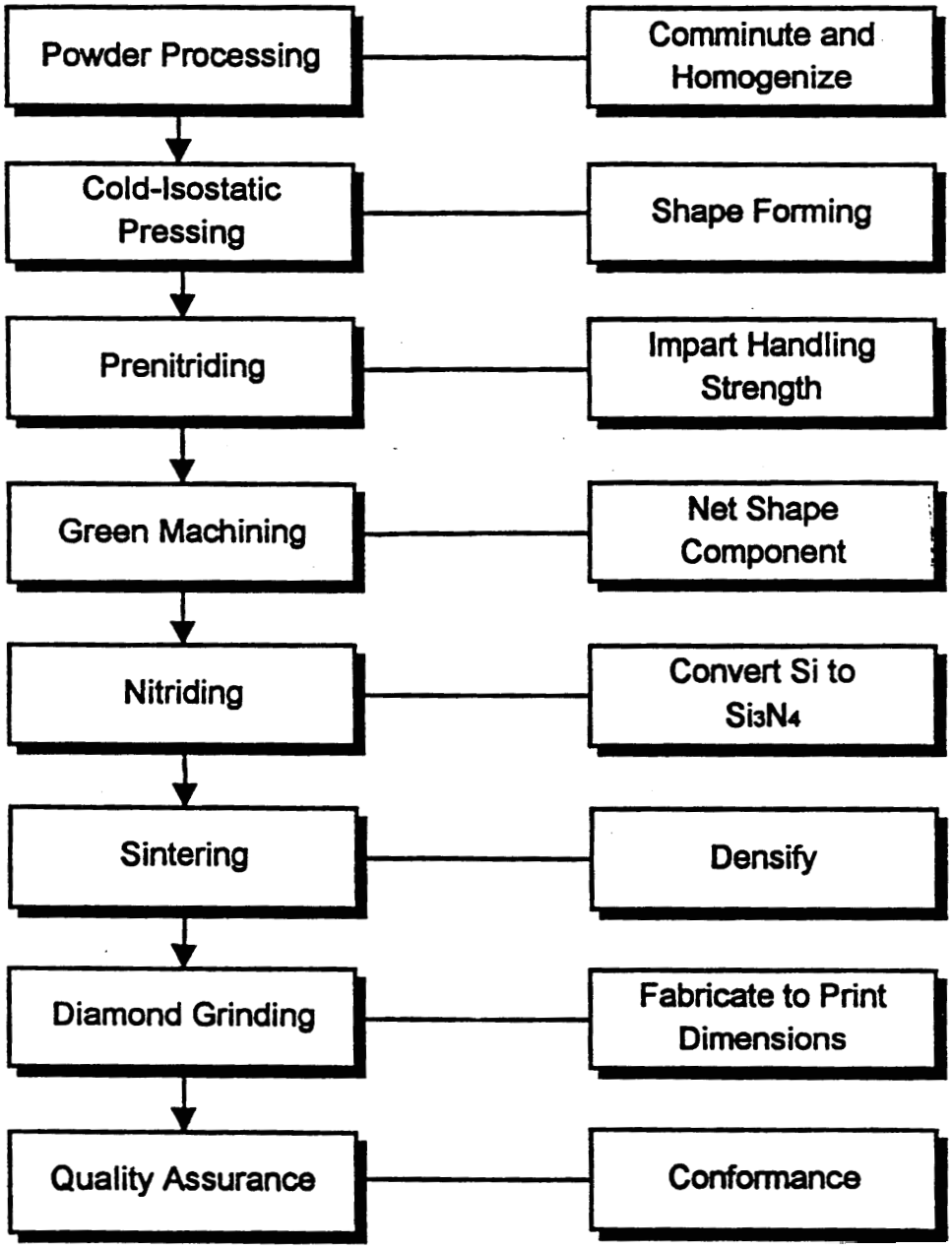

Figure 2. Fabrication process for PSX.

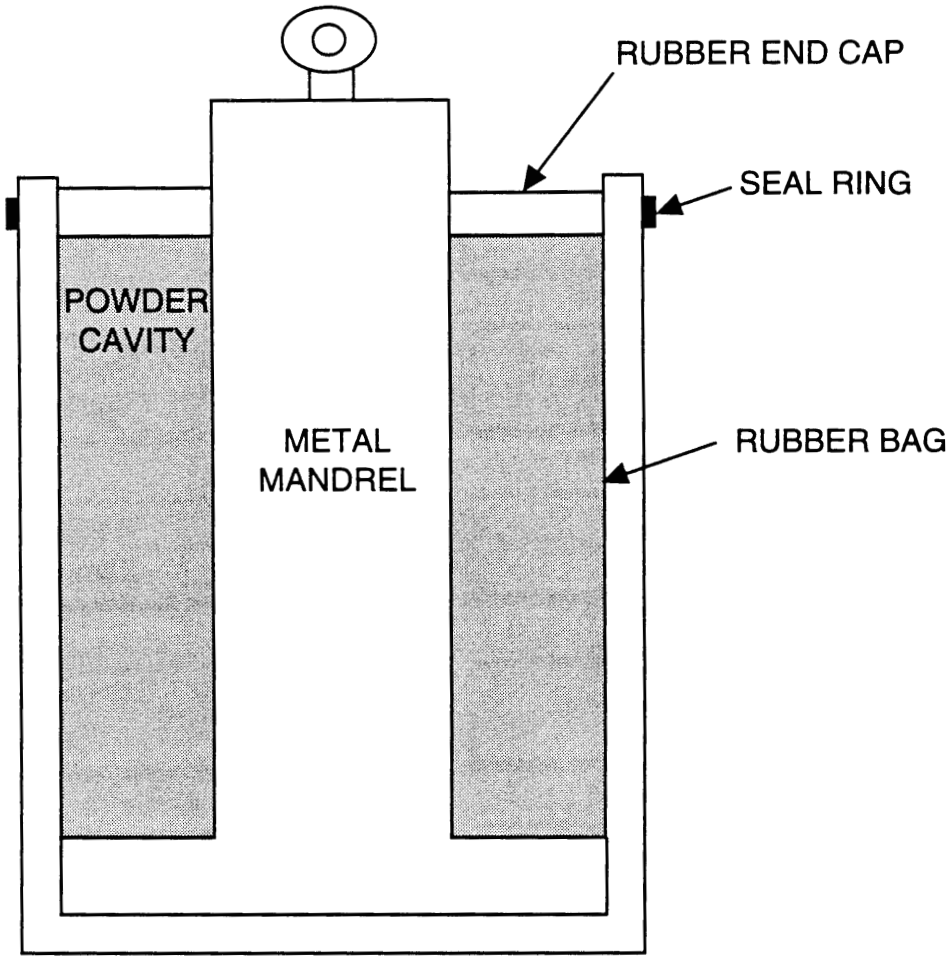

Figure 3. Schematic of cold isostatic-pressing tooling set.

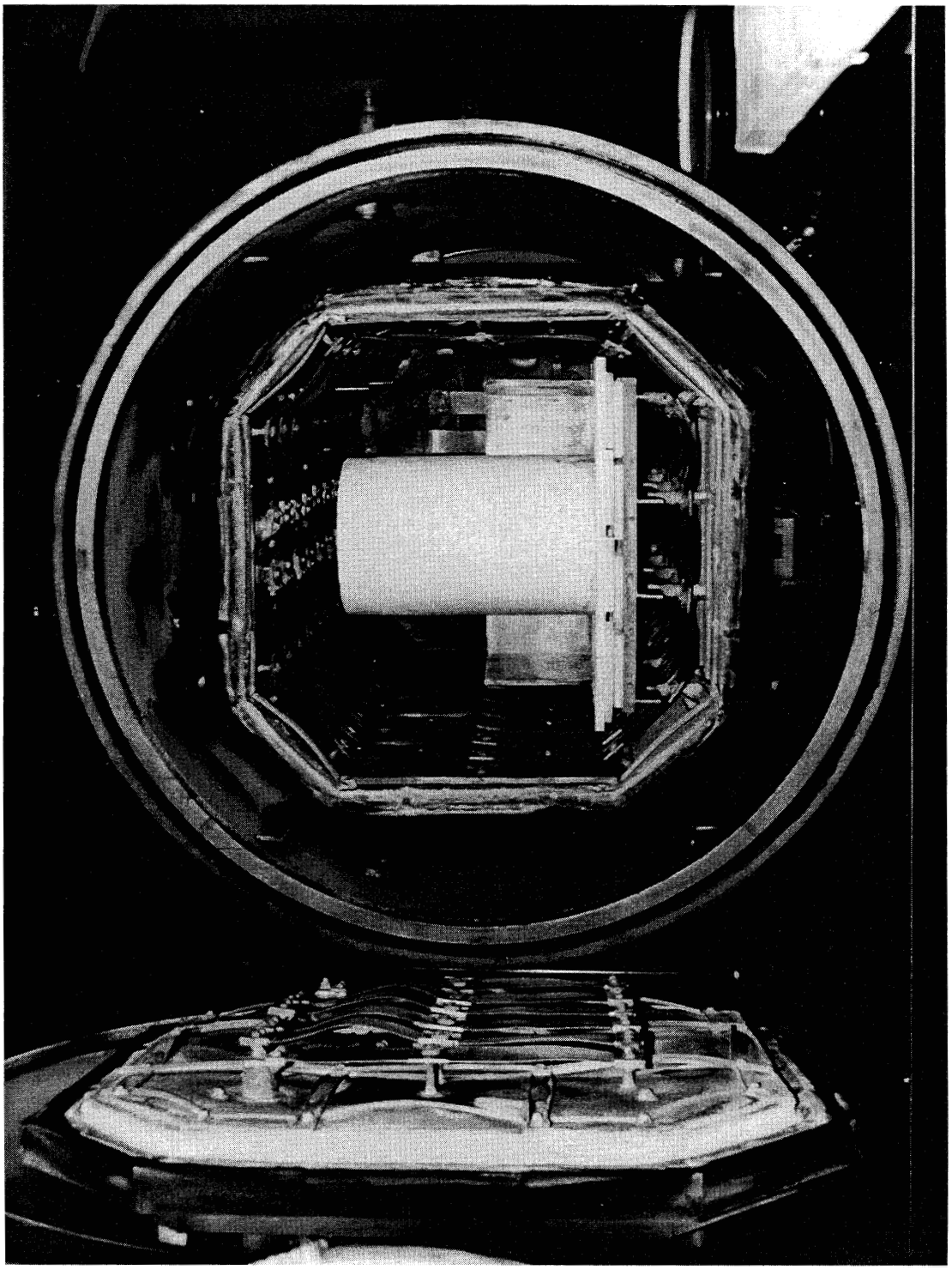

Figure 4. Cold-walled, vacuum-nitriding furnace shown with nitrided cylinder.

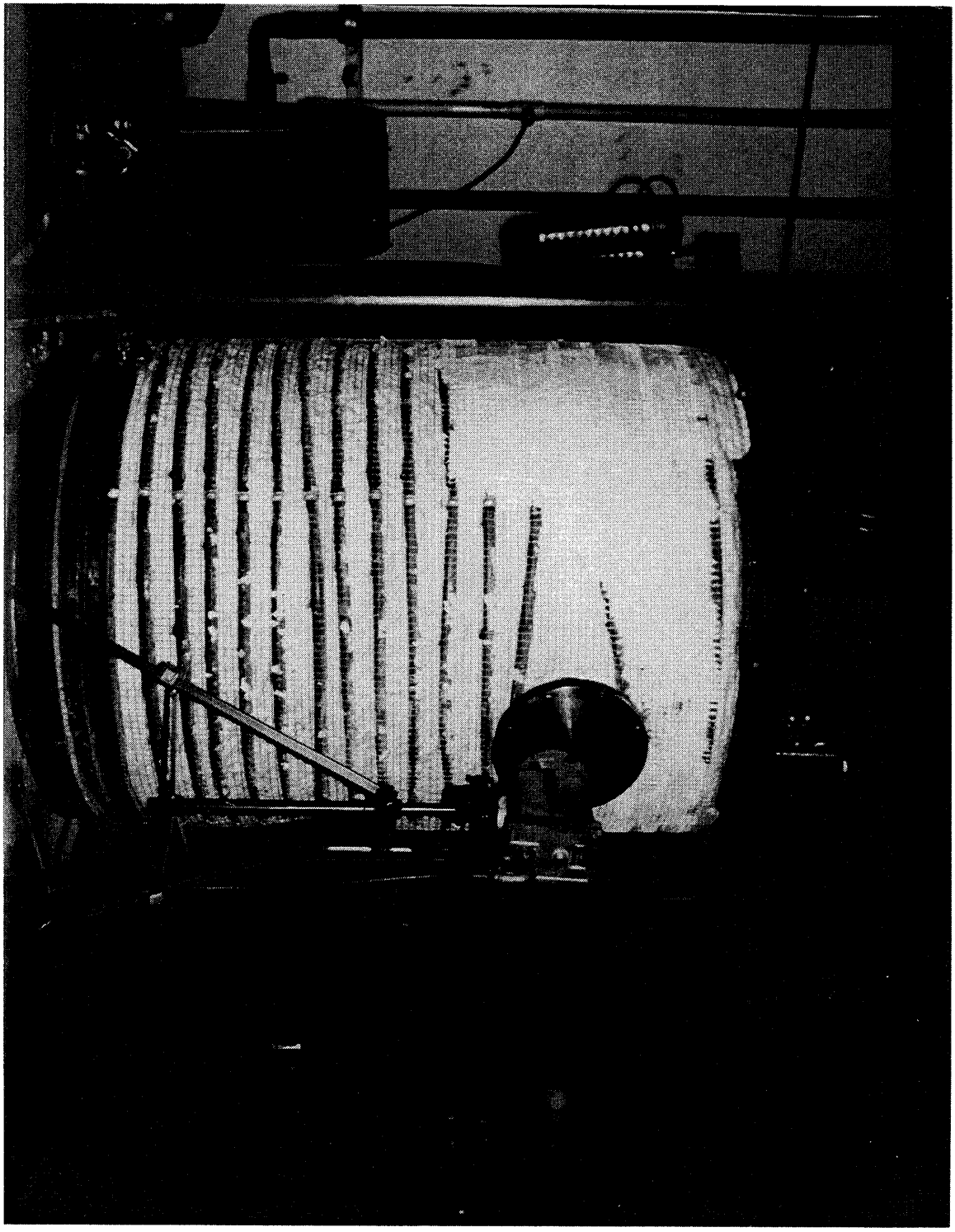

Figure 5. CERCOM's graphite-based (2200 degrees C) sintering furnace used for densifying Si_3N_4.

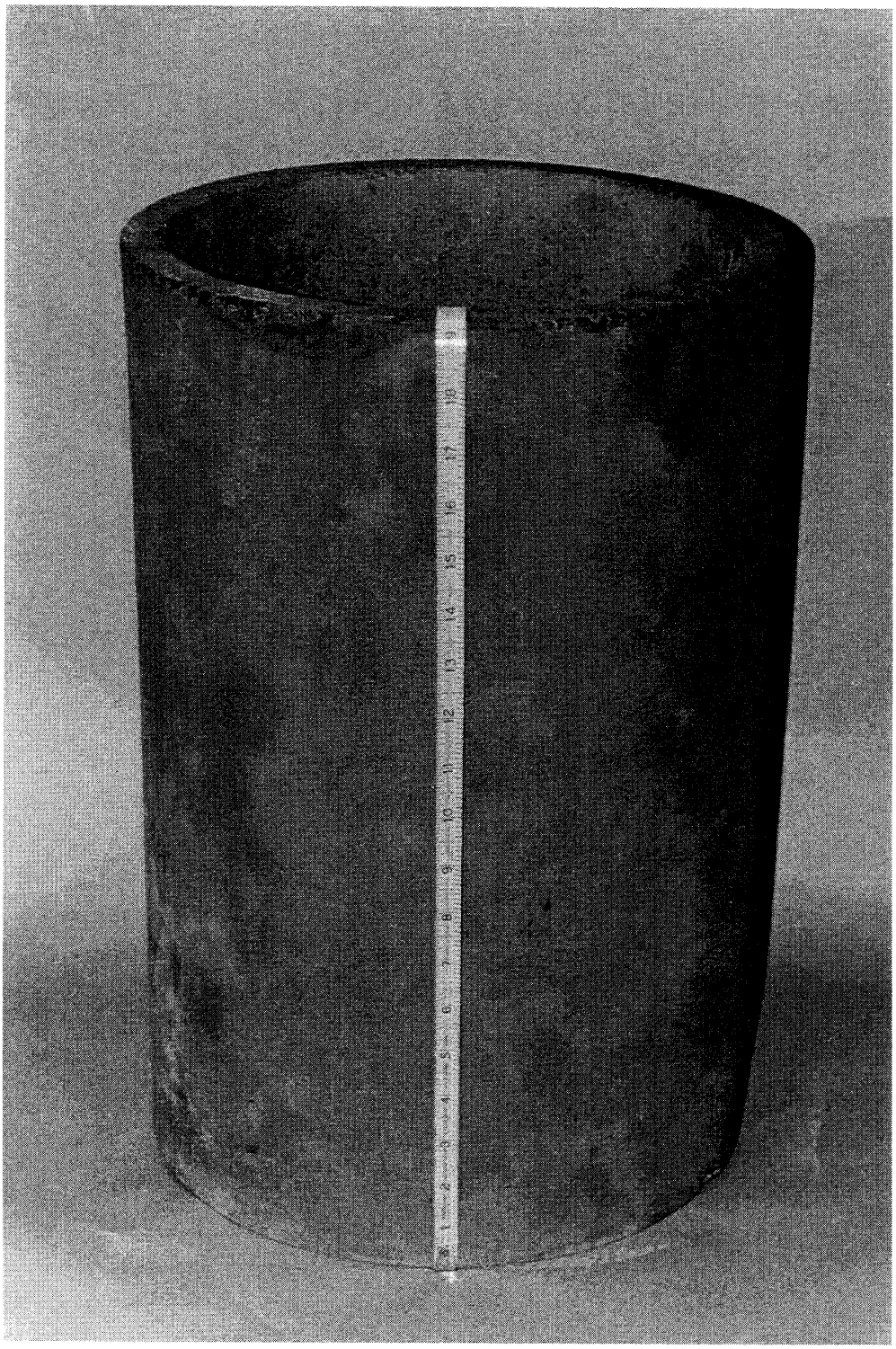

Figure 6. Sintered Si_3N_4 cylinder prior to grinding.

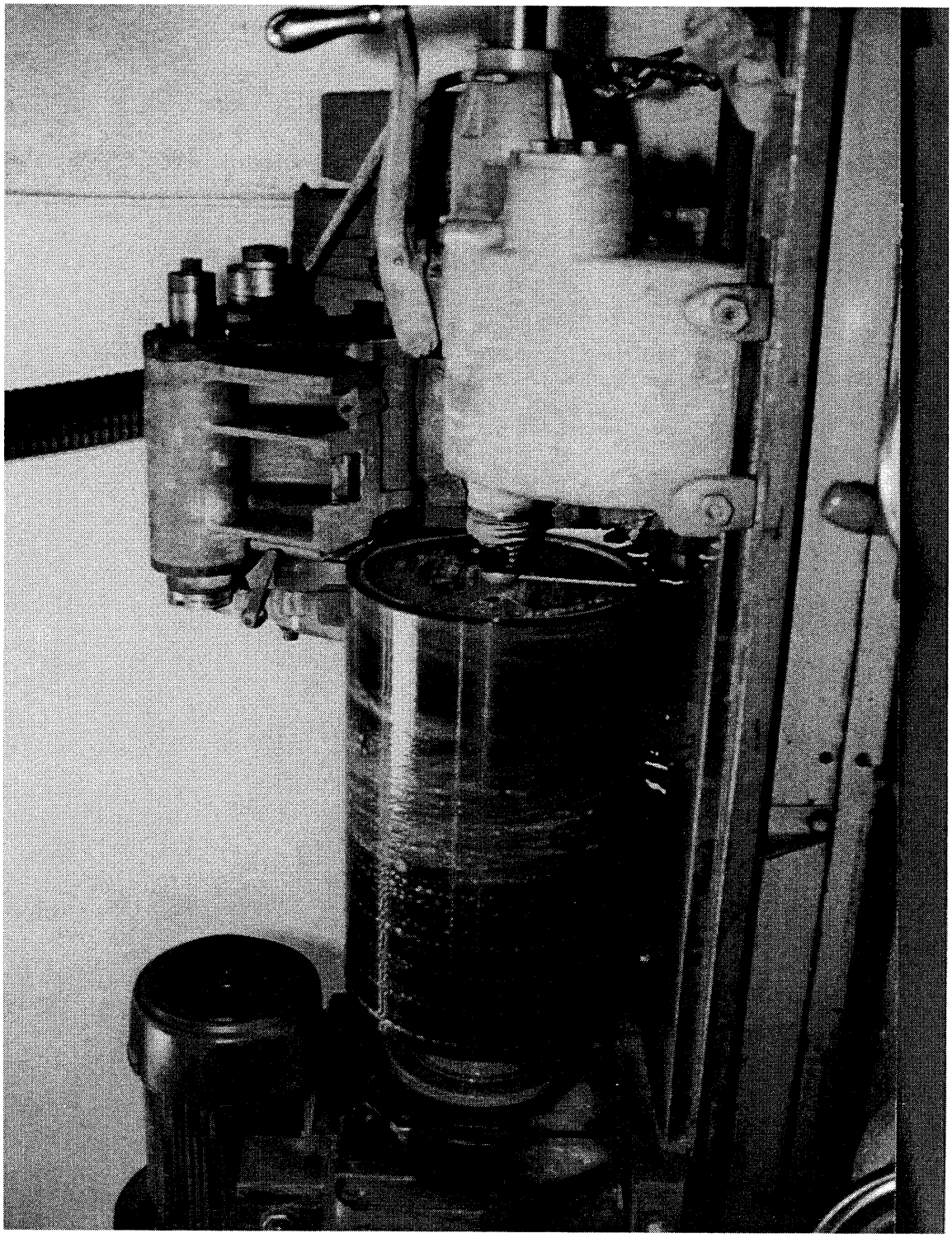

Figure 7. Diamond grinding of fully densified Si_3N_4 cylinder.

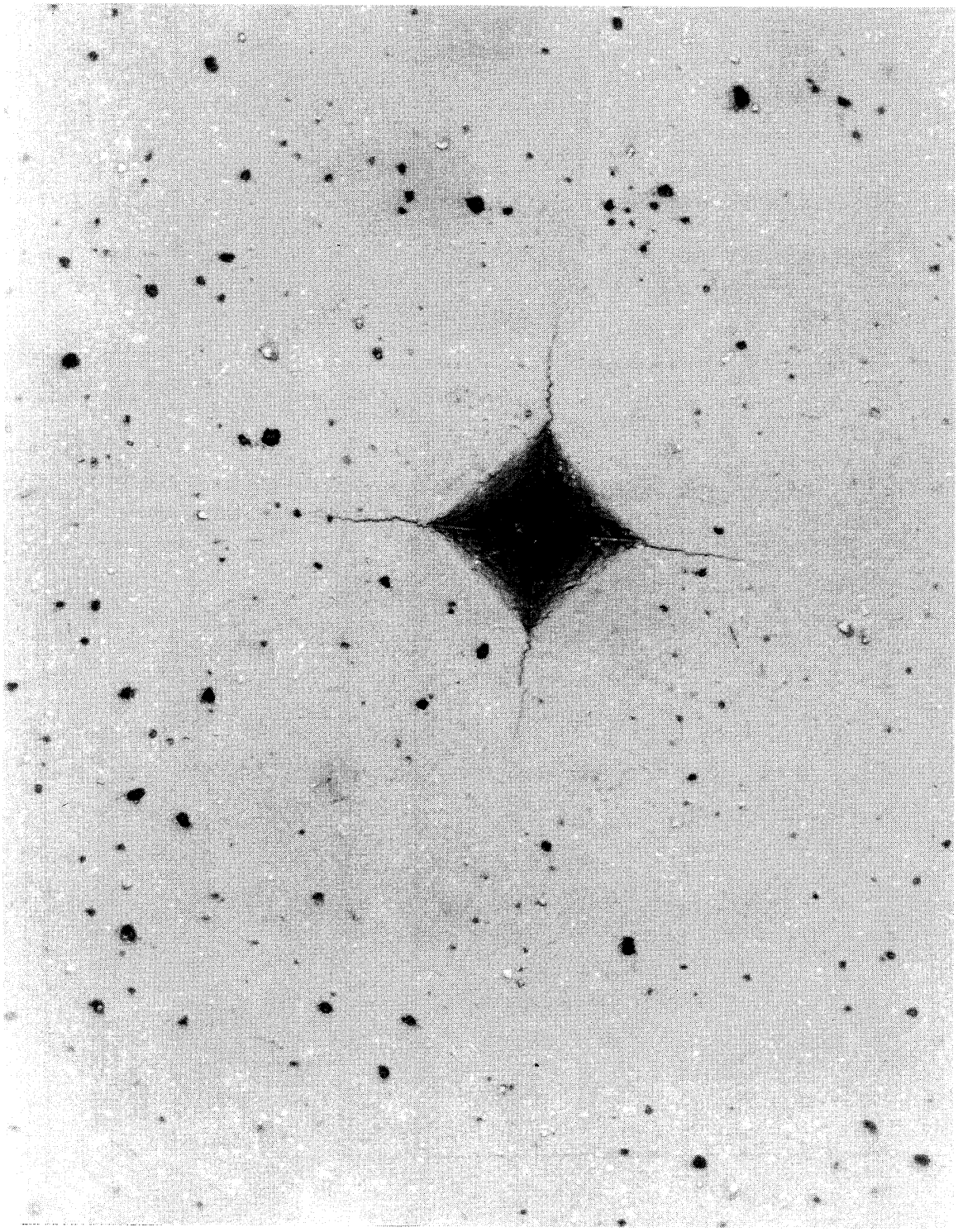

Figure 8. Typical Vikers indentation for measuring fracture toughness.

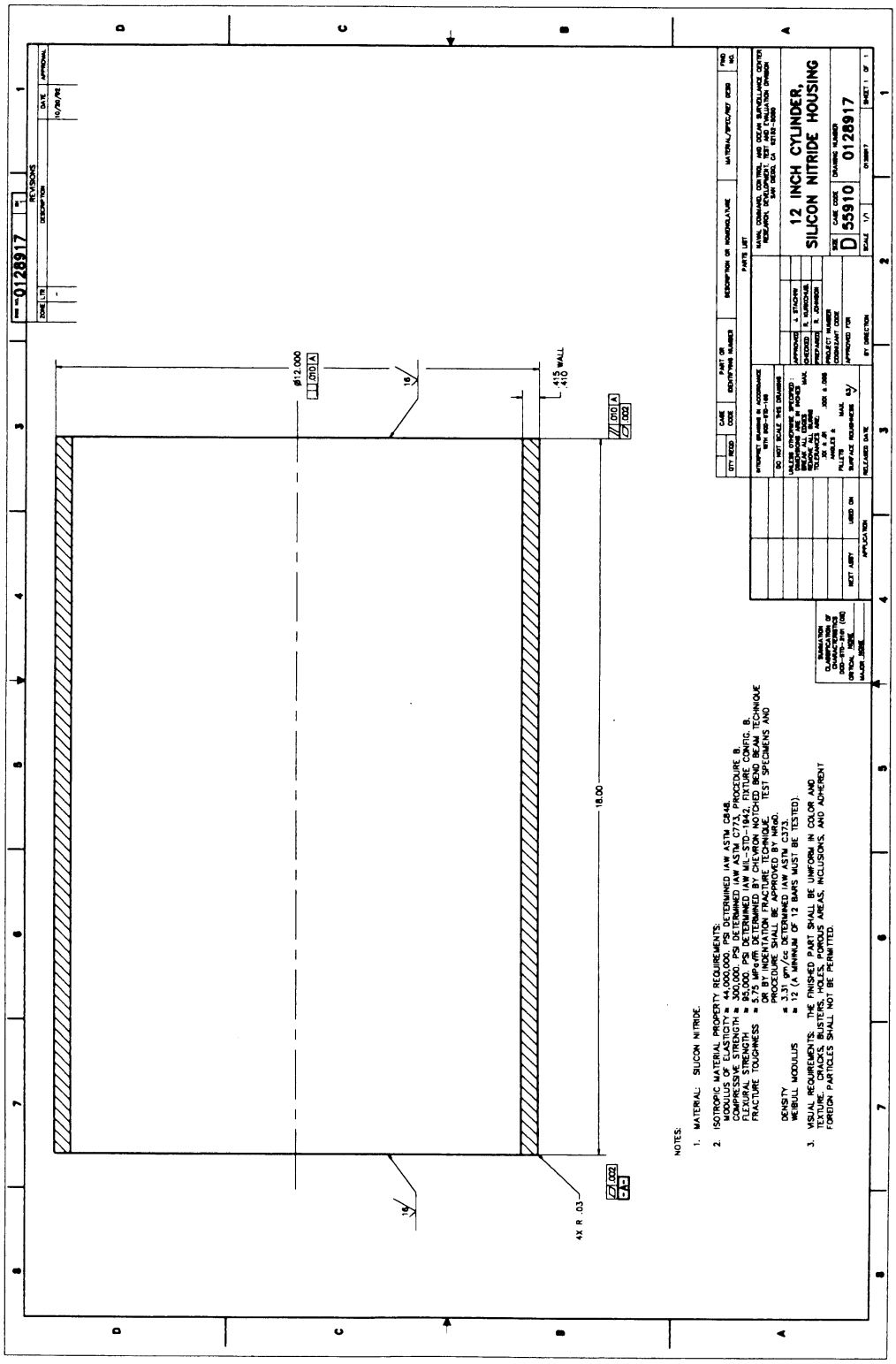

Figure 9. Engineering drawing for 12-inch-OD by 18-inch-long Si_3N_4 cylinder.

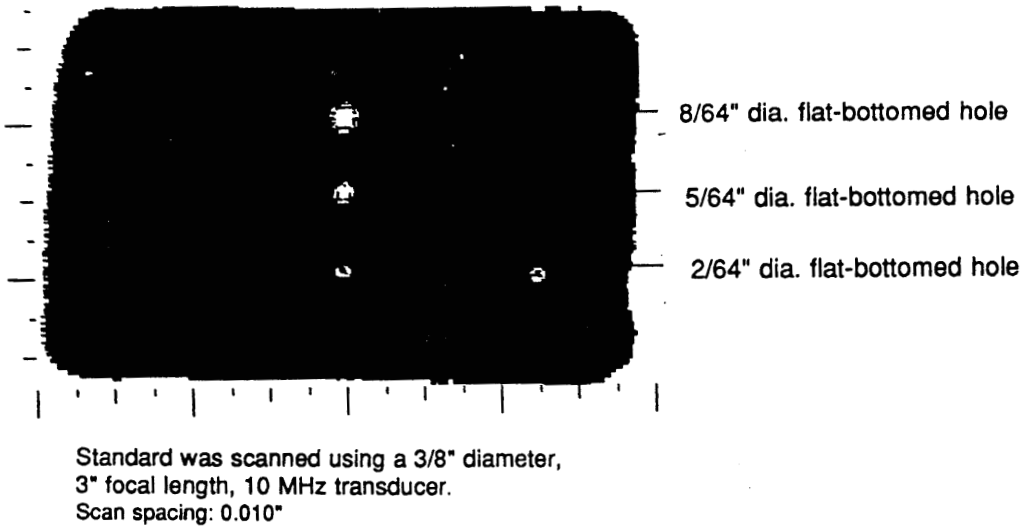

Figure 10. Pulse-echo C-scan of Si3N4 ceramic calibration standard used for inspection of deliverable components.

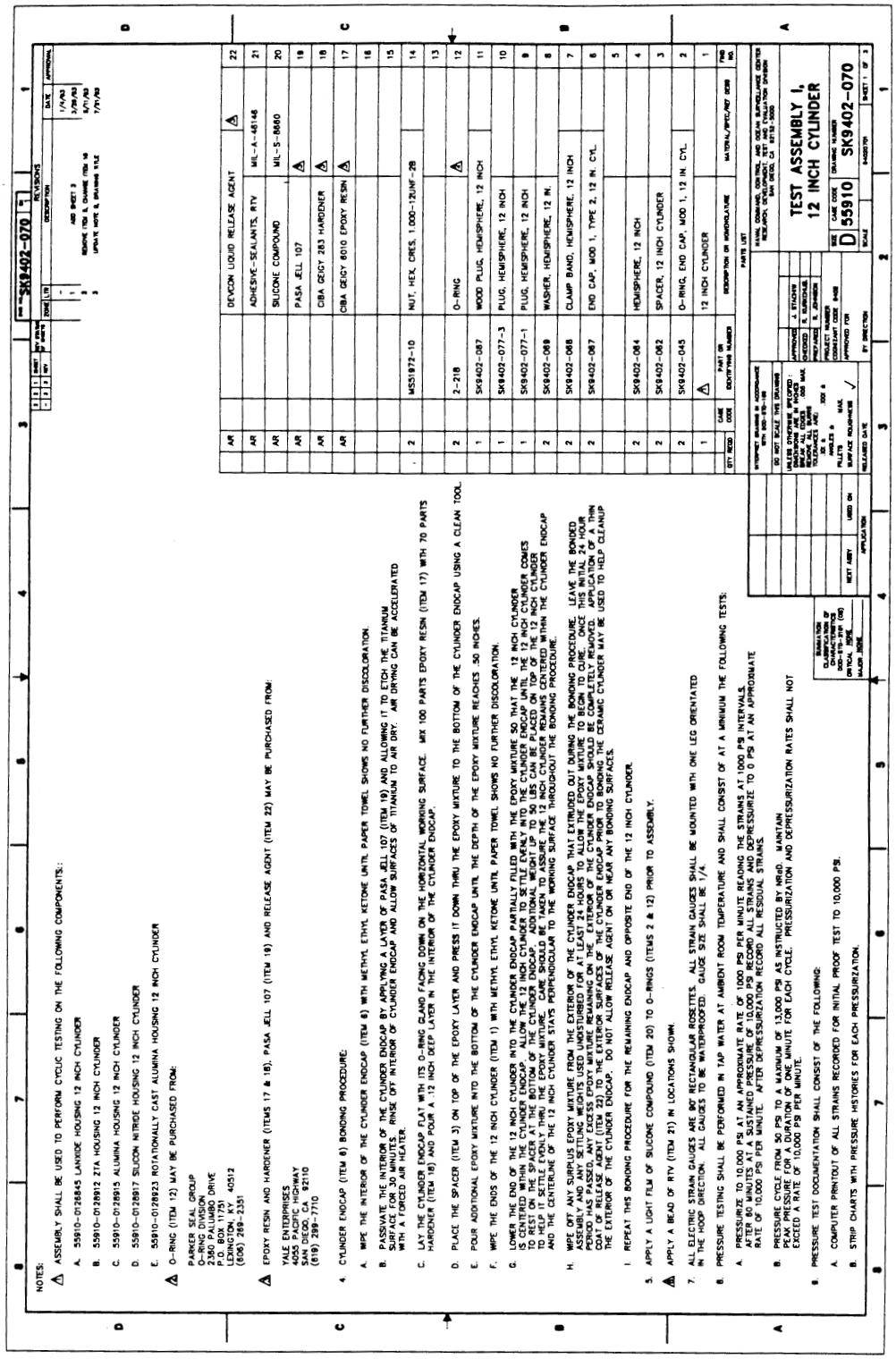

Figure 11. 12-inch cylinder test assembly, Type 1 configuration, Sheet 1.

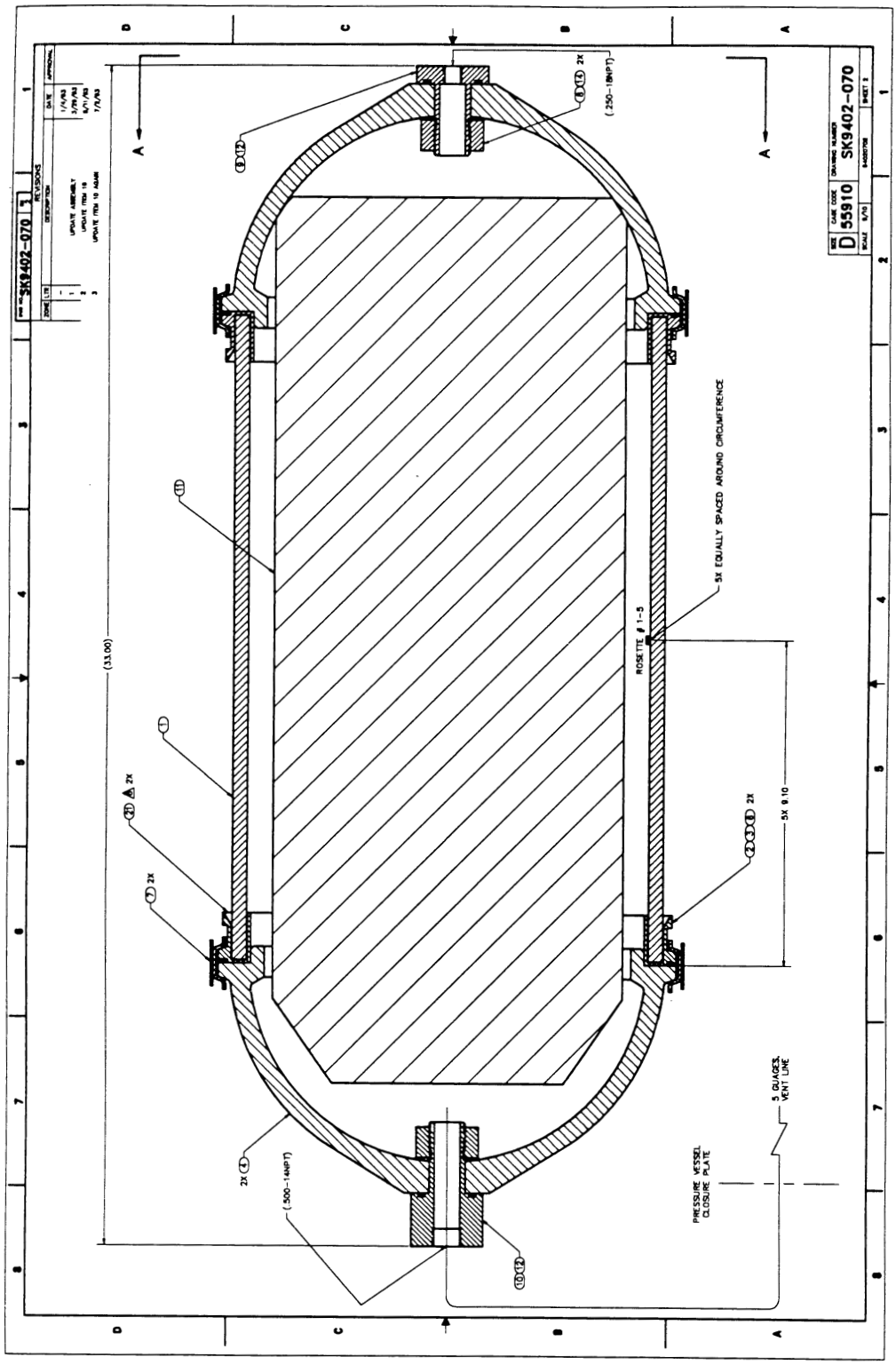

Figure 11. 12-inch cylinder test assembly, Type 1 configuration, Sheet 2.

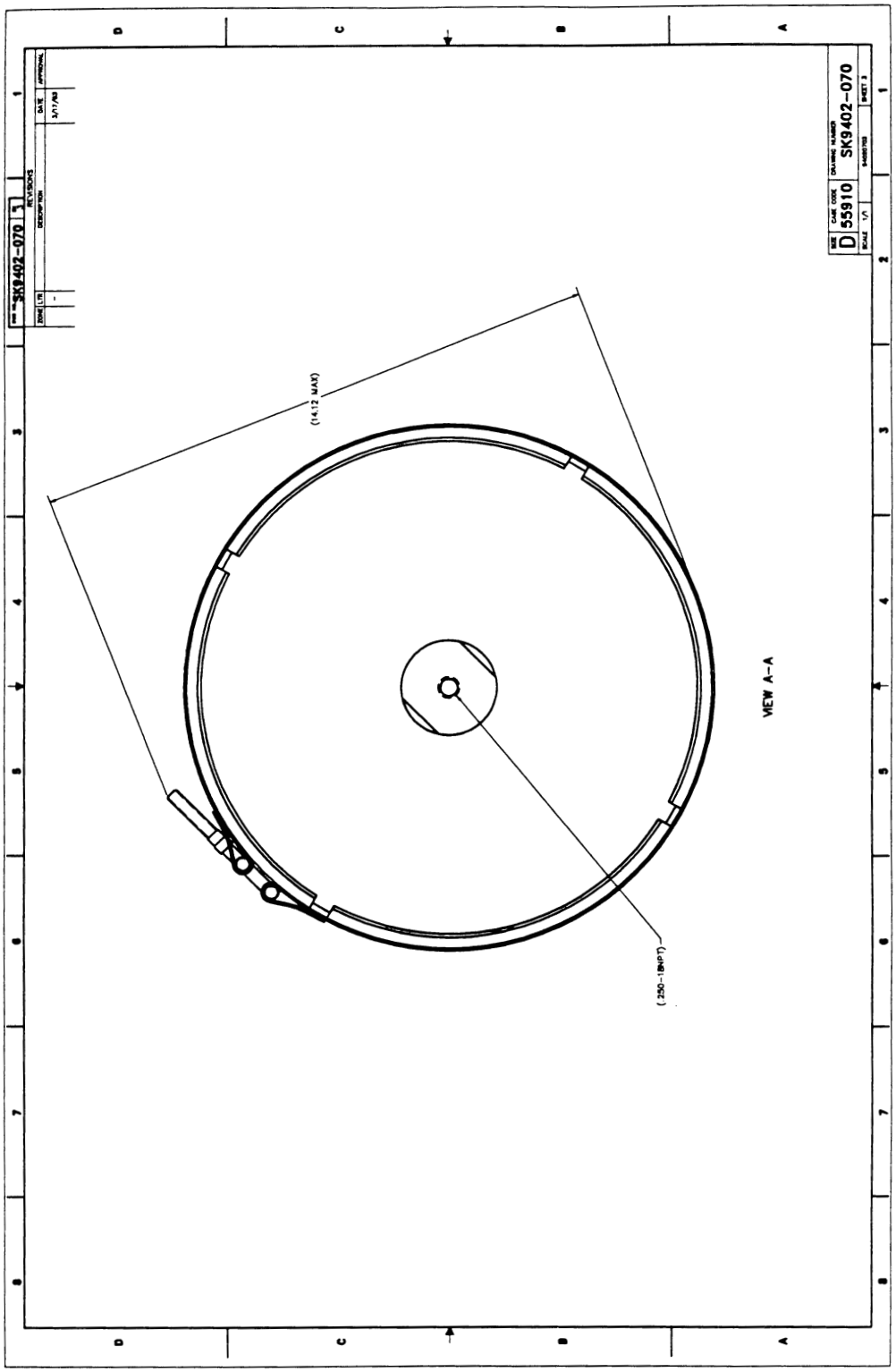

Figure 11. 12-inch cylinder test assembly, Type 1 configuration, Sheet 3.

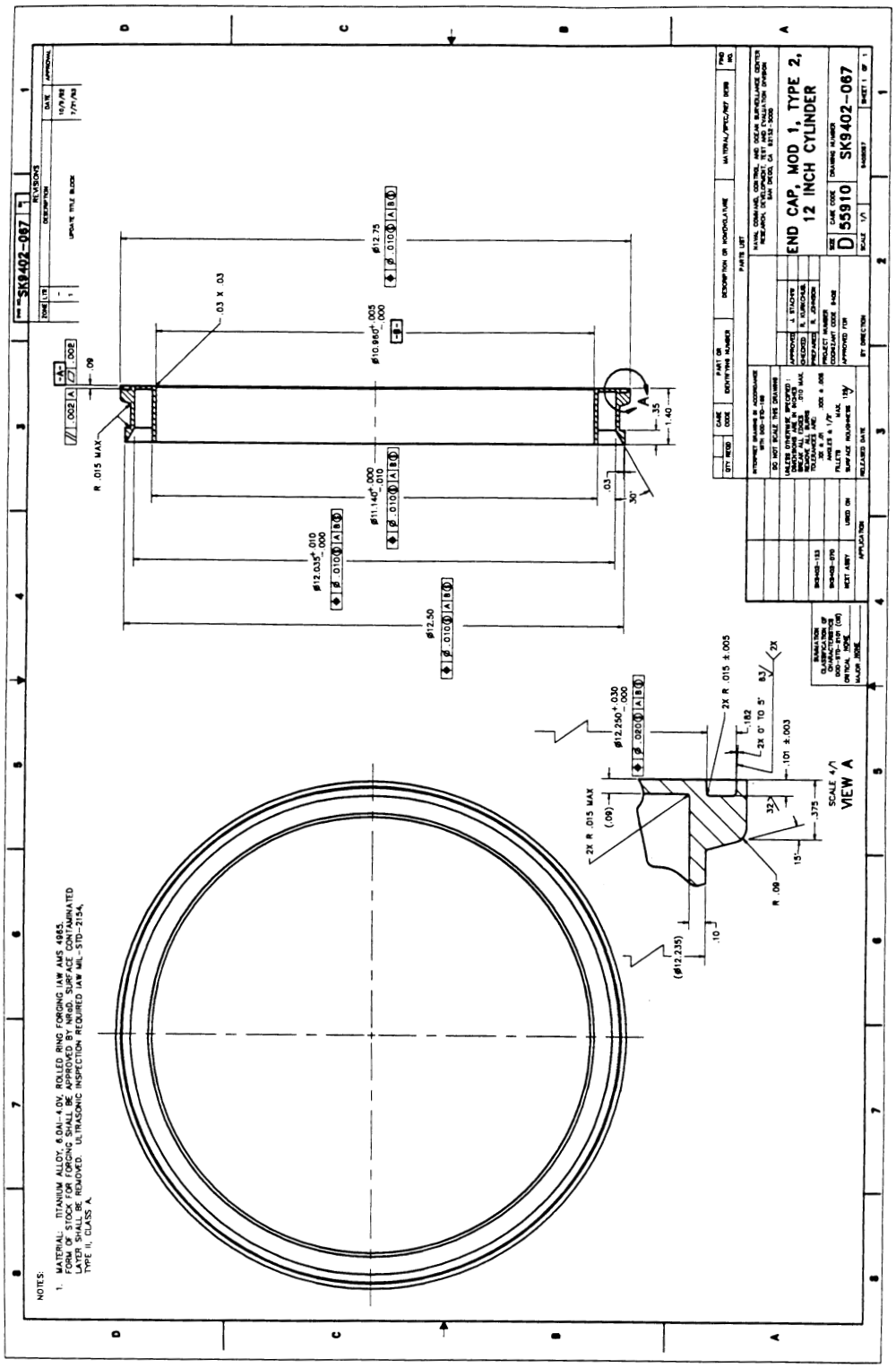

Figure 12. 12-inch cylinder Mod 1, Type 2 end-cap joint ring.

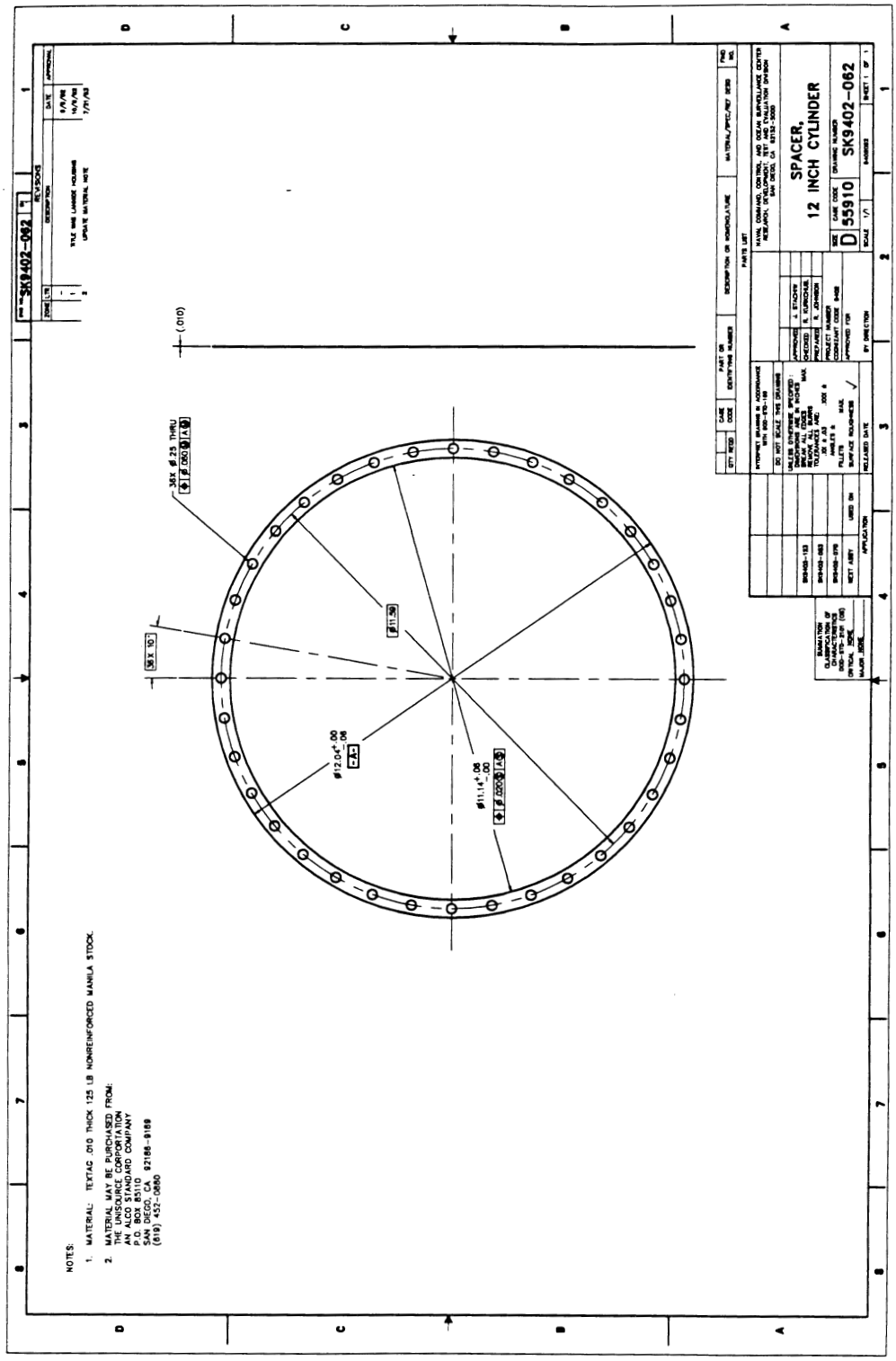

Figure 13. 12-inch cylinder spacer.

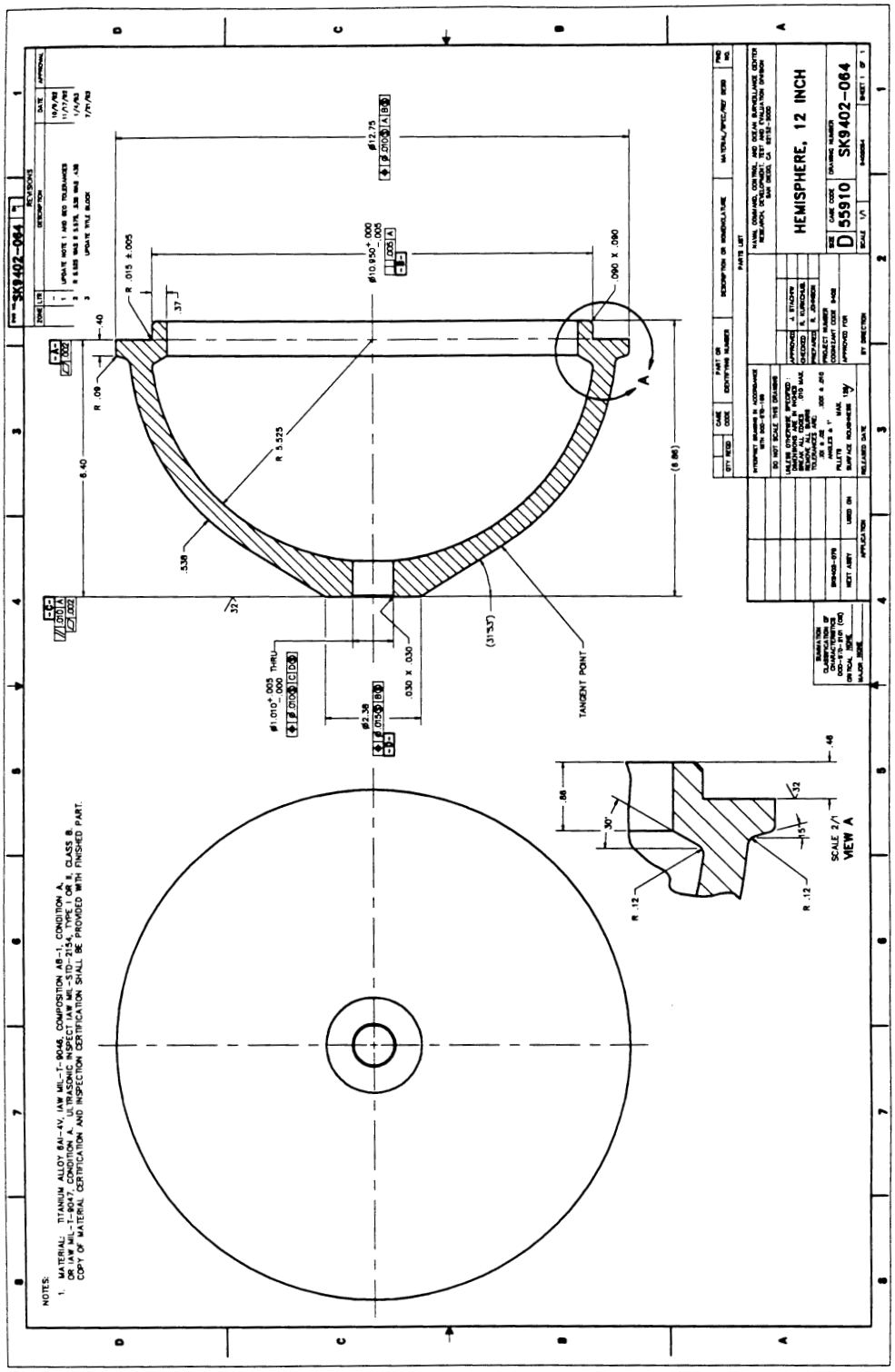

Figure 14. 12-inch hemisphere.

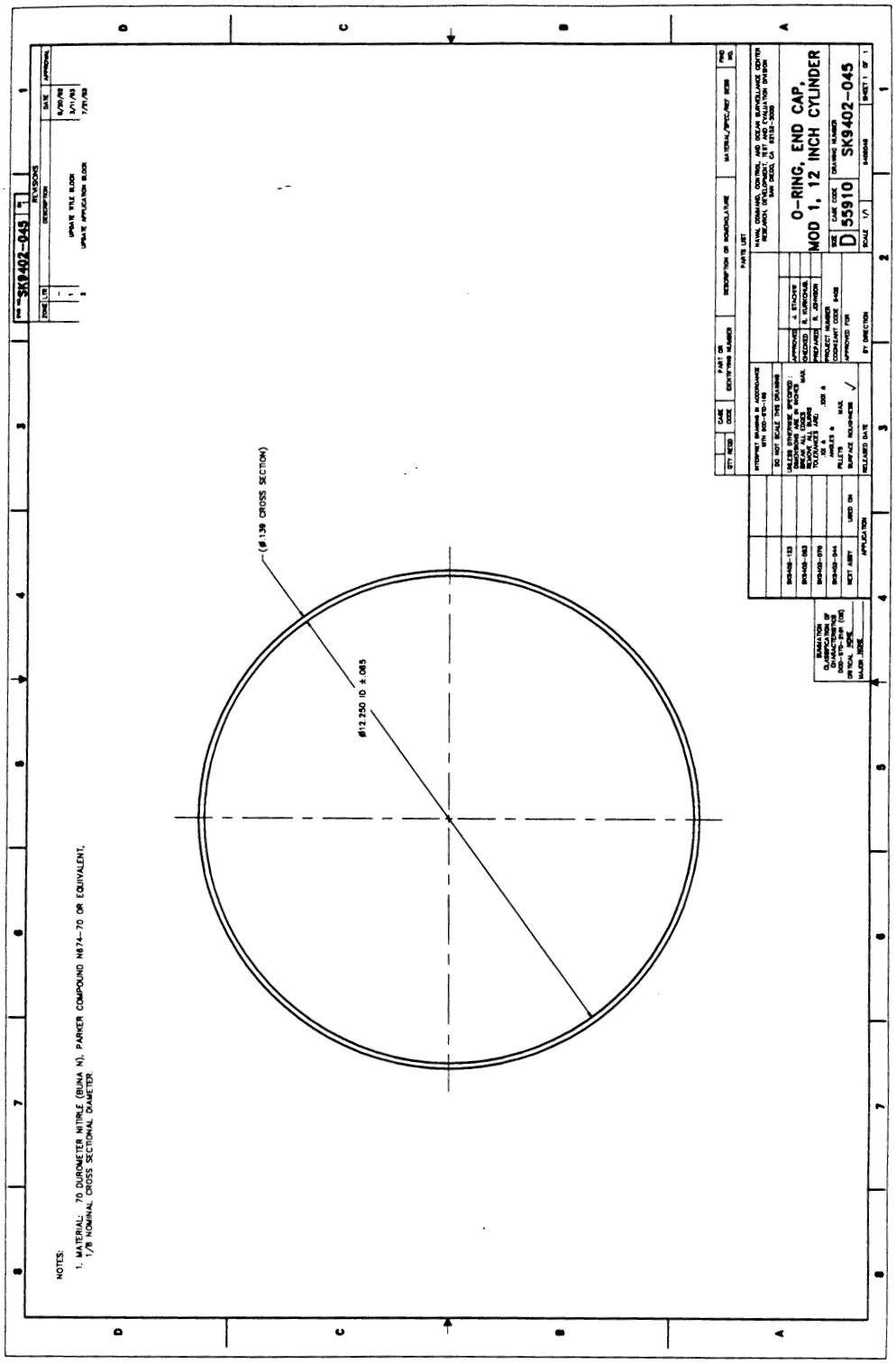

Figure 15. 12-inch cylinder Mod 1 end-cap joint O-ring.

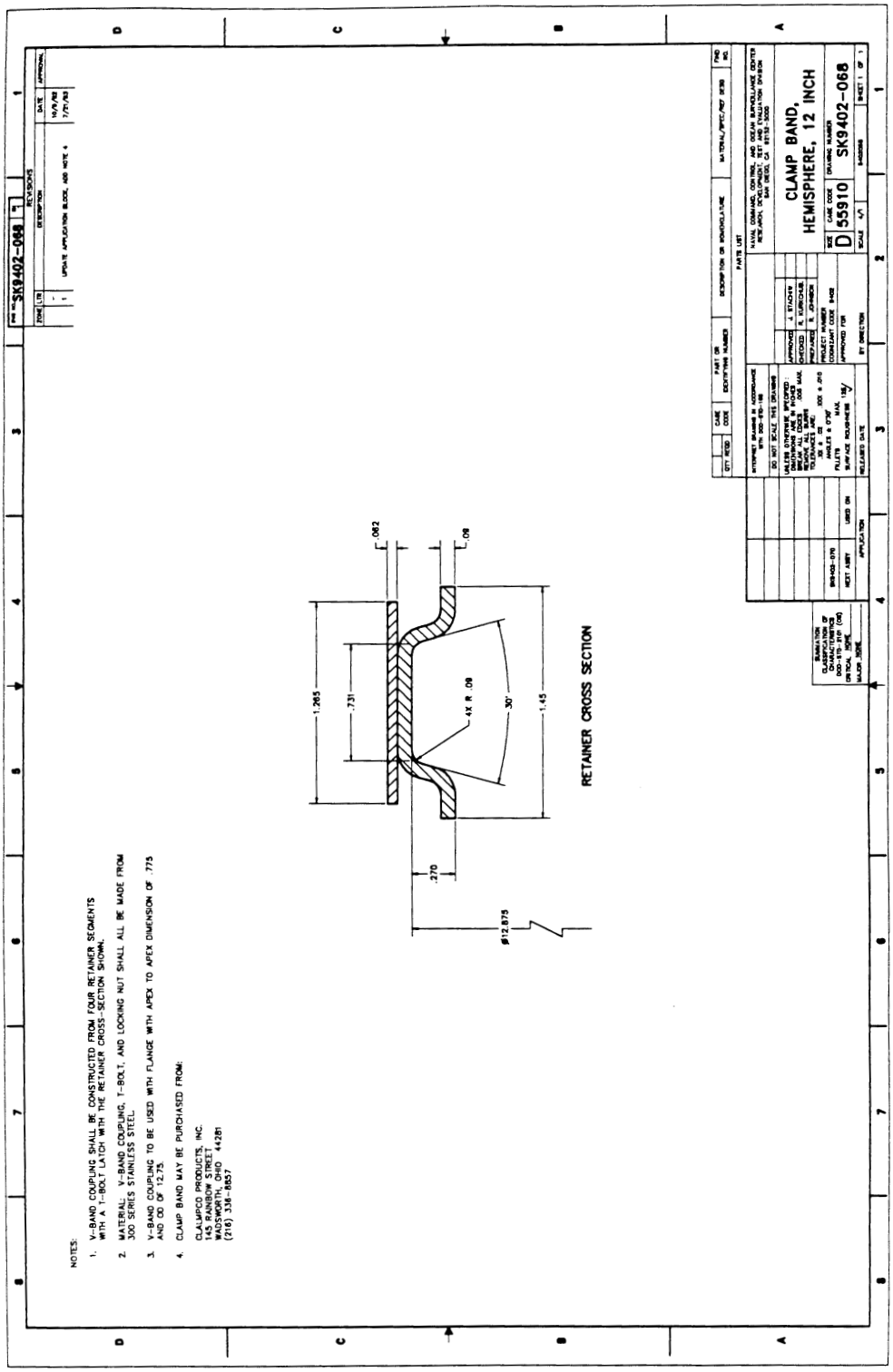

Figure 16. 12-inch hemisphere clamp band.

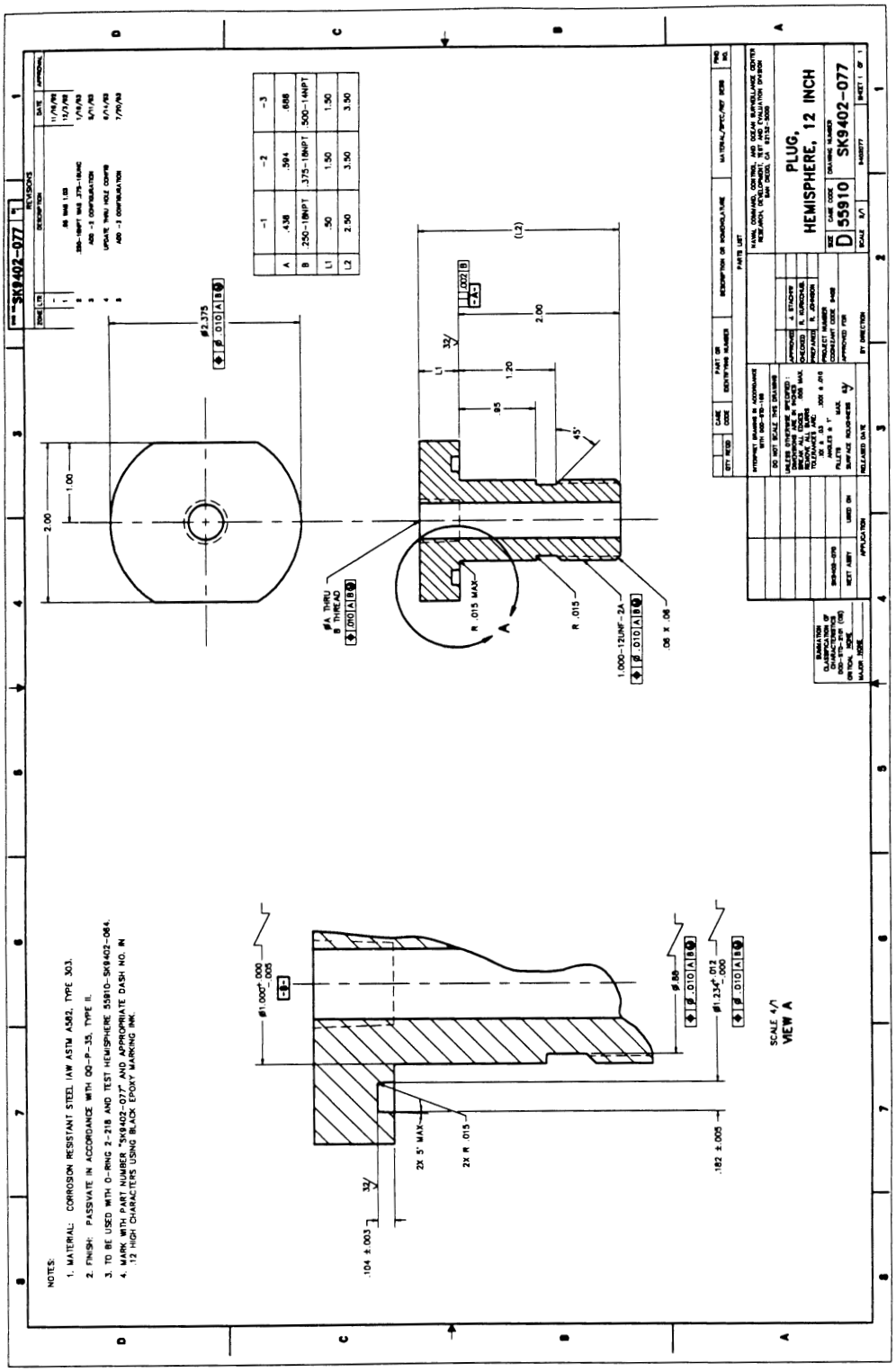

Figure 17. 12-inch hemisphere plug.

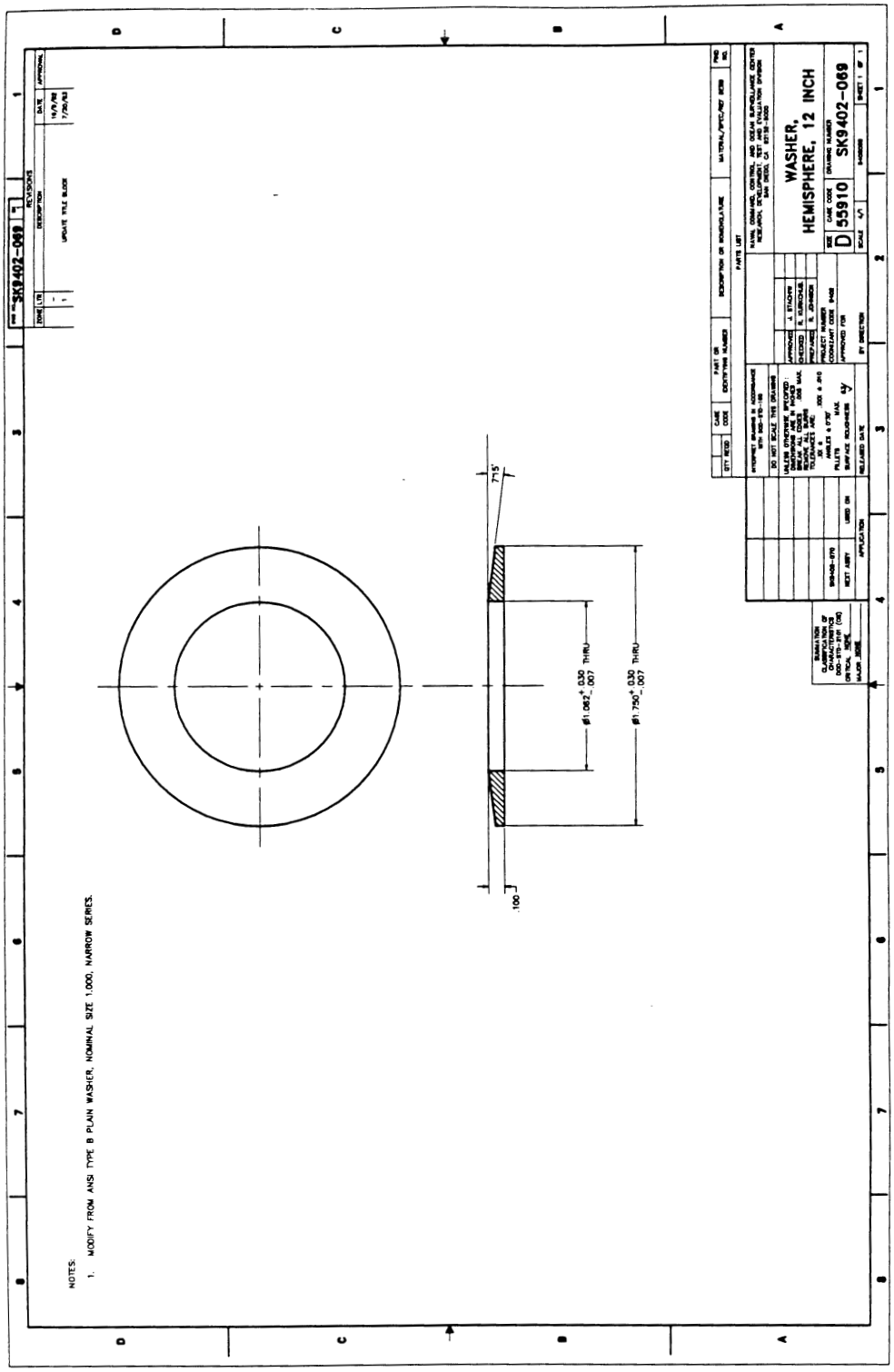

Figure 18. 12-inch hemisphere washer.

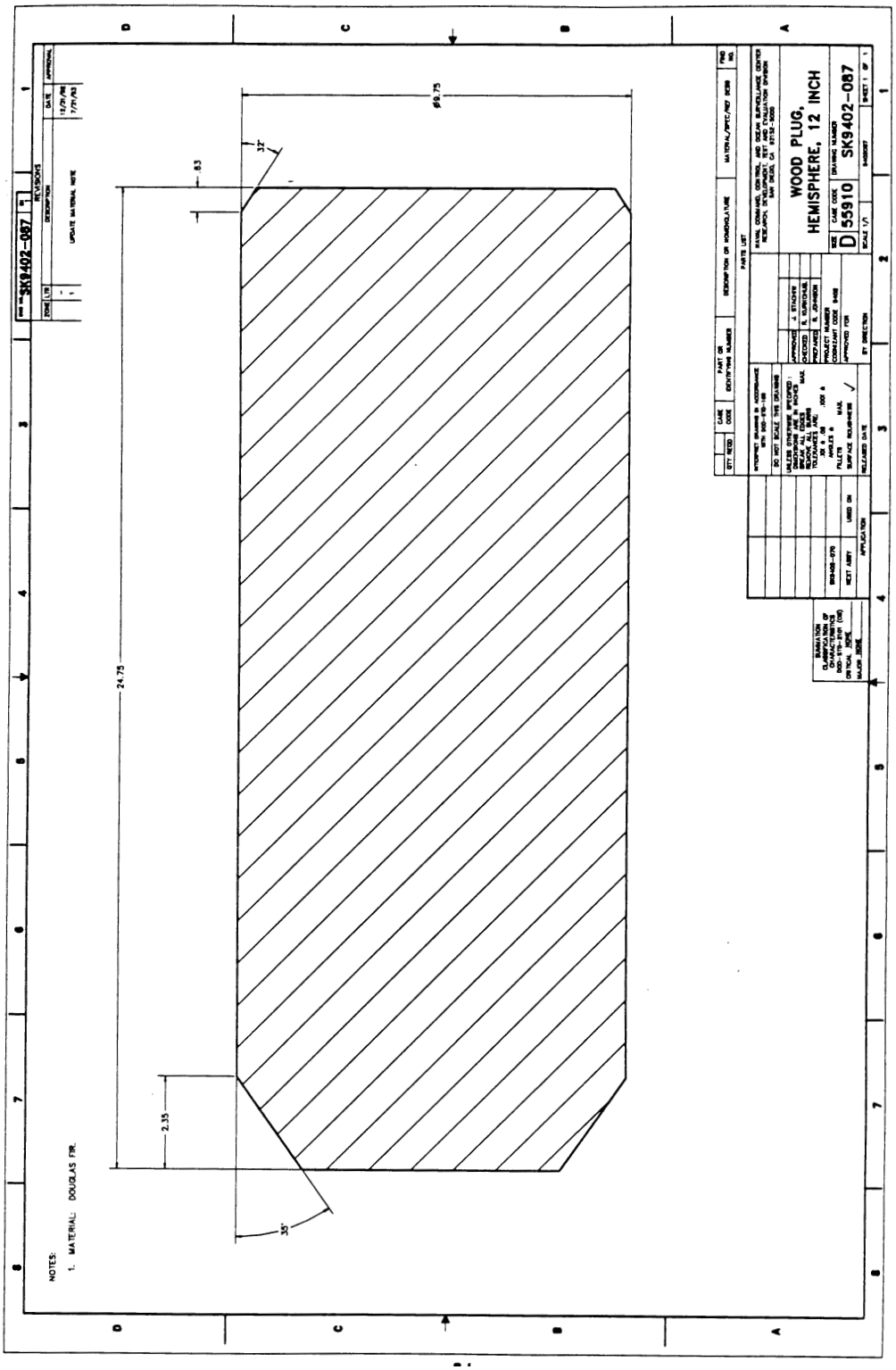

Figure 19. 12-inch hemisphere wooden plug.

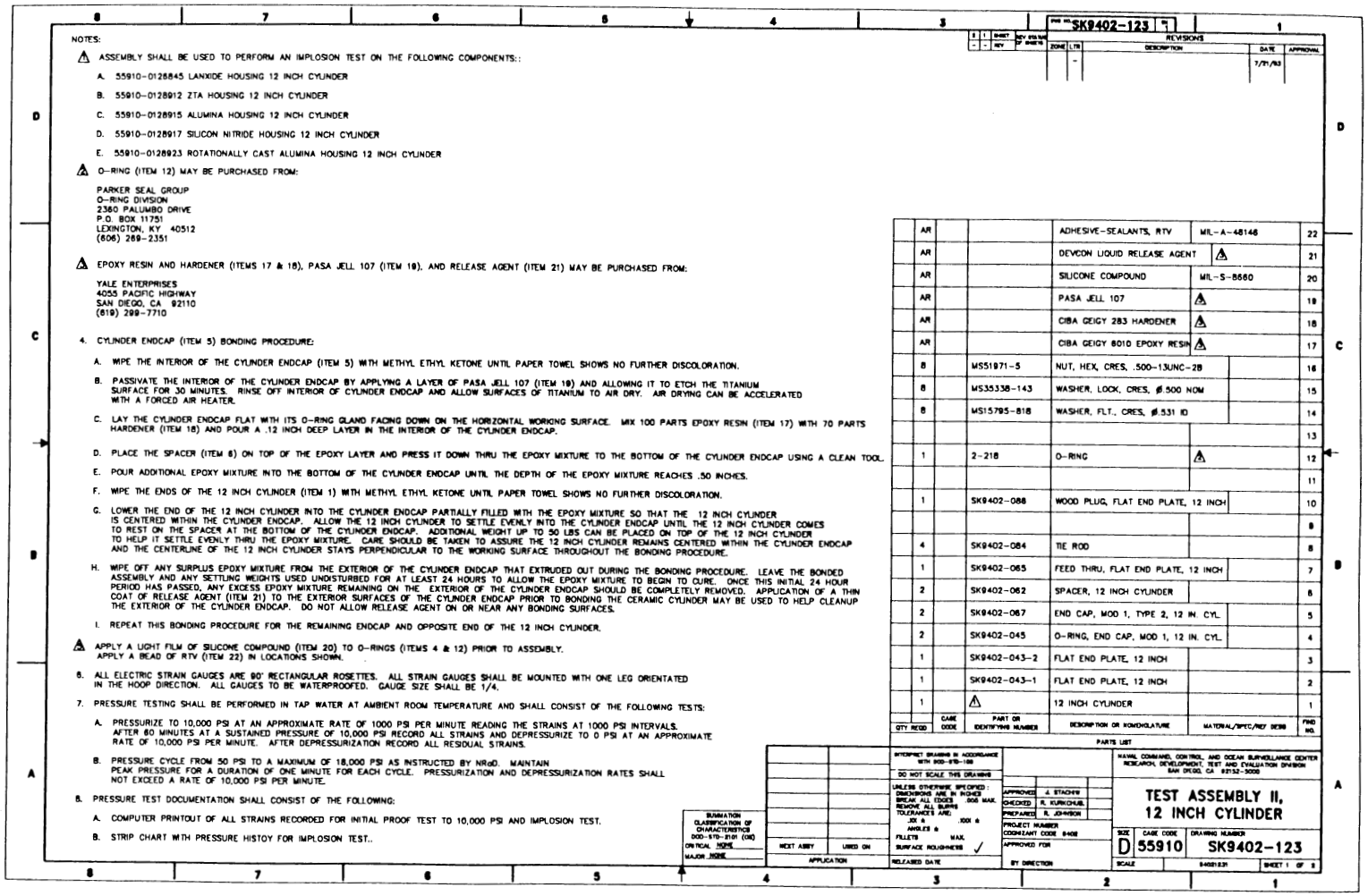

NOTES:

1. ASSEMBLY SHALL BE USED TO PERFORM AN IMPLOSION TEST ON THE FOLLOWING COMPONENTS::
   - A. 55910-0128845 LANXIDE HOUSING 12 INCH CYLINDER
   - B. 55910-0128912 ZTA HOUSING 12 INCH CYLINDER
   - C. 55910-0128915 ALUMINA HOUSING 12 INCH CYLINDER
   - D. 55910-0128917 SILICON NITRIDE HOUSING 12 INCH CYLINDER
   - E. 55910-0128923 ROTATIONALLY CAST ALUMINA HOUSING 12 INCH CYLINDER
2. O-RING (ITEM 12) MAY BE PURCHASED FROM:

   PARKER SEAL GROUP
   O-RING DIVISION
   2360 PALUMBO DRIVE
   P.O. BOX 11751
   LEXINGTON, KY 40512
   (606) 269-2351

3. EPOXY RESIN AND HARDENER (ITEMS 17 & 18), PASA JELL 107 (ITEM 19), AND RELEASE AGENT (ITEM 21) MAY BE PURCHASED FROM:

   YALE ENTERPRISES
   4055 PACIFIC HIGHWAY
   SAN DIEGO, CA 92110
   (619) 299-7710

4. CYLINDER ENDCAP (ITEM 5) BONDING PROCEDURE:
   - A. WIPE THE INTERIOR OF THE CYLINDER ENDCAP (ITEM 5) WITH METHYL ETHYL KETONE UNTIL PAPER TOWEL SHOWS NO FURTHER DISCOLORATION.
   - B. PASSIVATE THE INTERIOR OF THE CYLINDER ENDCAP BY APPLYING A LAYER OF PASA JELL 107 (ITEM 19) AND ALLOWING IT TO ETCH THE TITANIUM SURFACE FOR 30 MINUTES. RINSE OFF INTERIOR OF CYLINDER ENDCAP AND ALLOW SURFACES OF TITANIUM TO AIR DRY. AIR DRYING CAN BE ACCELERATED WITH A FORCED AIR HEATER.
   - C. LAY THE CYLINDER ENDCAP FLAT WITH ITS O-RING GLAND FACING DOWN ON THE HORIZONTAL WORKING SURFACE. MIX 100 PARTS EPOXY RESIN (ITEM 17) WITH 70 PARTS HARDENER (ITEM 18) AND POUR A .12 INCH DEEP LAYER IN THE INTERIOR OF THE CYLINDER ENDCAP.
   - D. PLACE THE SPACER (ITEM 6) ON TOP OF THE EPOXY LAYER AND PRESS IT DOWN THRU THE EPOXY MIXTURE TO THE BOTTOM OF THE CYLINDER ENDCAP USING A CLEAN TOOL.
   - E. POUR ADDITIONAL EPOXY MIXTURE INTO THE BOTTOM OF THE CYLINDER ENDCAP UNTIL THE DEPTH OF THE EPOXY MIXTURE REACHES .50 INCHES.
   - F. WIPE THE ENDS OF THE 12 INCH CYLINDER (ITEM 1) WITH METHYL ETHYL KETONE UNTIL PAPER TOWEL SHOWS NO FURTHER DISCOLORATION.
   - G. LOWER THE END OF THE 12 INCH CYLINDER INTO THE CYLINDER ENDCAP PARTIALLY FILLED WITH THE EPOXY MIXTURE SO THAT THE 12 INCH CYLINDER IS CENTERED WITHIN THE CYLINDER ENDCAP. ALLOW THE 12 INCH CYLINDER TO SETTLE EVENLY INTO THE CYLINDER ENDCAP UNTIL THE 12 INCH CYLINDER COMES TO REST ON THE SPACER AT THE BOTTOM OF THE CYLINDER ENDCAP. ADDITIONAL WEIGHT UP TO 50 LBS CAN BE PLACED ON TOP OF THE 12 INCH CYLINDER TO HELP IT SETTLE EVENLY THRU THE EPOXY MIXTURE. CARE SHOULD BE TAKEN TO ASSURE THE 12 INCH CYLINDER REMAINS CENTERED WITHIN THE CYLINDER ENDCAP AND THE CENTERLINE OF THE 12 INCH CYLINDER STAYS PERPENDICULAR TO THE WORKING SURFACE THROUGHOUT THE BONDING PROCEDURE.
   - H. WIPE OFF ANY SURPLUS EPOXY MIXTURE FROM THE EXTERIOR OF THE CYLINDER ENDCAP THAT EXTRUDED OUT DURING THE BONDING PROCEDURE. LEAVE THE BONDED ASSEMBLY AND ANY SETTLING WEIGHTS USED UNDISTURBED FOR AT LEAST 24 HOURS TO ALLOW THE EPOXY MIXTURE TO BEGIN TO CURE. ONCE THIS INITIAL 24 HOUR PERIOD HAS PASSED, ANY EXCESS EPOXY MIXTURE REMAINING ON THE EXTERIOR OF THE CYLINDER ENDCAP SHOULD BE COMPLETELY REMOVED. APPLICATION OF A THIN COAT OF RELEASE AGENT (ITEM 21) TO THE EXTERIOR SURFACES OF THE CYLINDER ENDCAP PRIOR TO BONDING THE CERAMIC CYLINDER MAY BE USED TO HELP CLEANUP THE EXTERIOR OF THE CYLINDER ENDCAP. DO NOT ALLOW RELEASE AGENT ON OR NEAR ANY BONDING SURFACES.
   - I. REPEAT THIS BONDING PROCEDURE FOR THE REMAINING ENDCAP AND OPPOSITE END OF THE 12 INCH CYLINDER.
5. APPLY A LIGHT FILM OF SILICONE COMPOUND (ITEM 20) TO O-RINGS (ITEMS 4 & 12) PRIOR TO ASSEMBLY. APPLY A BEAD OF RTV (ITEM 22) IN LOCATIONS SHOWN.
6. ALL ELECTRIC STRAIN GAUGES ARE 90° RECTANGULAR ROSETTES. ALL STRAIN GAUGES SHALL BE MOUNTED WITH ONE LEG ORIENTATED IN THE HOOP DIRECTION. ALL GAUGES TO BE WATERPROOFED. GAUGE SIZE SHALL BE 1/4.
7. PRESSURE TESTING SHALL BE PERFORMED IN TAP WATER AT AMBIENT ROOM TEMPERATURE AND SHALL CONSIST OF THE FOLLOWING TESTS:
   - A. PRESSURIZE TO 10,000 PSI AT AN APPROXIMATE RATE OF 1000 PSI PER MINUTE READING THE STRAINS AT 1000 PSI INTERVALS. AFTER 60 MINUTES AT A SUSTAINED PRESSURE OF 10,000 PSI RECORD ALL STRAINS AND DEPRESSURIZE TO 0 PSI AT AN APPROXIMATE RATE OF 10,000 PSI PER MINUTE. AFTER DEPRESSURIZATION RECORD ALL RESIDUAL STRAINS.
   - B. PRESSURE CYCLE FROM 50 PSI TO A MAXIMUM OF 18,000 PSI AS INSTRUCTED BY NRaD. MAINTAIN PEAK PRESSURE FOR A DURATION OF ONE MINUTE FOR EACH CYCLE. PRESSURIZATION AND DEPRESSURIZATION RATES SHALL NOT EXCEED A RATE OF 10,000 PSI PER MINUTE.
8. PRESSURE TEST DOCUMENTATION SHALL CONSIST OF THE FOLLOWING:
   - A. COMPUTER PRINTOUT OF ALL STRAINS RECORDED FOR INITIAL PROOF TEST TO 10,000 PSI AND IMPLOSION TEST.
   - B. STRIP CHART WITH PRESSURE HISTOY FOR IMPLOSION TEST..

QTY REQD	CAGE CODE	PART OR IDENTIFYING NUMBER	DESCRIPTION OR NOMENCLATURE	MATERIAL/SPEC/REF DESIG	FIND NO.
AR			ADHESIVE-SEALANTS, RTV	MIL-A-48146	22
AR			DEVCON LIQUID RELEASE AGENT		21
AR			SILICONE COMPOUND	MIL-S-8660	20
AR			PASA JELL 107		19
AR			CIBA GEIGY 283 HARDENER		18
AR			CIBA GEIGY 8010 EPOXY RESIN		17
8		MS51971-5	NUT, HEX, CRES, .500-13UNC-2B		16
8		MS35338-143	WASHER, LOCK, CRES, ø.500 NOM		15
8		MS15795-818	WASHER, FLT., CRES, ø.531 ID		14
					13
1		2-218	O-RING		12
					11
1		SK9402-088	WOOD PLUG, FLAT END PLATE, 12 INCH		10
					9
4		SK9402-084	TIE ROD		8
1		SK9402-065	FEED THRU, FLAT END PLATE, 12 INCH		7
2		SK9402-062	SPACER, 12 INCH CYLINDER		6
2		SK9402-067	END CAP, MOD 1, TYPE 2, 12 IN. CYL.		5
2		SK9402-045	O-RING, END CAP, MOD 1, 12 IN. CYL.		4
1		SK9402-043-2	FLAT END PLATE, 12 INCH		3
1		SK9402-043-1	FLAT END PLATE, 12 INCH		2
1			12 INCH CYLINDER		1

PARTS LIST

REVISIONS			
ZONE	LTR	DESCRIPTION	DATE	APPROVAL
	-		7/21/93	

NAVAL COMMAND, CONTROL, AND OCEAN SURVEILLANCE CENTER RESEARCH, DEVELOPMENT, TEST AND EVALUATION DIVISION SAN DIEGO, CA 92152-5000

TEST ASSEMBLY II, 12 INCH CYLINDER

SIZE D | CAGE CODE 55910 | DRAWING NUMBER SK9402-123

SCALE | SHEET 1 OF 3

APPROVED: A. STACHIW
CHECKED: R. KURKCHUB
PREPARED: R. JOHNSON

DO NOT SCALE THIS DRAWING

UNLESS OTHERWISE SPECIFIED: DIMENSIONS ARE IN INCHES. BREAK ALL EDGES .005 MAX. REMOVE ALL BURRS. TOLERANCES ARE: .XX ±, .XXX ±, ANGLES ±, FILLETS MAX, SURFACE ROUGHNESS ✓

SUMMATION CLASSIFICATION OF CHARACTERISTICS DOD-STD-2101 (OS)
CRITICAL NONE
MAJOR NONE

NEXT ASSY | USED ON | APPLICATION

Figure 20. 12-inch cylinder test assembly, Type 2 configuration, Sheet 1.

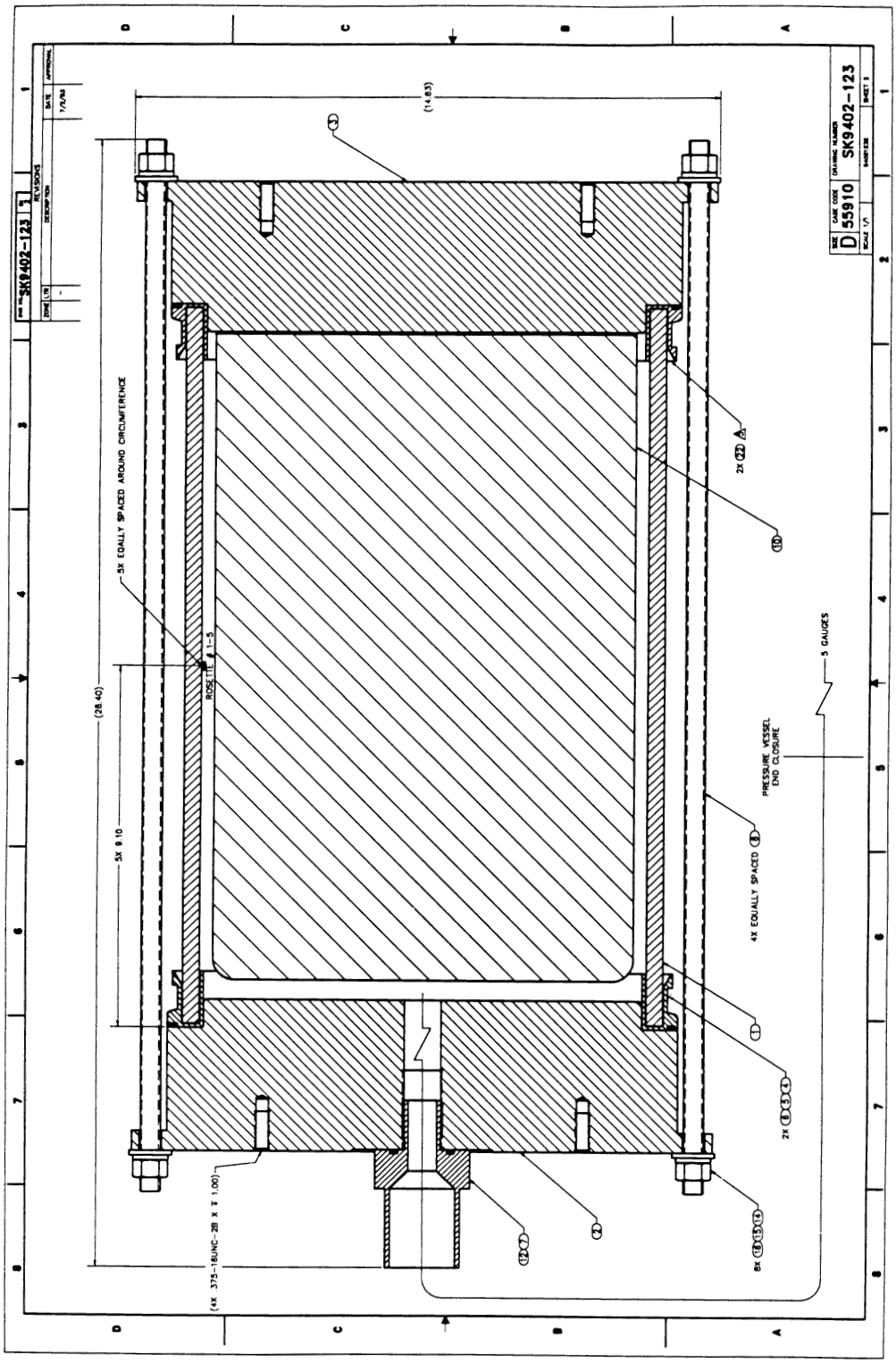

Figure 20. 12-inch cylinder test assembly, Type 2 configuration, Sheet 2.

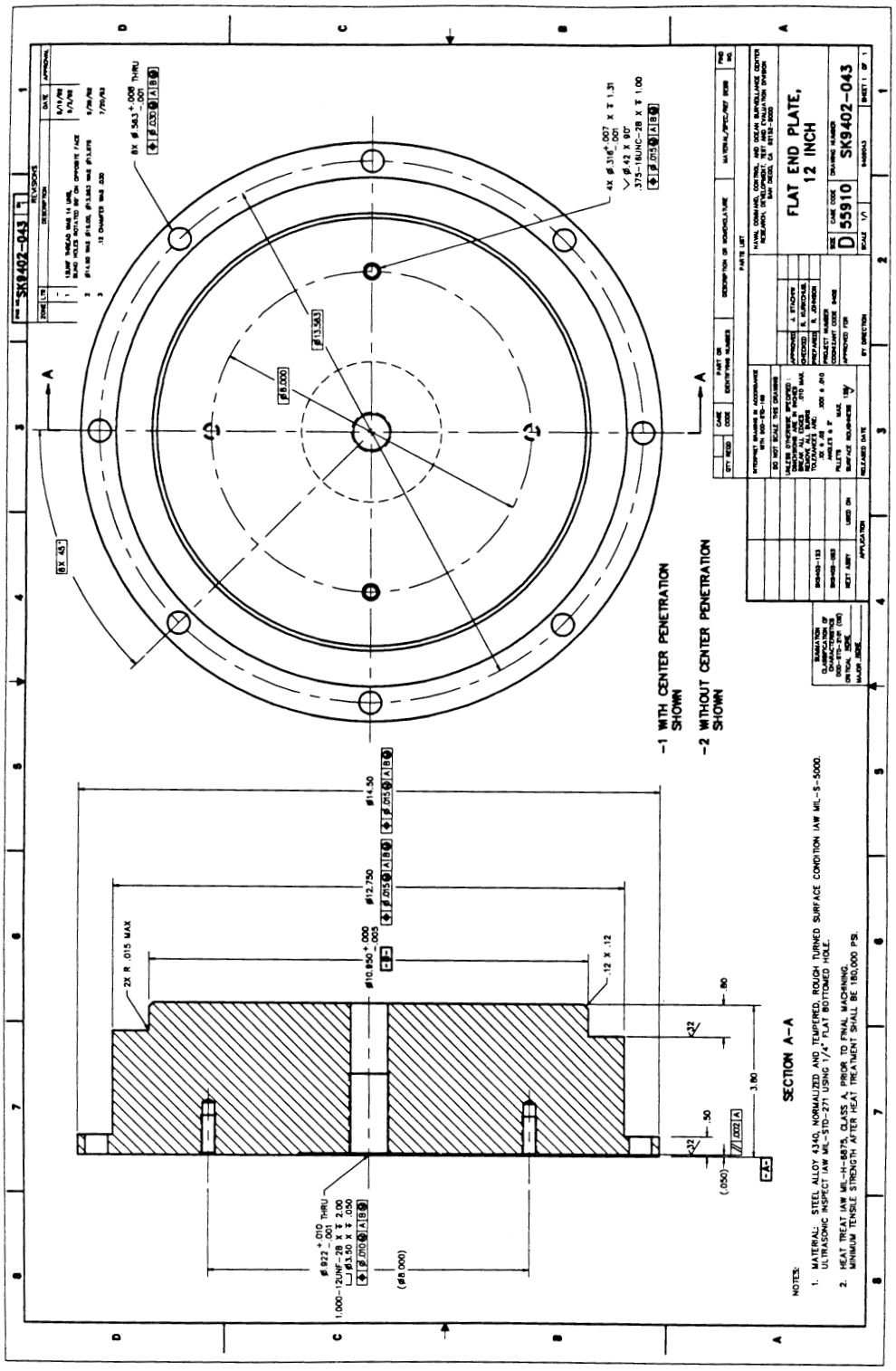

Figure 21. 12-inch flat plate.

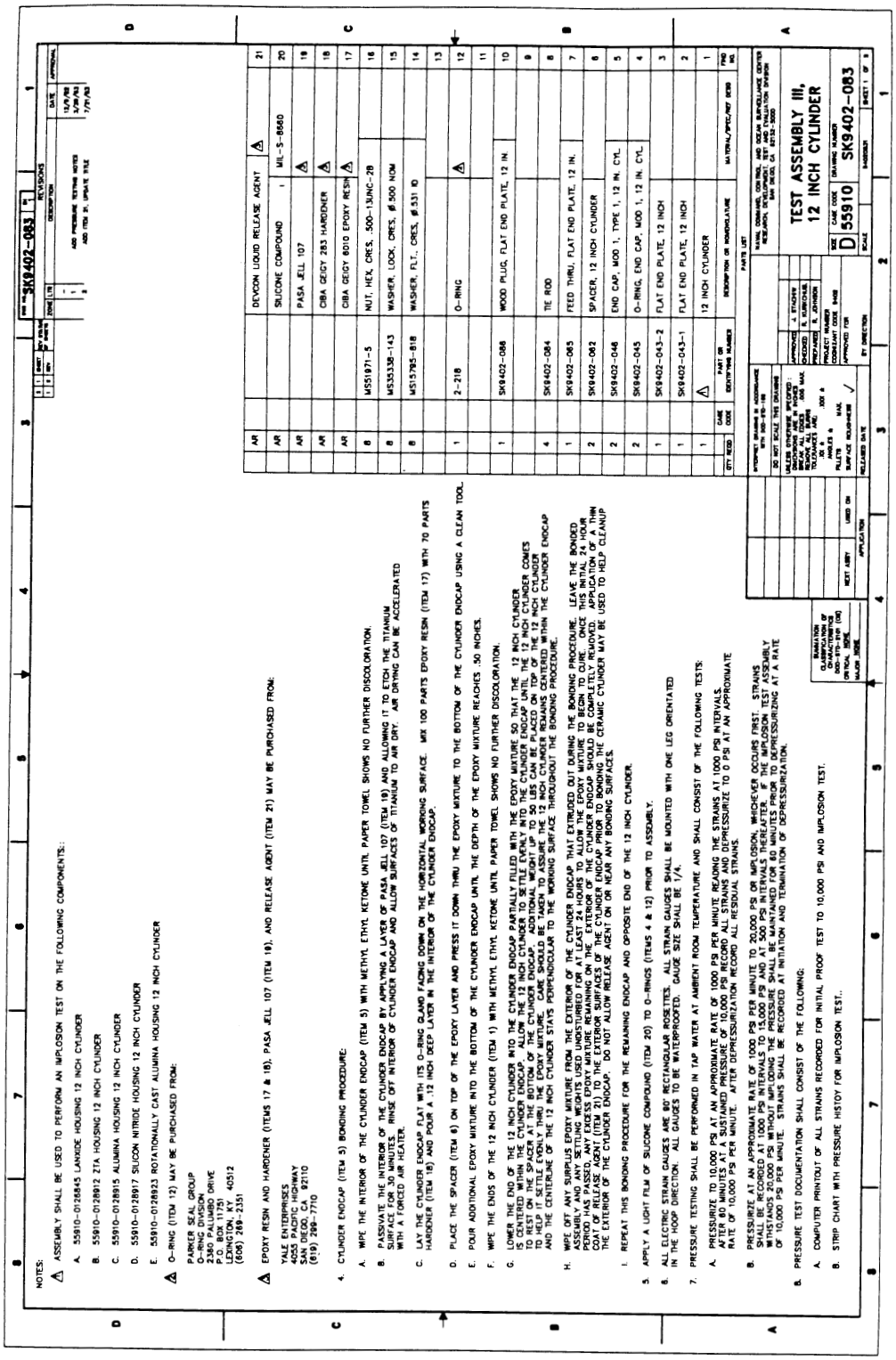

Figure 22. 12-inch cylinder test assembly, Type 3 configuration, Sheet 1.

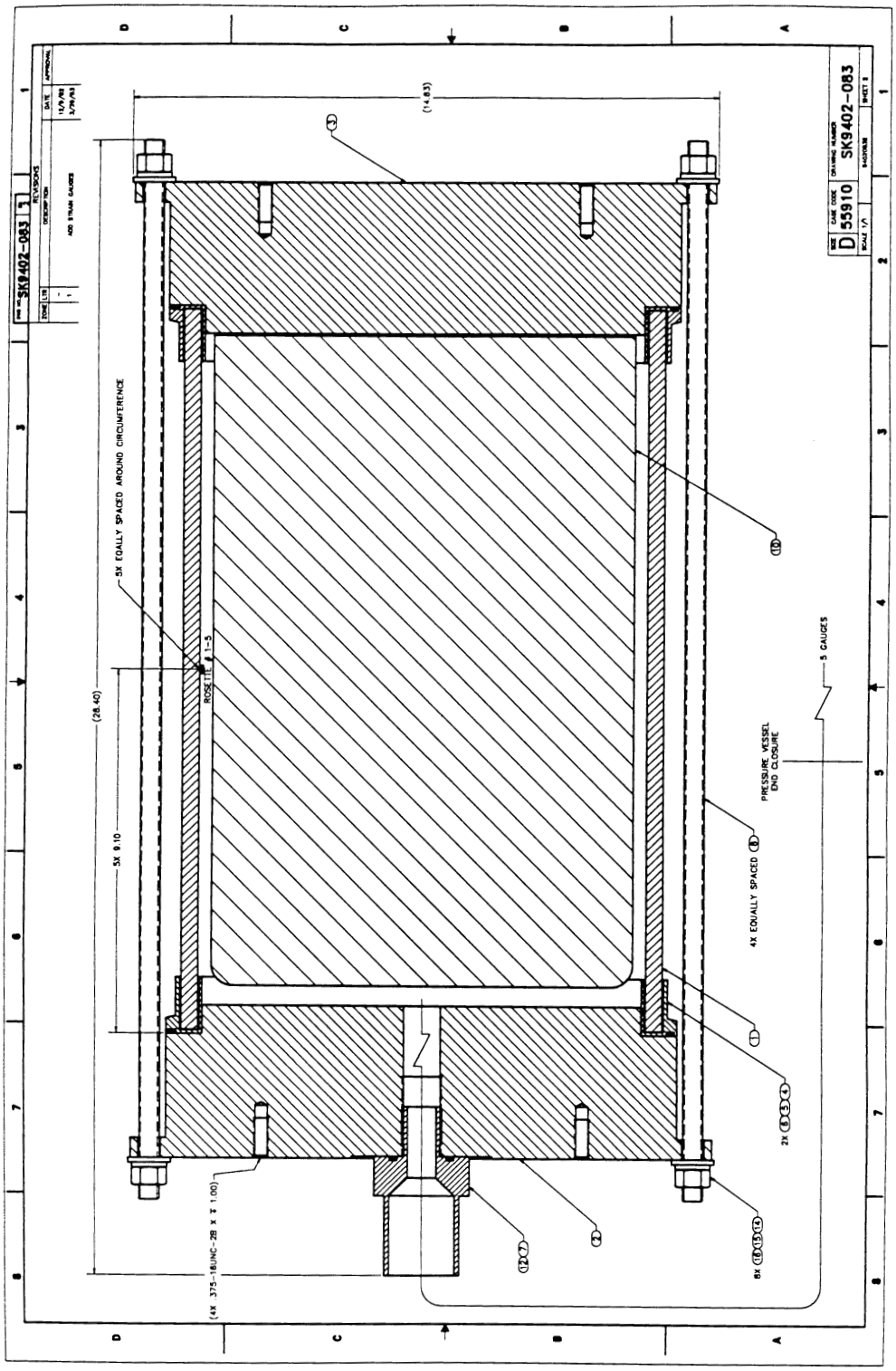

Figure 22. 12-inch cylinder test assembly, Type 3 configuration, Sheet 2.

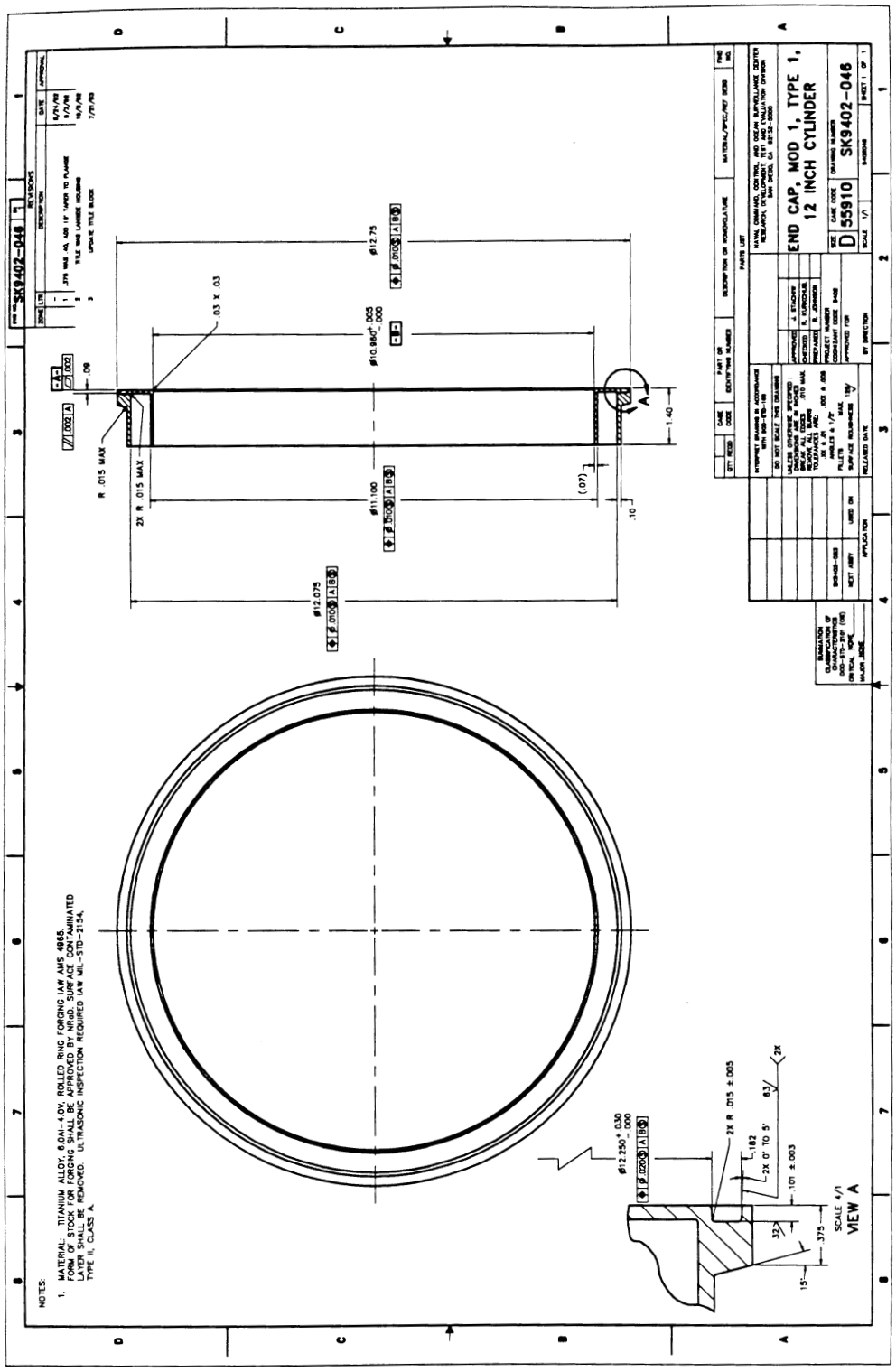

Figure 23. 12-inch cylinder Mod 1, Type 1 end-cap joint ring.

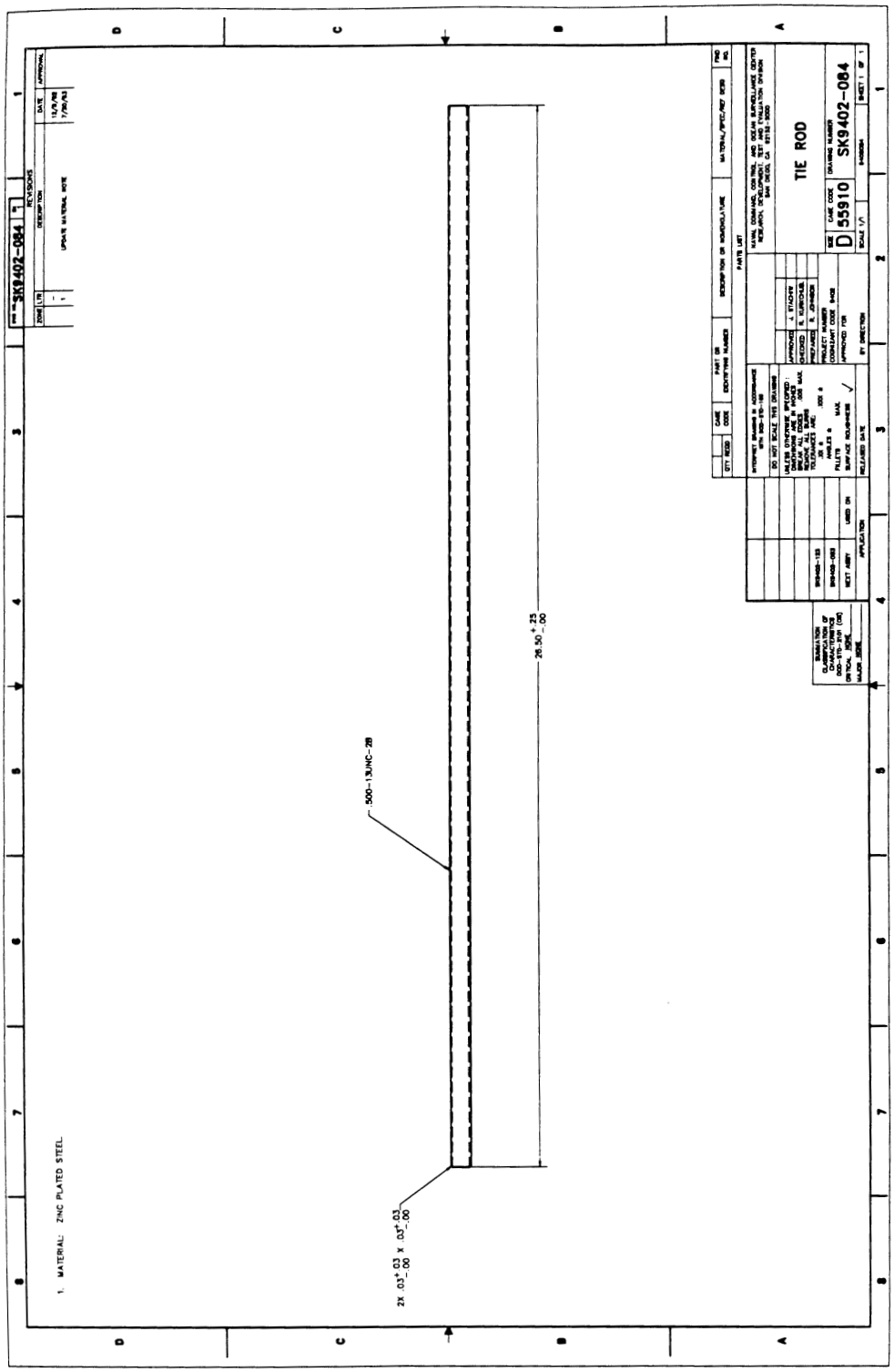

Figure 24. 12-inch flat end-plate tie rod.

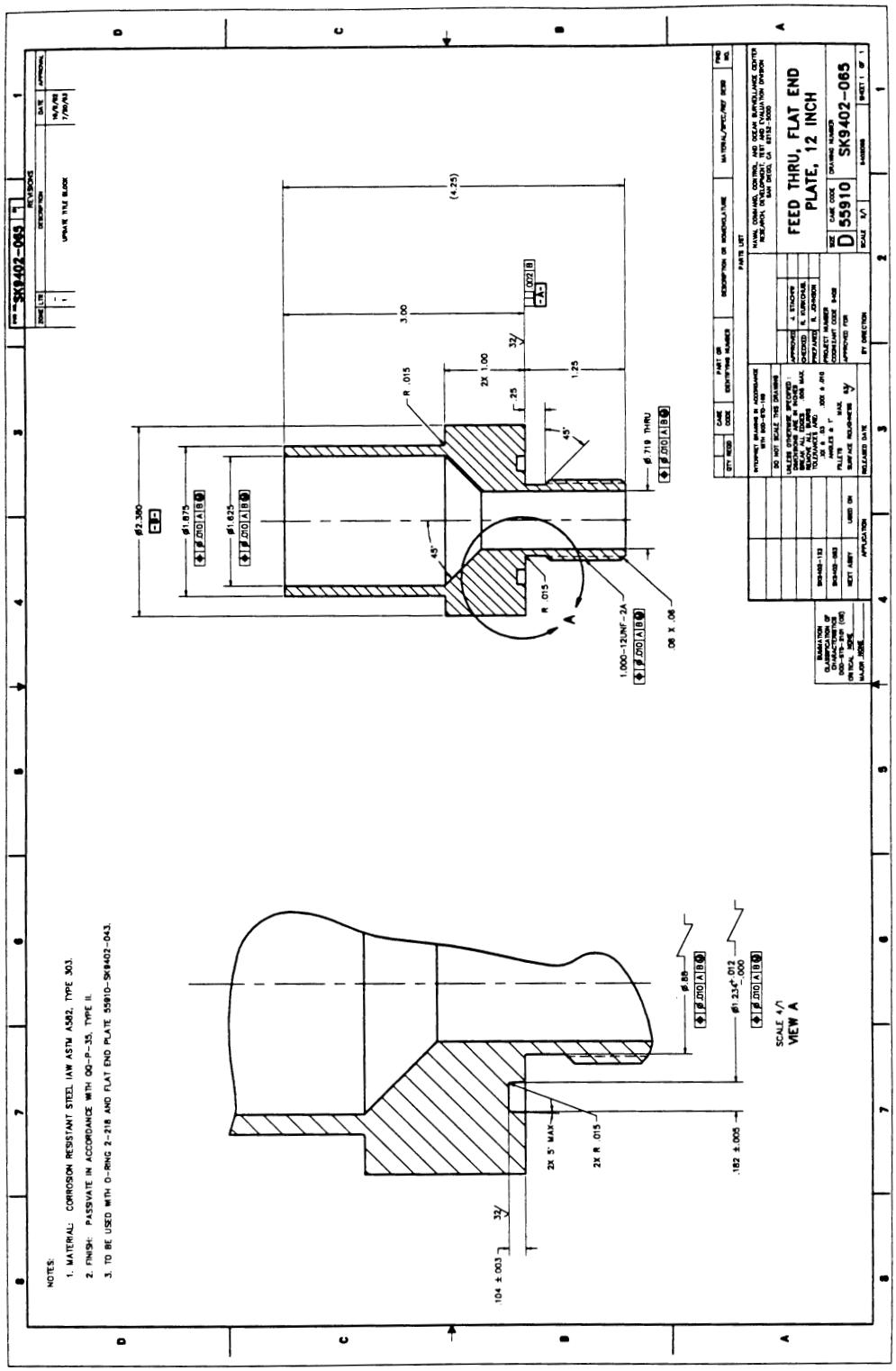

Figure 25. 12-inch flat end-plate feed through.

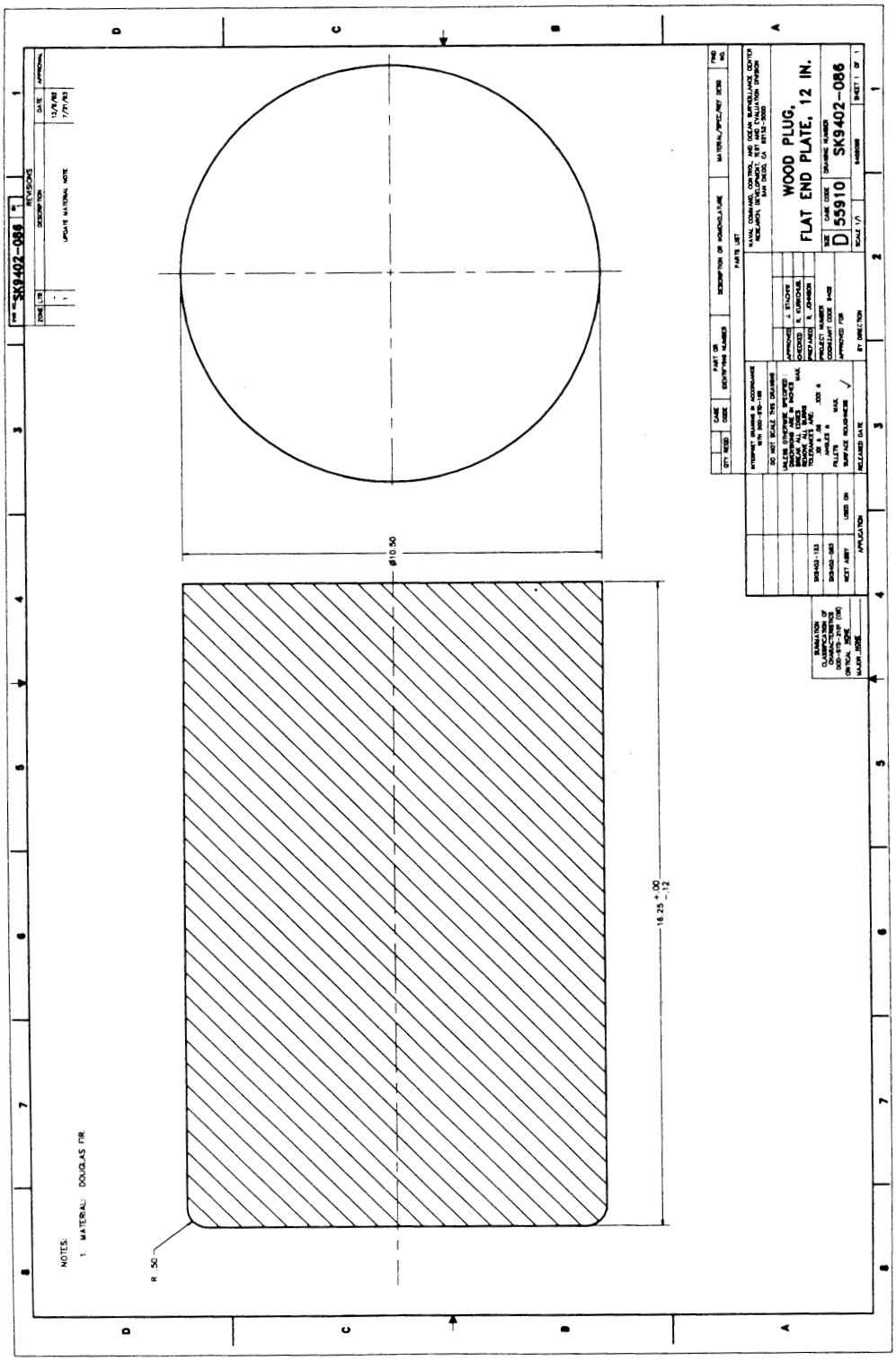

Figure 26. 12-inch end-plate wooden plug.

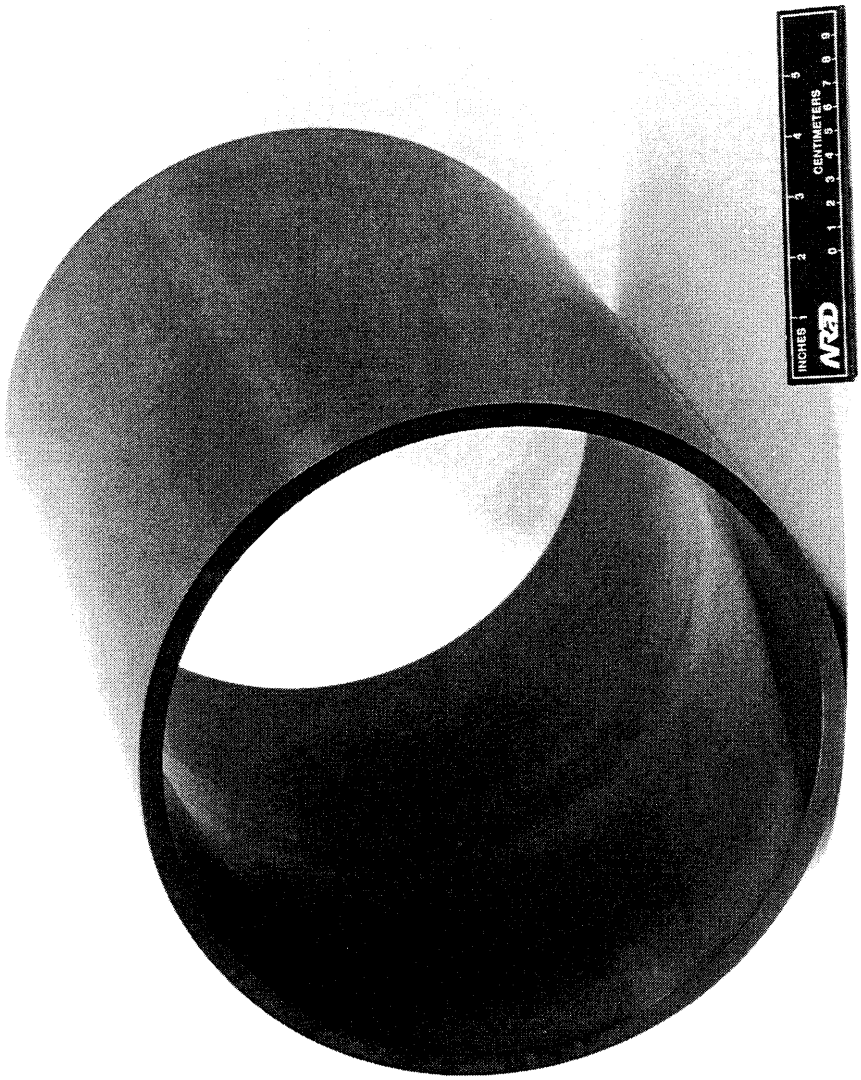

Figure 27. Photo of fully machines Si_3N_4 ceramic cylinder prior to bonding of titanium end rings.

Figure 28. Photo of fully machined Si3N4 ceramic cylinder with titanium end rings bonded in place.

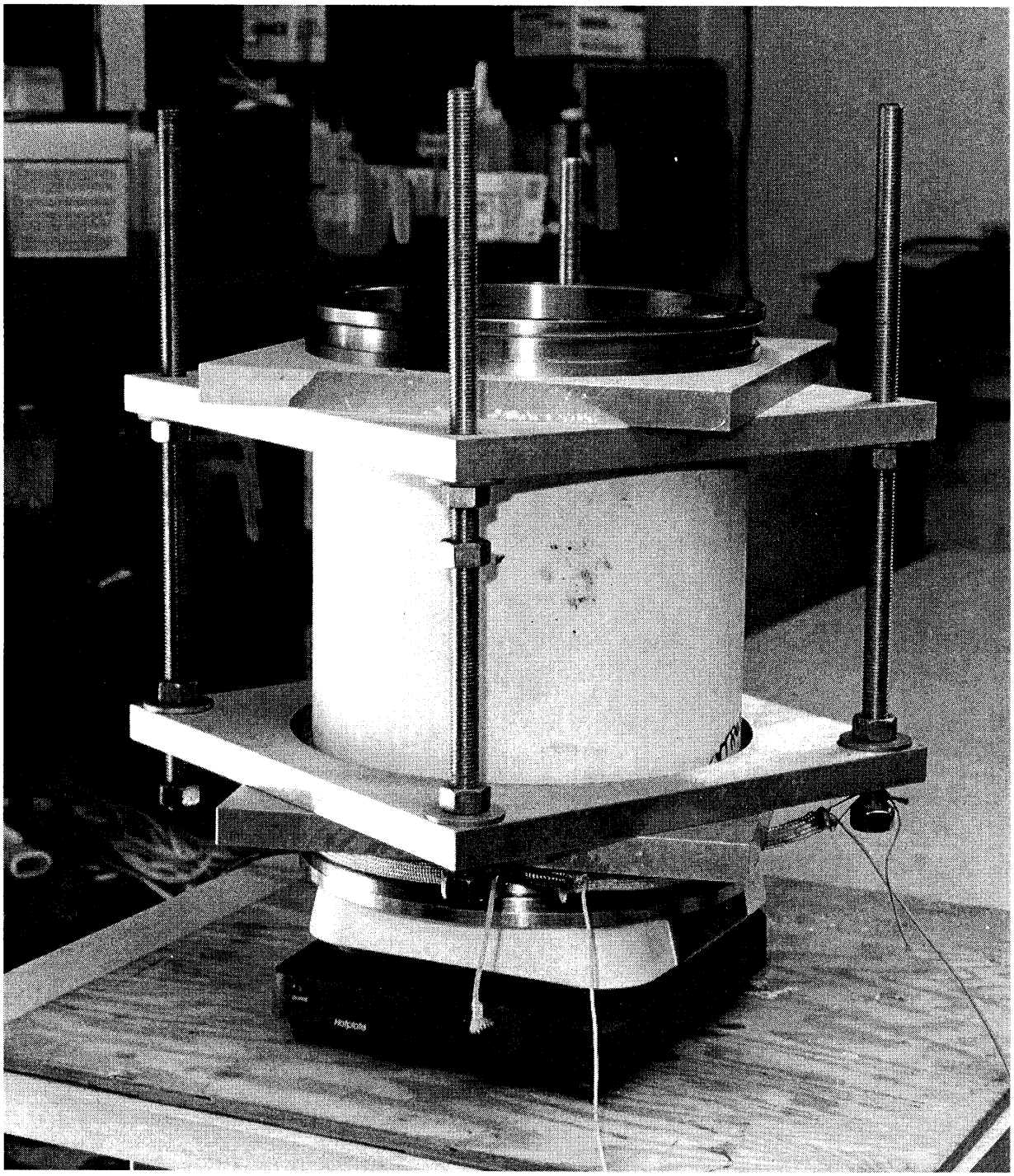

Figure 29. End-cap joint ring removal fixture.

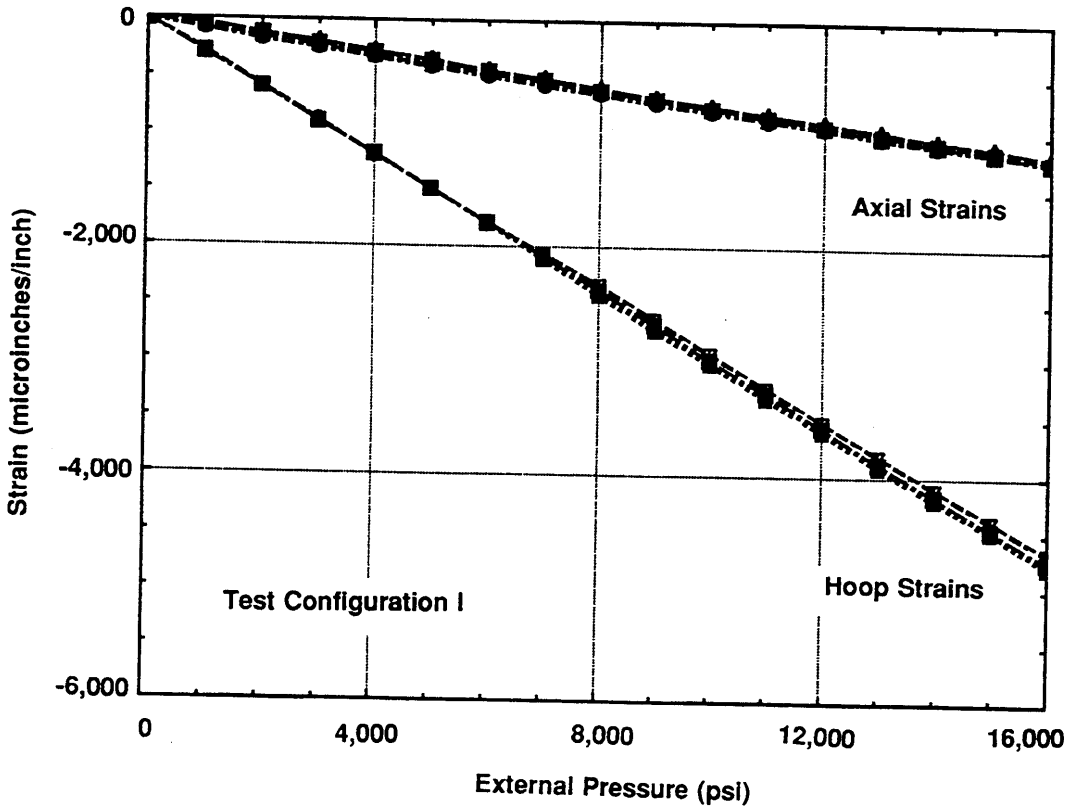

Figure 30. Pressure vs. strain plot for cylinder 001.

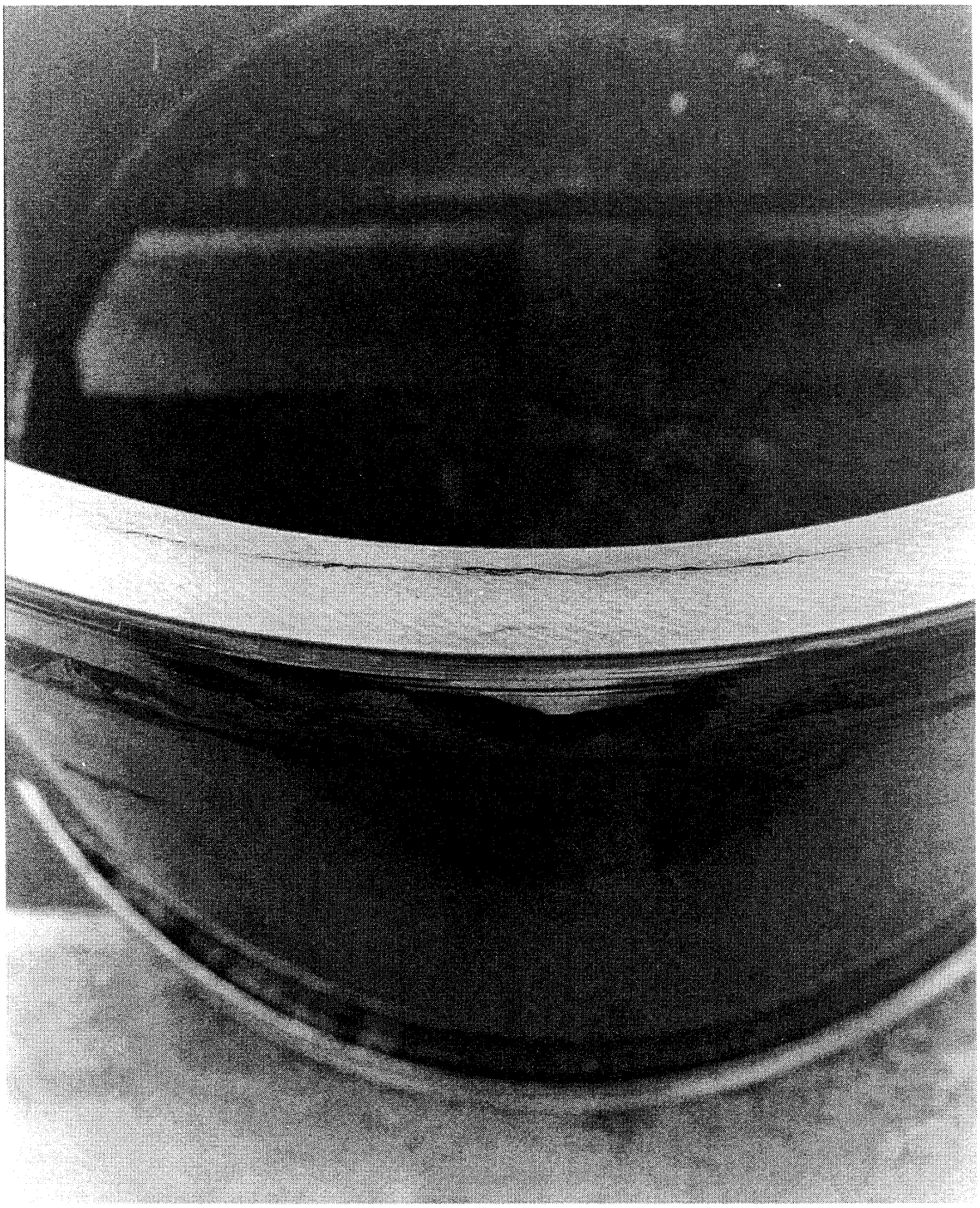

Figure 31. Circumferential cracking on the bearing surface of cylinder 001. The titanium end-cap joint ring was removed after pressure testing to inspect for cracking.

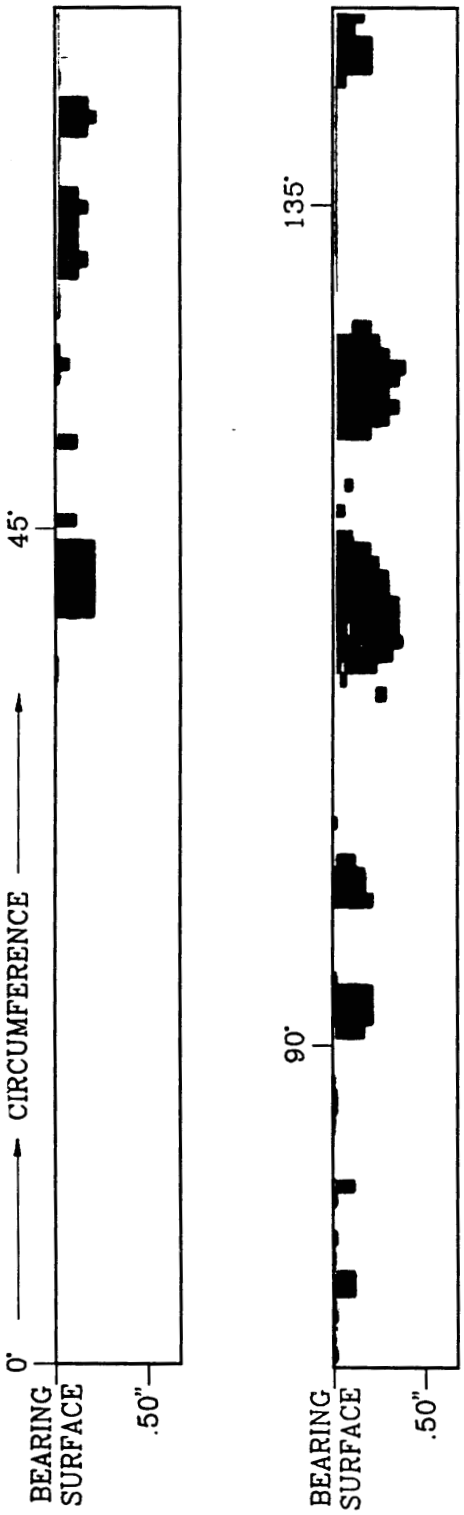

Figure 32. Pulse-echo C-scan of cylinder 001, Sheet 1.

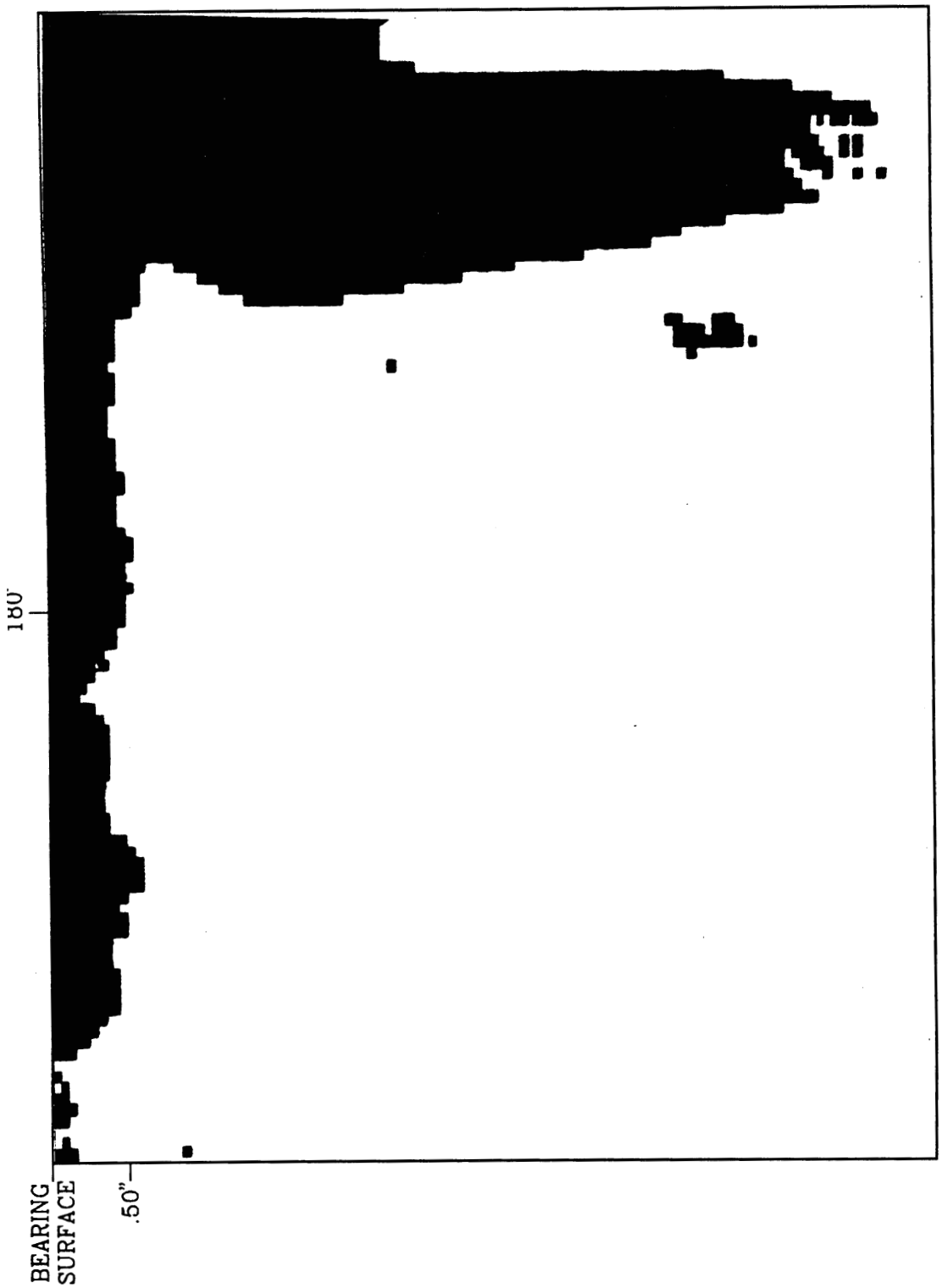

Figure 32. Pulse-echo C-scan of cylinder 001, Sheet 2.

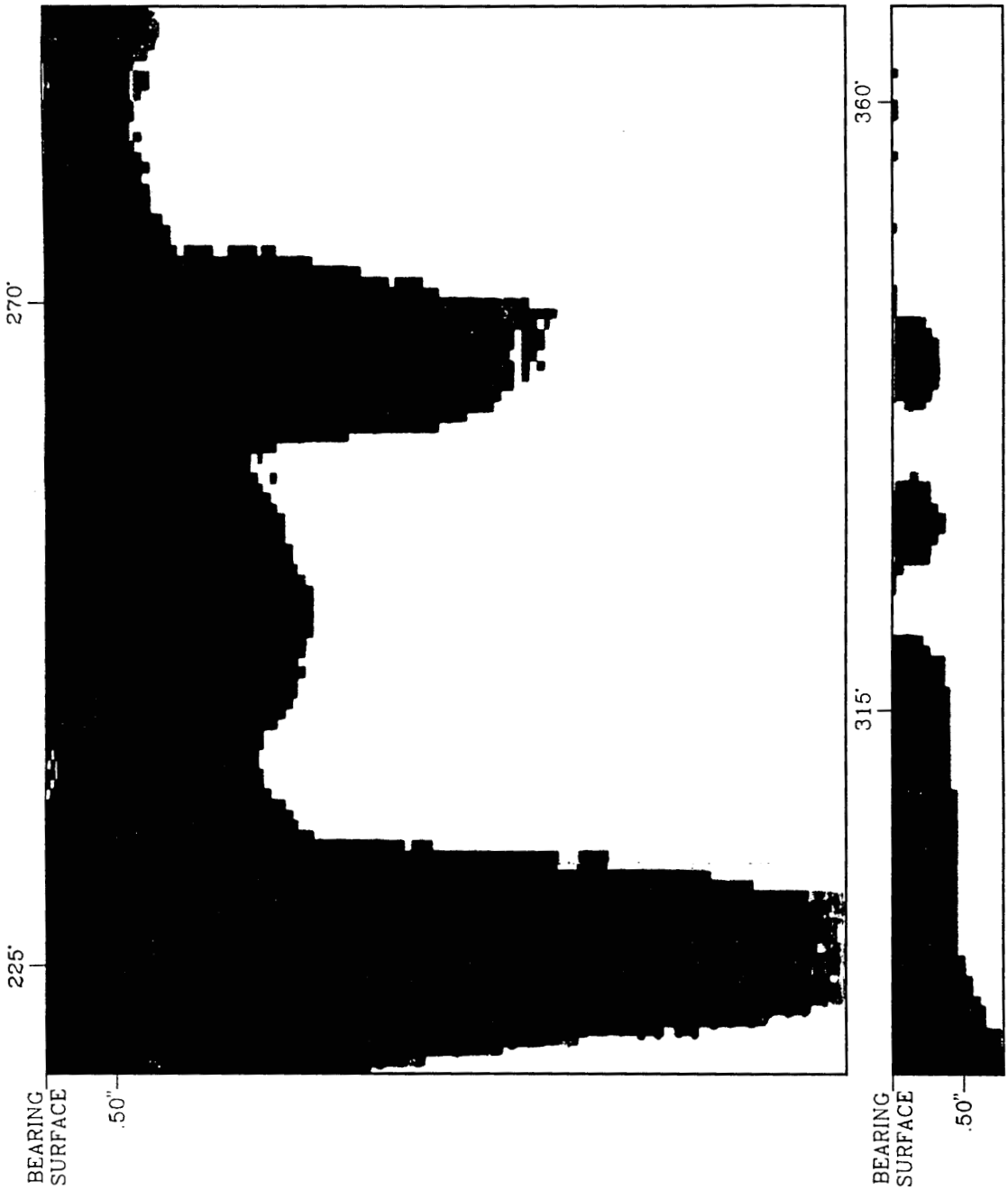

Figure 32. Pulse-echo C-scan of cylinder 001, Sheet 3.

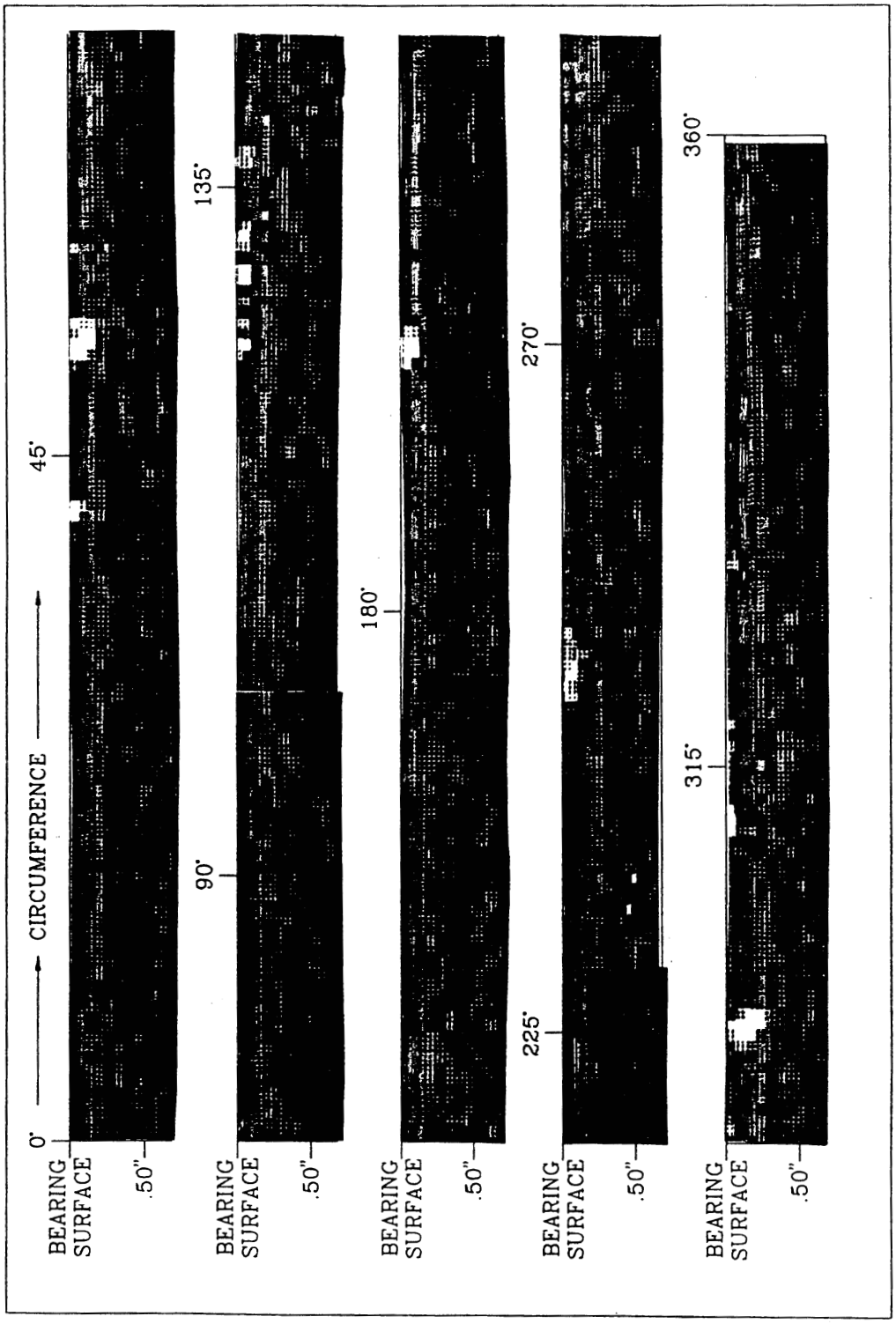

Figure 33. Pulse-echo C-scan of the other end of cylinder 001.

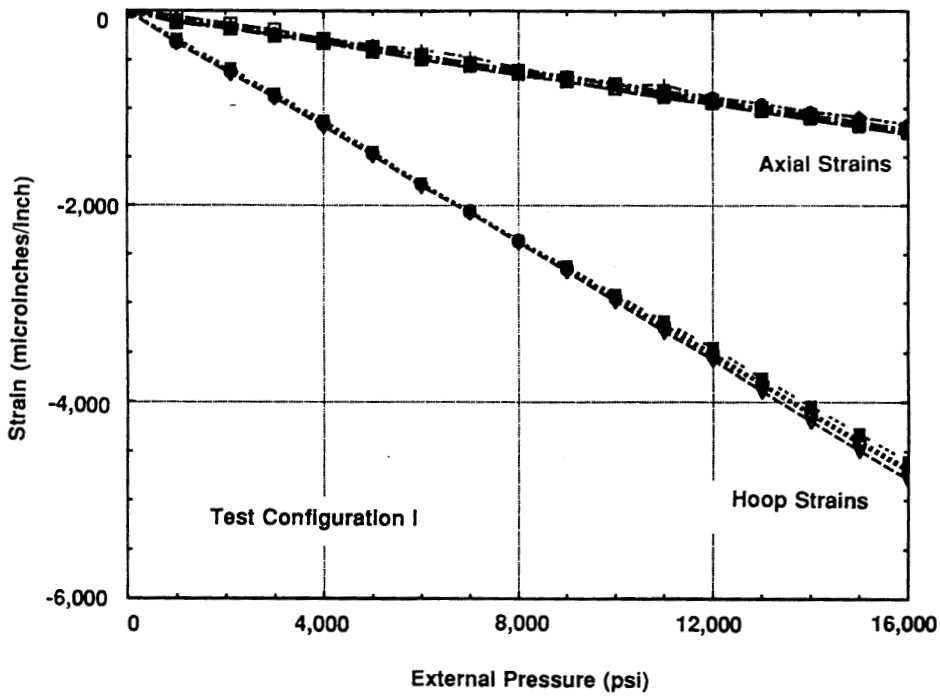

Figure 34. Pressure vs. strain plot for cylinder 002.

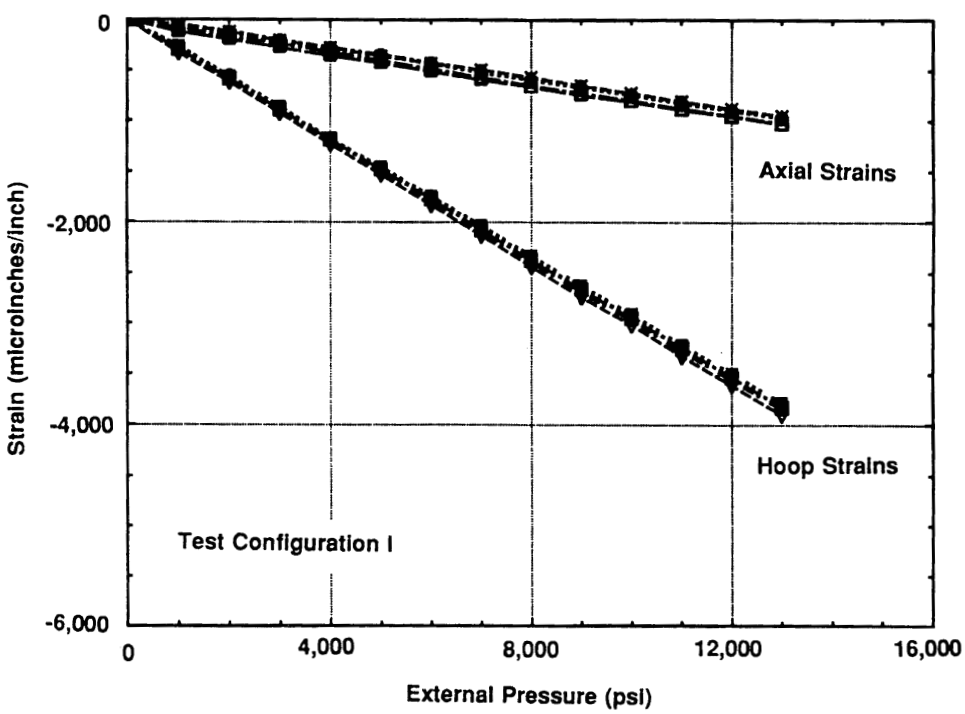

Figure 35. Pressure vs. strain plot for cyllinder 003.

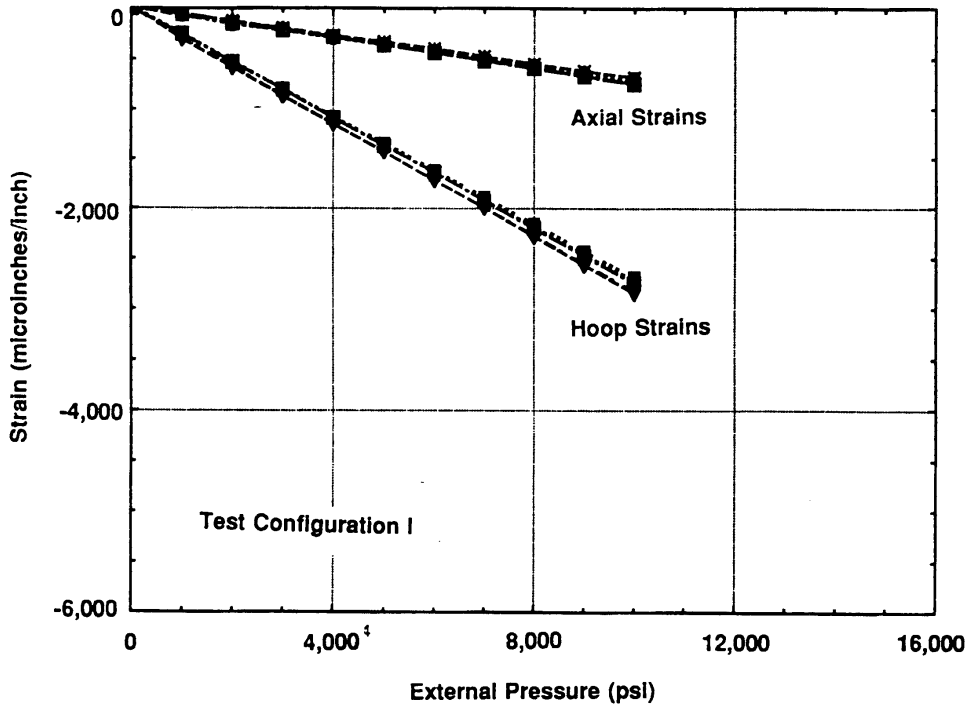

Figure 36. Pressure vs. strain plot for cylinder 004.

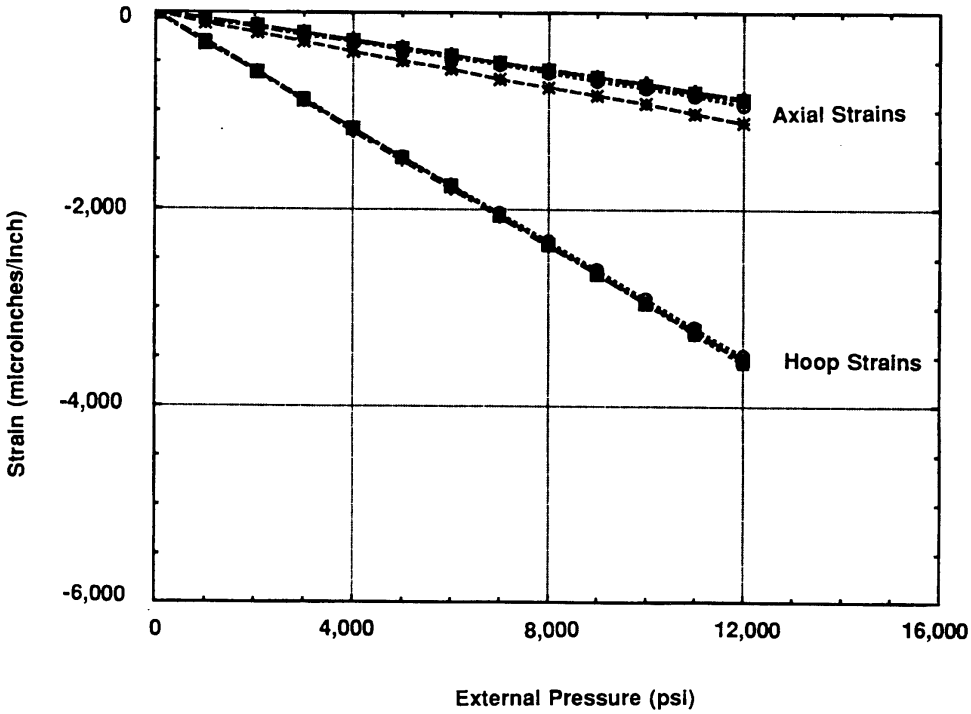

Figure 37. Pressure vs. strain plot for cyllinder 005.

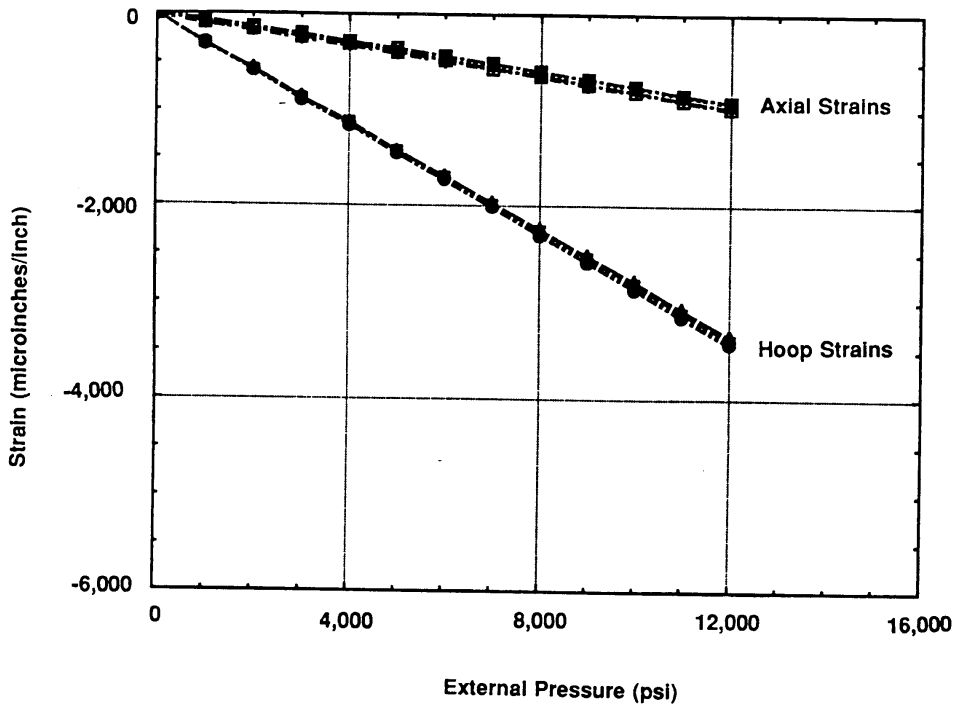

Figure 38. Pressure vs. strain plot for cylinder 006.

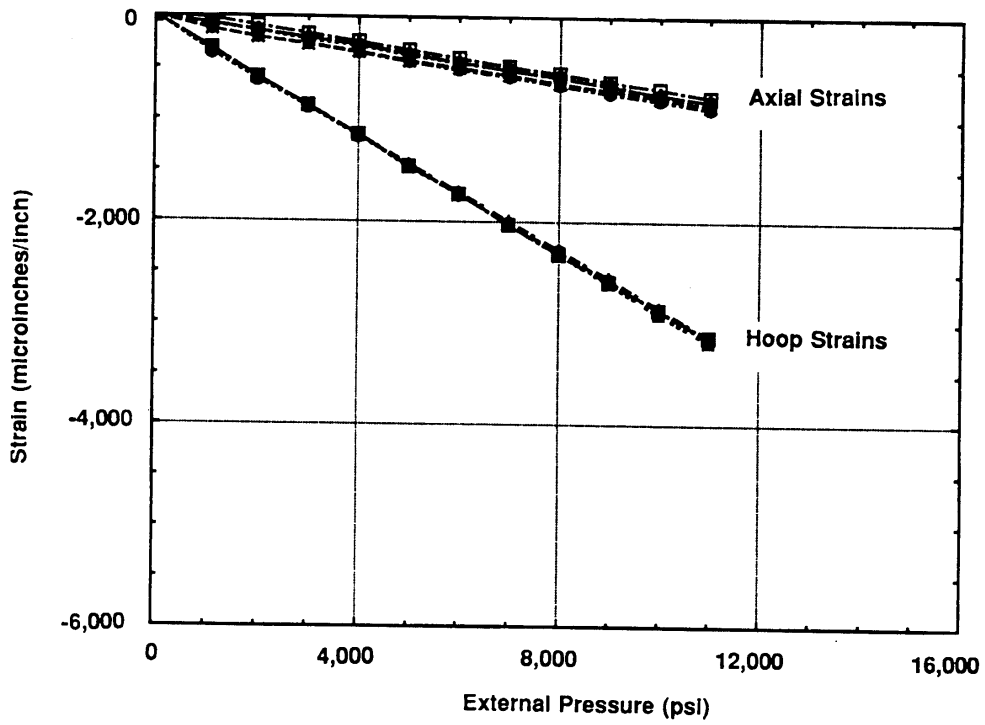

Figure 39. Pressure vs. strain plot for cyllinder 007.

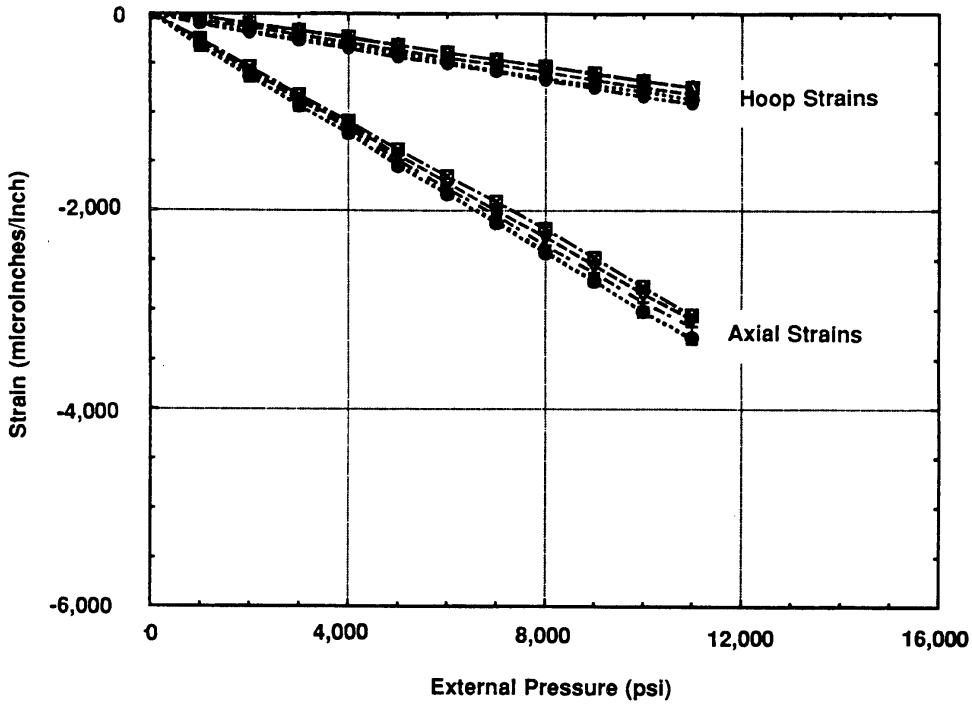

Figure 40. Pressure vs. strain plot for cylinder 008.

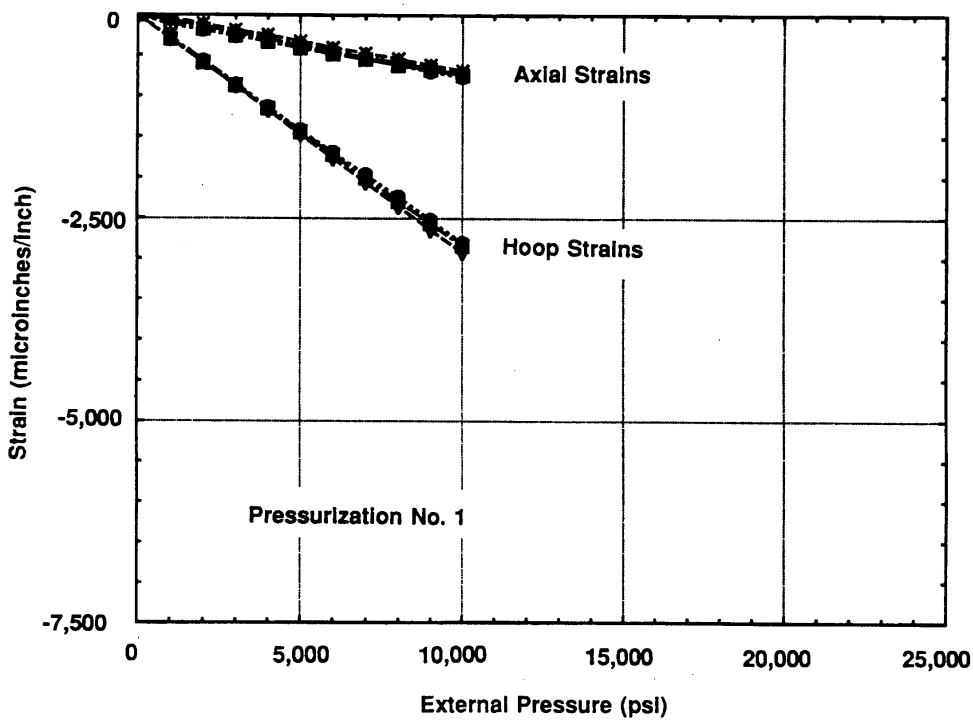

Figure 41. Pressure vs. strain plot for cylinder 009, pressurization No. 1.

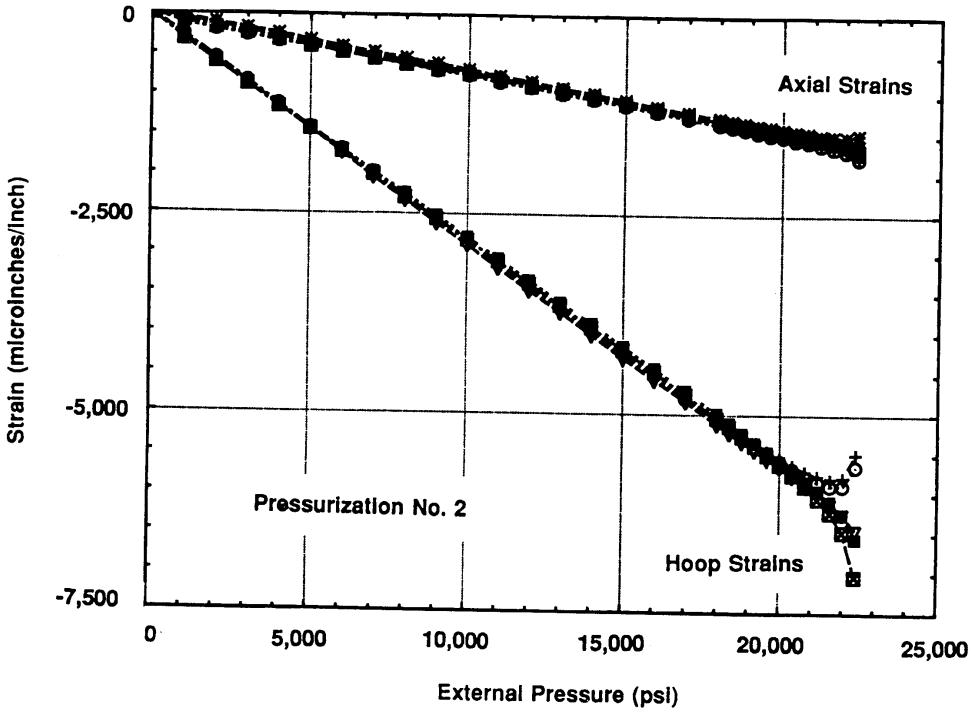

Figure 42. Pressure vs. strain plot for cylinder 009, pressurization No. 2.

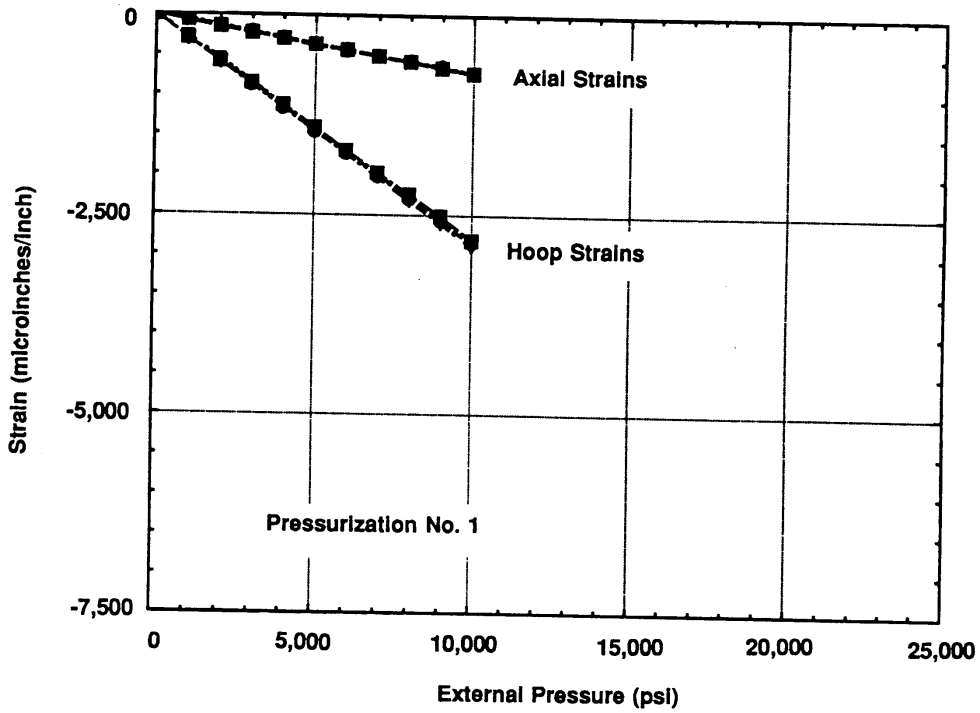

Figure 43. Pressure vs. strain plot for cylinder 010, pressurization No. 1.

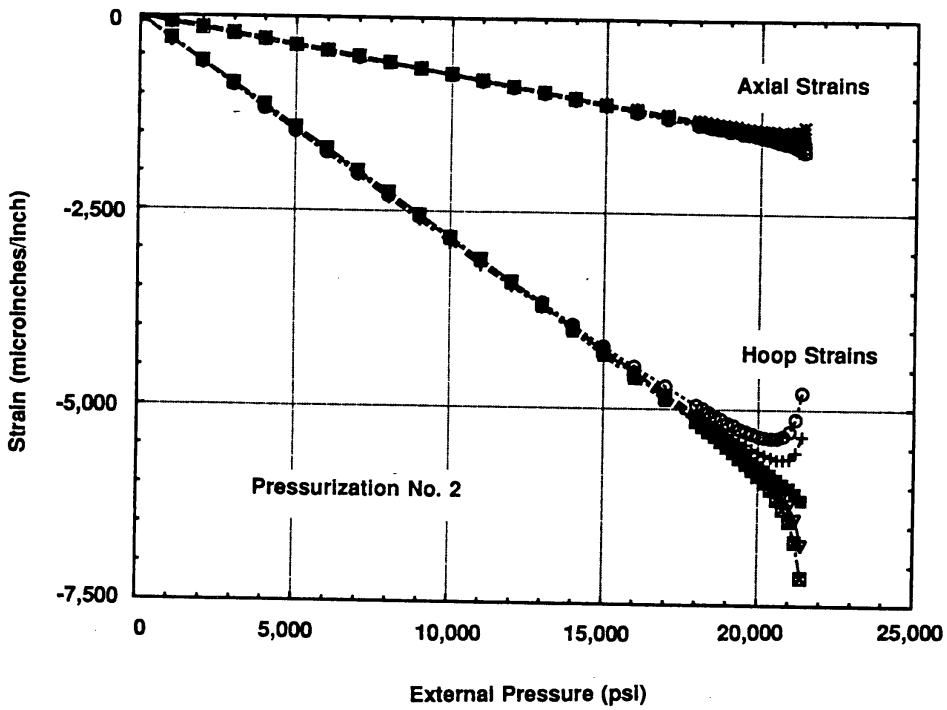

Figure 44. Pressure vs. strain plot for cylinder 010, pressurization No. 2.

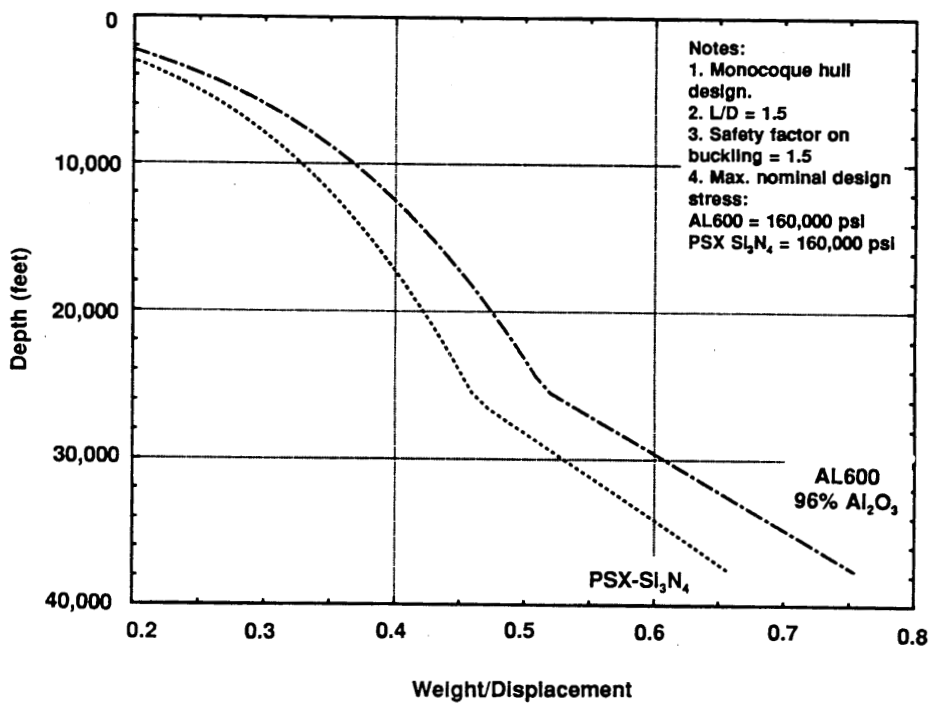

Figure 43. W/D vs. depth curves for AL-600 96-percent alumina ceramic and PSX ceramic.

Table 1. Typical properties for PSX commercial grade of silicon nitride.

Bulk Density	3.29	g/cm^3
Flexural Strength (MOR) @ RT, 4 point average	703 102	MPa ksi
Characteristic Strength @ RT, 4 point	744 108	MPa ksi
Weibull Modulus (m)	14	
Elastic Modulus (E)	317 46	Gpa Mpsi
Poisson's Ratio (v)	0.24	
Hardness (Knoop 1 kg)	1480	kg/mm^2
Fracture Toughness (Vickers)	6.0	$MPa{\cdot}m^{1/2}$
Thermal Expansion (RT-1000°C)	3.3	$10^{-6}/°C$
Thermal Conductivity (RT)	30.0	W/mK
Thermal Shock Resistance (ΔT_c)	700	°C

Table 2. Actual dimensions of deliverable PSX cylinders.

Cylinder No.	Outer diameter	Wall thickness	Length
Si_3N_4 001	12	0.412	18
Si_3N_4 002	12	0.412	18
Si_3N_4 003	12	0.412	18
Si_3N_4 004	12	0.412	18
Si_3N_4 005	12	0.412	18
Si_3N_4 006	12.077	0.418	13.0
Si_3N_4 007	12.056	0.413	16.0
Si_3N_4 008	12.070	0.416	17.938
Si_3N_4 009	12.058	0.415	18.0
Si_3N_4 010	12.041	0.406	18.0

Table 3. Measured material properties of deliverable PSX cylinders.

Cylinder No.	Density (gm/cc)	Young's Modulus (Msi)	Shear Modulus (Msi)	Poisson's Ratio	Compressive Strength (ksi)	Flexural Strength (ksi)	Weibull Modulus	Fracture Toughness MPa · m1/2
Si_3N_4 001	3.264	44.69	17.66	0.27	501.0 ± 13.0	106.6 ± 9.0	13.0	6.2 ± 0.3
Si_3N_4 002	3.275	43.50	17.22	0.26	506.9 ± 18.5	105.1 ± 11.0	11.1	6.2 ± 0.3
Si_3N_4 003	3.265	43.86	17.42	0.26	474.4 ± 27.4	108.5 ± 17.2	6.2	5.8 ± 0.4
Si_3N_4 004	3.275	44.00	17.44	0.26	519.3 ± 15.5	104.6 ± 11.7	9.3	6.2 ± 0.5
Si_3N_4 005	3.271	43.63	17.38	0.26	485.7 ± 18.5	97.8 ± 11.6	8.9	5.9 ± 0.4
Si_3N_4 006	3.266	44.19	17.52	0.26	480.0 ± 20.7	92.9 ± 12.1	8.6	6.2 ± 0.4
Si_3N_4 007	3.269	43.66	17.37	0.26	460.2 ± 22.9	101.8 ± 8.8	13.1	6.2 ± 0.3
Si_3N_4 008	3.266	44.00	17.38	0.27	477.1 ± 11.2	100.3 ± 10.9	10.1	6.0 ± 0.4
Si_3N_4 009	2.272	43.95	17.36	0.27	472.1 ± 26.1	100.8 ± 10.8	10.0	5.8 ± 0.3
Si_3N_4 010	3.279	44.12	17.60	0.25	489.3 ± 18.6	110.8 ± 6.0	20.4	6.0 ± 0.3
Mean	3.270	43.96	17.44	0.26	486.6	102.9	11.1	6.1
St. Dev.	0.005	0.34	0.13	0.01	17.9	5.3	3.9	0.2

Table 4. Summary of findings made in PSX cylinders using pulse-echo ultrasonic inspection.

Cylinder No.	Number of Indications	Indication/Depth (return signal amplitude*/inches below surface)
Si_3N_4 001	2	32% @0.2; 45% @0.3
Si_3N_4 002	4	57% @0.3; 59% @0.12; 69% @0.12; **4dB @0.27**
Si_3N_4 003	4	43% @0.10; 46% @0.2; 62% @0.3; 63% @0.18
Si_3N_4 004	4	21% @0.3; 24% @0.2; 32% @0.2; 42% @0.2
Si_3N_4 005	4	66% @0.12; **83% @0.1; 92% @0.13; 4dB @0.13**
Si_3N_4 006	9	47% @0.15; 50% @0.15; 51% @0.2; 51% @0.3; 54% @0.2; 56% @0.2; 58% @0.3; 62% @0.2; **80% @0.25**
Si_3N_4 007	13	40% @0.35; 46% @0.2; 49% @0.3; 53% @0.2; 55% @0.15; 59% @0.3; 67% @0.2; 79% @0.1; **80% @0.15; 80% @0.15; 90% @0.1; 90% @0.3; 93% @0.15**
Si_3N_4 008	17	47% @0.35; 52% @0.3; 54% @0.2; 54% @0.3; 61% @0.3; 62% @0.35; 77% @0.15; 78% @0.3; **82% @0.3; cluster up to 85% @0.1-0.3; 1dB@0.2; 2dB @0.15; 2dB @0.2; 3dB @0.3; 4dB @0.3; 6dB @0.15; 8dB @0.3**
Si_3N_4 009	22	30% @0.35; 45% @0.23; 65% @0.2; 65% @0.15; 70% @0.15; 70% @0.2; 75% @0.25; 75% @0.2; 76% @0.2; **80% @0.3; 80% @0.2; 80% @0.35; 83% @0.15; 85% @0.3; 90% @0.20; 90% @0.15; 90% @0.3; 95% @0.15; 95% @0.3; 95% @0.15**
Si_3N_4 010	10	24% @0.3; 26% @0.3; 38% @0.2; 42% @0.3; 56% @0.15; 62% @0.15; 70% @0.35; 74% @0.25; **7dB @0.2; 28% @0.25**

* Note: Return signal amplitude is calibrated so that 80% amplitude is equal to that returned by a 1/32" flat-bottom drilled hole. Indications which are theoretically larger than 1/32" dia. are shown bold.

Table 5. Average hoop and axial strains measured on inner mid-bay diameter of PSX cylinders at 10,000-psi external hydrostatic pressure.

Cylinder	Strains at 10,000 psi external pressure (microinches/inch)		Measured Poisson's Ratio	Calculated Poisson's Ratio	Measured Compressive Modulus (Msi)	Calculated Compressive Modulus (Msi)
	Axial	Hoop				
Si_3N_4 001	773 + 22	2981 + 45	0.27	0.277	44.69	43.59
Si_3N_4 002	767 + 31	2854 + 208	0.26	0.267	43.50	45.78
Si_3N_4 003	759 + 39	2952 + 43	0.26	0.279	43.86	43.97
Si_3N_4 004	714 + 33	2765 + 68	0.26	0.278	44.00	46.97
Si_3N_4 005	774 + 84	2934 + 20	0.26	0.272	43.63	44.41
Si_3N_4 006	776 + 33	2832 + 36	0.26	0.262	44.19	45.92
Si_3N_4 007	759 + 42	2871 + 23	0.26	0.272	43.66	45.49
Si_3N_4 008	745 + 70	2913 + 109	0.27	0.280	44.00	44.36
Si_3N_4 009	732 + 30	2841 + 48	0.27	0.281	43.95	45.54
	724 + 28*	2840 + 40*				
Si_3N_4 010	723 + 8	2843 + 31	0.25	0.281	44.12	46.38
	727 + 9*	2859 + 29*				
Mean			0.262	0.275	43.96	45.24
St.Dev.			0.006	0.006	0.34	1.11

* Note: Strains on second pressurization to 10,000 psi external hydrostatic pressure.

Table 6. Summary of test plans and results for cylinders 001 through 010, Sheet 1.

Cylinder No.	Test Configuration	Test Plan/Test Result
Si_3N_4 001	II	Proof test cylinder to 16,000 psi, read strains. Cycle cylinder to 16,000 psi, stop testing after 2,000 cycles.
		1-proof cycle to **16,000 psi**. Cylinder **withstood 581 cycles to 16,000 psi**. Testing was terminated due to leakage.
Si_3N_4 002	II	Proof test cylinder to 16,000 psi, read strains. Cycle cylinder to 16,000 psi, stop testing after 2,000 cycles.
		1-proof cycle to **16,000 psi**, no damage noted. Cylinder **failed on cycle number 337** during pressurization.
Si_3N_4 003	II	Proof test cylinder to 13,000 psi, read strains. Cycle cylinder to 13,000 psi, stop testing after 2,000 cycles.
		1-proof cycle to **13,000 psi**, no damage noted. Cylinder **failed on cycle number 1,379** during pressurization.
Si_3N_4 004	I	Proof test cylinder to 9,000 psi, read strains. Cycle cylinder to 9,000 psi, stop testing after 3,000 cycles.
		1-proof cycle to **9,000 psi**, no damage noted. Cylinder **withstood 3,008 cycles to 9,000 psi** without visisble damage.
Si_3N_4 005	II	Proof test cylinder to 12,000 psi, read strains. Cycle cylinder to 12,000 psi, stop testing after 3,000 cycles.
		1-proof cycle to **12,000 psi**, no damage noted. Cylinder **failed on cycle number 743** during pressurization.

Table 6. Summary of test plans and results for cylinders 001 through 010, Sheet 2.

Cylinder No.	Test Configuration	Test Plan/Test Result
Si_3N_4 006	II sand-blasted ends	Proof test cylinder to 12,000 psi, read strains. Cycle cylinder to 12,000 psi, stop testing after 3,000 cycles.
		1-proof cycle to 12,000 psi, no damage noted. Cylinder **withstood 2,241 cycles to 12,000 psi** without visible damage.
Si_3N_4 007	II sand-blasted ends	Proof test cylinder to 11,000 psi, read strains. Cycle cylinder to 11,000 psi, stop testing after 3,000 cycles.
		1-proof cycle to **11,000 psi**, no damage noted. Cylinder **withstood 3,010 cycles to 11,000 psi** without visible damage.
Si_3N_4 008	II sand-blasted ends	Proof test cylinder to 11,000 psi. Cycle cylinder to 11,000 psi, stop testing after 3,000 cycles.
		1-proof cycle to **11,000 psi**. No damage noted. Cylinder **failed on cycle number 1,665**.
Si_3N_4 009	III sand-blasted ends	Proof test cylinder to 10,000 psi, read strains. Then pressurize to failure while reading strains.
		1-proof cycle to 10,000 psi, no damage noted. Cylinder was **pressurized to failure which occured at 22,600 psi**.
Si_3N_4 010	III sand-blasted ends	Proof test cylinder to 10,000 psi, read strains. Then pressurize to failure while reading strains.
		1-proof cycle to 10,000 psi, no damage noted. Cylinder was **pressurized to failure which occured at 21,600 psi**.

Table 7. Comparison of cyclic pressure testing performance of PSX Silicon Nitride cylinders and of AL-600 96-percent alumina-ceramic cylinders.

External hydrostatic pressure (psi)	Maximum nominal hoop stress (psi)	Number of pressurizations	
		Cercom PSX Si_3N_4 cylinder	Wesgo AL600 96% Al_2O_3 cylinder
9,000	131,067	withstood 3,008	withstood 3,000
10,000	145,631		
11,000	160,194	withstood 3,000 failure at 1,665	withstood 1,380 failure at 2,969
12,000	174,757	withstood 2,241 failure at 743	failure at 1,065
12,500	182,039		
13,000	189,320	failure at 1,379	failure at 762
14,000	203,883		failure at 214
15,000	218,447		failure at 707
16,000	233,010	Leakage at 581 failure at 337	

Table 8. Comparison of the material compositions evaluated for the application of ceramics to large housings for UUVs.

Material Property	WESGO AL600 96-percent Al_2O_3	CERCOM PSX-Si_3N_4	WESGO ZTA	LANXIDE Comp. 90-X-089 $SiC/Al_2O_3/Al$
Compressive strength (ksi)	350	**487**	416	301
Compressive modulus (Msi)	**47.0**	43.9	43.5	41.6
Flexural strength (ksi)	47.0	**102.9**	48.1	56.2
Fracture toughness ($ksi \cdot in^{1/2}$)	2.5	6.7	6.1	**7.6**
Specific gravity (gm/cc)	3.749	**3.270**	4.065	3.365
Weibull modulus	20	11	**38**	N/A
Relative cost (cost factor)	**Low (1)**	Med-High (5.8)	Low-Med (2.6)	High (21.7)